CR-137759

PILOT PERFORMANCE IN ZERO-VISIBILITY PRECISION APPROACH

BY

ARYE R. EPHRATH

B.S., UNIVERSITY OF FLORIDA
1969

S.M., MASSACHUSETTS INSTITUTE OF TECHNOLOGY
1972

SUBMITTED IN PARTIAL FULFILLMENT
OF THE REQUIREMENTS FOR THE DEGREE
OF
DOCTOR OF PHILOSOPHY

AT THE
MASSACHUSETTS INSTITUTE OF TECHNOLOGY
JUNE 1975

Signature of Author Arye R. Ephrath.

Certified by Ronald E. Curry
Thesis Supervisor

Certified by Laurence R. Young
Thesis Supervisor

Certified by John J. Deyst Jr.
Thesis Supervisor

Accepted by Wallace E. Vander Velde
Chairman
Departmental Doctoral Committee

ACKNOWLEDGEMENTS

A research effort of this magnitude is obviously not the work of one person alone and I am very fortunate to have had the assistance of the members of my Doctoral Committee: Professor R.E. Curry, the Chairman, who initiated this research and to whom I am indebted for his helpful advice and his expert guidance; Professor L.R. Young, on whose enormous experience in man-machine systems I depended heavily and whose friendship I value; and Dr. J.J. Deyst Jr. of the Charles Stark Draper Laboratory, who reviewed the manuscript and who provided many helpful comments.

Very special thanks are due the pilots of American, Delta and Eastern Airlines and the MIT personnel who contributed their free time to serve as subjects in the experiments. They are, in alphabetical order:

Paul H. Bauer
Carl A. Beatrice
Frank Buselli
Ronald Harrod
Stanley L. Henderson
Jack D. Howell
George Kyrazis
Lawrence C. Malarsky
Paul D. McCarthy
Gray B. Newman
Richard A. Osborne
Guy D. Paris
Eugene P. Rooney
Stafford A. Short
Robert W. Simpson
Frederic Stanwood
Michael G. Sweeney
Carl W. Vietor
Charles S. Williams
Marc Wolf

And, finally, I would like to express my gratitude to my wife, Linda. While working on doctoral research of her own she had the patience and the sense of humor that made her a friend in need.

This research was supported by NASA grant NGR 22-009-733.

TABLE OF CONTENTS

LIST OF FIGURES

LIST OF TABLES

CHAPTER I

INTRODUCTION

1.1 The Instrument Landing Approach

The instrument landing system (ILS) has been in civil use since 1947 and is in operation at about 600 airports throughout the world, half of them in the United States. Its name, however, is a misnomer. It should more properly be called an instrument low-approach system, as a pilot must establish visual reference with the ground in the last phase of the approach to complete the landing. This is the "see-to-land" concept (DeCelles, 1970).

The minimum height above the runway elevation at which a pilot must abort the approach if the required visual reference has not been established is the "decision height". At present, five categories of instrument landing approaches are classified by the International Civil Aviation Organization, with different decision heights (ICAO, 1965 and 1970):

Table 1.1 ICAO Categories

Category	Decision Height (ft.)	Runway Visual Range (ft.)
I	200	2400
II	100	1200
IIIA	0	700
IIIB	0	150
IIIC	0	0

The category under which an ILS approach is conducted depends on the certification of the particular aircraft and its crew and on the available ground equipment at the airport. Category I landings have been carried out for almost thirty years; the first eight United States airports were certificated for Category II operations in August of 1968. At the present time there is only one runway in the United States which is certificated for Category IIIA operations.

The ILS is a precision approach system which provides accurate course alignment and glide slope descent information during the approach by way of specialized equipment on the ground and on board the aircraft:

1. The glide slope transmitter, usually installed between

750 and 1250 feet from the approach end of the runway, establishes a radiation pattern in space from which a signal is derived proportional to the aircraft's vertical angular displacement from the glide path. This signal drives the up-down glide slope deviation indicator (GSI) needle and is one of the inputs to the longitudinal flight-director in the aircraft. The glide slope beam width is approximately 1.5°, half above and half below the glide slope line. The glide slope line elevation is usually 2.5° to 3.5° above the horizontal.

2. The localizer transmitter is usually installed approximately 1000 feet beyond and 300 feet to the side of the far end of the runway with the antenna in line with the runway centerline. The localizer establishes a radiation pattern in space from which a signal is derived proportional to the lateral angular displacement from the vertical plane through the runway centerline. This signal drives the left-right course deviation indicator (CDI) needle and is one of the inputs to the lateral flight director in the aircraft. The localizer beam width is approximately 5°, half to the right and half to the left of the runway centerline extension.

3. Marker beacons and optional compass locators provide definite fixes along the approach as distance spot checks. The outer marker is placed on the runway centerline extension at a distance of from 4 to 7 miles from the runway threshold; the middle marker is placed where the glide slope is 200 feet above the runway elevation and identifies the Category I decision height; the inner marker is

placed where the glide slope is at the Category II decision height or to indicate runway threshold passage. In addition to an audible tone, the outer marker lights a purple lamp on the instrument panel; the middle marker, an amber lamp; and the inner marker, a white lamp.

1.2 Background

In the last decade, a great deal of thought has been given to Category III landings and their implications. One area of intensive investigation centered around the role of the crew during the approach, and current thought is polarized around two extremes:

1. The crew is in the control loop and flies the aircraft in accordance with instrument-generated signals.
2. Steering signals are coupled directly into the autopilot, with the crew monitoring the system.

Crew control based on the steering signals is favored by many crewmen and operations personnel (Kayton, 1969), and comprehensive manual control-display theories have been developed (Clement *et al.*, 1968; McRuer *et al.*, 1967) to facilitate the design of optimal equipment. For reasons of economy, civil aviation authorities and commercial carriers prefer to retain the ILS for Category III guidance and are

working to set standards for compatible airborne equipment. The ILS localizer can probably be made usable for lateral guidance during Category III touchdowns. The ILS glide slope is not usable, however, below approximately 100 feet of altitude, because of the parabolic shape of the beam in that region. Thus, for vertical guidance near the runway, Category III landing systems must be based on non-ILS equipment such as microwave guidance or a radio altimeter.

During the early phases of an uncoupled final approach, at altitudes greater than the decision height, steering information is presented to the pilot by the flight director. This system incorporates as inputs not only the raw GSI and CDI position data but also rate information and thus relieves the pilot of the need to generate large leads in synthesizing the information (DeCelles, 1970). New features are constantly being added to existing flight director systems (Monroe *et al.*, 1968); they are, however, inadequate as a mode of guidance during the final phase of the landing (DeCelles, *op. cit.*) and their performance during simulated Category III landing studies has been disappointing (Gainer *et al.*, 1967), presumably because of increased workloads caused by the manual control mode and because of excessive dispersion at touchdown.

The first British European Airways Trident had been certificated for automatic touchdowns in 1965 (St. John and Morgan, 1966) and

the first fully automatic landing in airline passenger service occurred two years later. Since then, great progress has been achieved in the development of automatic landing systems. The simplex, fail-hard couplers of yore have been replaced by redundant duplex systems and triply-redundant autopilots which provide fail-soft capability in the event of two simultaneous failures. Many systems are available today, such as TALAR, FLARESCAN and AUTOLAND, to name just a few.

Yet computers are only human, and crews demand the capability of monitoring the progress of the landing via displays which utilize signals and data processors completely independent of the autopilot (DeCelles, *op. cit.*). Indeed, a number of independent landing monitor (ILM) concepts and configurations have been proposed to date, both the conventional panel-mounted variety (Bencivenga, 1970) and the heads-up display (HUD) type (Parks and Tubb, 1970; Jenney *et al.*,1971). Some of these concepts have been evaluated in flight: An instrument panel display for monitoring automatic landings was flight-tested in a DC-7 at the National Aviation Facilities Experimental Center (Pursel, 1968), while in France a HUD all-weather approach and landing monitor is being flown on board a Nord-262 (Dunbar and Collins, 1972).

1.3 Objectives of the Thesis

It is axiomatic that a pilot should be capable of detecting and identifying failures in the automatic landing system accurately, reliably and with minimal time delay. To this end, extensive studies have been conducted in which the pilot was treated as a controlling element in a one-dimensional task; his decision processes (Schrenk, 1969) and his adaptive behavior following a sudden change in the controlled plant dynamics were investigated (Young *et al.*, 1964; Phatak and Bekey, 1969). Other studies investigated the failure-detection performance, treating the operator as a pure monitor (Gai and Curry, 1975). In reality, the pilot is faced with multi-axes, not single-axis, tasks; although models for interference among multiple control tasks have been derived (Levison, 1970), the inter-relationships between simultaneous control and monitoring tasks are not as yet well understood (Levison, 1971).

Young *et al.* (*op. cit.*) found that in single-axis tracking tasks the human operator's performance as a failure detector was better when he was in the control loop; simulated Category III landing studies, on the other hand, revealed that the pilot's failure detection performance deteriorated when he was faced with a manual control task, compared to the monitoring mode (Vreuls *et al.*, 1968a

and 1968b). When faced with split-axis tasks, pilots' monitoring and decision making was impaired (Monroe *et al.*, 1968) and they sometimes completely overlooked the occurrence of a failure, presumably because of the increased workload associated with split-axis tasks compared to a monitoring task (Gainer *et al.*, 1967). The inadequacy of the human operator as a fault detector led to the development of performance-monitoring hardware (Smith *et al.*, 1972) which has been installed in many modern aircraft (Jester, 1973). Even with the aid of such annunciator panels the pilot's performance, under certain conditions, leaves much to be desired (Semple *et al.*, 1968).

It has been recognized that when the role of the human operator changes from monitoring to that of an active controller, corresponding changes take place in his workload level (Ekstrom, 1962; Wewerinke). However, in pilot performance studies to date these effects were completely confounded. It is the primary purpose of this investigation to separate these effects and to document pilot performance during a Category III landing as a function of the particular control mode at different workload levels. We wish to isolate and identify the effects on performance due to the variations in the control mode alone - and hence, variations in the operator's mode of behavior - apart from the effects on performance due to the variations in the workload level.

1.4 Research Method

As stated, the purpose of this research was the study of the pilot's short term decisions regarding performance assessment and failure monitoring. We wished to investigate the relationship between the pilot's ability to detect failures, his degree of participation in the control task and his over-all workload level. Also, we wished our findings to be applicable to the general population of pilots who fly low-visibility approaches in commercial jet transport aircraft.

To this end, this research consisted of an experimental investigation which was carried out in a static ground simulator. Airline pilots flew zero-visibility landing approaches with different degrees of automation and at different workload levels, which were induced by simulated wind disturbances. The pilots' ability to detect failures and to provide a reliable manual back-up capability was monitored and recorded.

The data were analyzed to identify statistically significant relationships among the experimental treatments and the factors which produced the optimal performance were sought.

1.5 Results of the Thesis Research

The investigation has examined the effects of the pilot's participation mode in the flying task on his workload level and failure-detection performance. We found that the participation mode had a strong effect on the pilot's workload, the induced workload being lowest when the pilot acted as a monitoring element during a coupled approach and highest when the pilot was an active element in the control loop. In addition, a very marked increase in workload at altitudes below approximately 500 feet was documented at all participation modes; this increase was inversely related to distance-to-go.

The effects of workload and participation mode on failure detection were separated. The participation mode was shown to have a dominant effect on the failure detection performance, with a failure in a monitored (coupled) axis being detected significantly faster than a comparable failure in a manually controlled axis.

Touchdown performance was also documented and the findings of previous investigators were supported, namely that the conventional instrument panel and its associated displays were quite inadequate for zero-visibility operations in the final phases of the simulated landing approach.

CHAPTER II

THE EXPERIMENT

2.1 Hypotheses

In analyzing his performance as a systems component, the human can be assumed to possess information-processing capacity which is fixed and constant in any given set of conditions (Brown, 1964). As long as the information processing demands, which are imposed on the operator, are considerably less than this maximal capacity, the human's information sampling rate will be limited only by the presentation rate and by his own display scan rate limitations. When the demands are increased, however, the human must reduce his information sampling rate.

If the human serves as a controlling element in the system, the reduced sampling rate will manifest itself in increased lag and hence, to maintain an adequate phase margin, the operator will reduce his gain which, in turn, will effect an increased RMS tracking error. If he acts as a failure-monitoring element, then failure-detection times will be increased. These assumptions underline our hypotheses:

1. Both operator participation level in the control task and his overall workload affect the information-processing requirements. The effects, then, of the operator's participation level and workload on his failure detection performance are additive. Manual tracking will result in longer detection times than will monitoring a coupled automatic approach, and high workloads will manifest themselves in longer detection times than will low workload levels.

2. As the flight instruments display angular, rather than linear, deviations from the localizer course and glide path, they increase in sensitivity as distance to touch-down decreases. In addition, the penalty for error increases with increased proximity to the ground. Additional processing demands are therefore placed on the pilot and hence his workload increases in inverse proportion to the altitude or to distance-to go.

The validity of these hypotheses will be tested experimentally in a fixed-base cockpit simulator with the aid of a workload-measurement device.

2.2 Workload Measurement Theory

As was already stated in Section 2.1, the human operator is postulated to possess finite, fixed capacity to perform well on

tasks such as manual tracking or information processing (Brown, 1964). This total capacity, TC, is assumed to be constant in a given set of conditions such that the performance is inversely related to the amount of workload required in excess of this level.

When the human operator is performing a task which requires less than his total capacity, then his total capacity is divided into the expended capacity, EC, and the fraction which is unused, the residual capacity, RC:

$$TC = EC + RC \tag{2.1}$$

A now classic example of these concepts was given during evaluation of alternative control modes for the X-15 research aircraft (Ekstrom, 1962). The subject first performed a self-paced choice-reaction pushbutton task, and his scores were recorded. As this was a self-paced task and the subject was well-motivated, these scores were assumed to represent his total capacity. Next, the subject performed the primary control task concurrently with and at the expense of the subsidiary pushbutton task. If the subsidiary task response was reduced to 40 percent of the level obtained when performing the subsidiary task alone, then this would be taken as an indication that the operator needed 100 - 40 = 60 percent of his attention to perform the primary control task. The results of this analysis

showed that the pilot could use both control modes equally well but that one mode required less of the pilot's attention and therefore, in terms of workload penalty, was superior to the other.

In this application, the auxiliary task is introduced as a measuring tool. It is used to determine the price paid in operator effort in meeting the performance criteria of the primary task. The rationale for using the subsidiary task is that as the load of the primary task is increased, performance on the subsidiary task will deteriorate, thus giving a measure of how much additional work the operator can handle while still meeting system criteria of the primary task. The situation is illustrated schematically in Figure 2.1.

2.3 Requirements of the Auxiliary Task

The problem of defining the requirements of the auxiliary task is complicated by the simple fact that different experiments impose different specific demands upon the auxiliary task, thus hampering the development of a universal subsidiary task.

A generalized set of desired characteristics, however, can be described for the auxiliary task. These characteristics do not

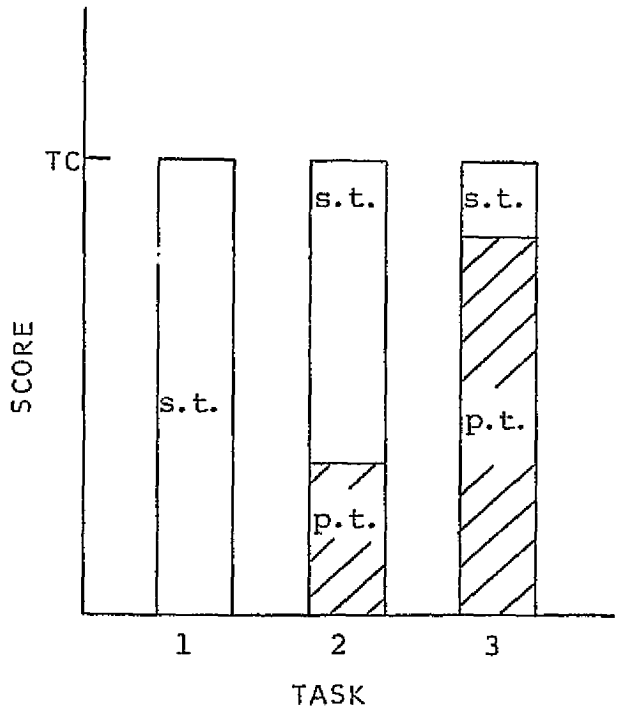

Task 1: s.t. alone
Task 2: p.t.#1 + s.t.
Task 3: p.t.#2 + s.t.

s.t.=subsidiary task
p.t.=primary task

Fig. 2.1 Auxiliary Task Score Reflects Primary Task Difficulty

define any one particular auxiliary task; they merely narrow down the selection to a smaller number of possible alternatives, of which the one is chosen which satisfies the additional requirements of the case in point.

2.3.1 The Multiplex Model

The subsidiary task is used to measure the reserve capacity of the operator during what is essentially normal performance of the primary task. It should, therefore, be subtle in its effect on the primary task; it should be demanding enough so that the operator cannot ignore it, yet not so demanding as to stress the primary task to the point of disruption (Knowles, 1963). In analyzing the specific requirements of subsidiary tasks, it is helpful to turn to a rather simple, yet effective, single channel multiplex model which has been proposed to summarize the basic notions of operator loading and its measurement by subsidiary task scores (Knowles, 1973; Broadbent, 1957). A multiplex system uses a single, fixed capacity channel to transmit messages from several sources to several destinations. Only messages from one source to one destination can be processed at a time, but the information flow rate can be maximized by proper coding and switching routines. A schematic representation of the model is given in Figure 2.2. In this model S is an information source, D is a destination, S_1-D_1 represent the flow of the primary task information, S_2-D_2 represent the flow

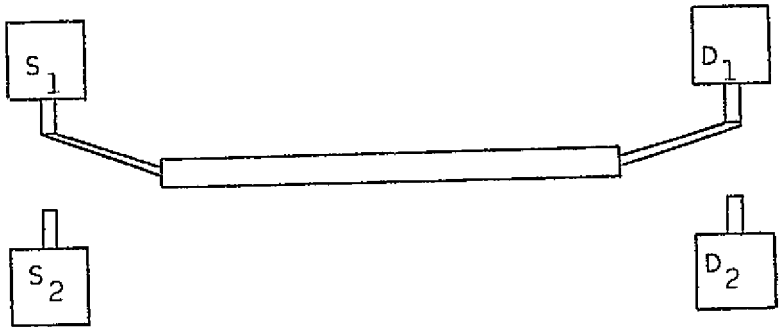

Fig. 2.2 Single Channel Multiplex Model

of the subsidiary task information.

In measuring operator workload it is assumed that, by appropriate motivation, priority is given to primary task information, and that subsidiary task information is processed within the residual channel capacity.

Some important requirements of the subsidiary task are illustrated by reference to this simple model:

1. The switching points at the input and at the output represent opportunities for task interference that must be minimized. At the input end, priority must be given to the primary task. Hence, by appropriate motivation, the subject should perform the subsidiary task only when he feels that he can respond with no decrement in his performance on the primary task. It should be noted here that in practice complete non-interference between the subsidiary and primary tasks is difficult to achieve. It should, however, be minimized by using a subsidiary task which is different in form from the primary task and which requires different effectors at the output end.

2. The subsidiary task should be self-paced.

3. It has been mentioned that information flow-rate through the multiplex channel is a function of the efficiency of the coding

method adopted by the subject, that is, the degree of learning achieved. The learning effects of the subsidiary task should be minimized if a meaningful measure of the workload is to be obtained. Consequently, the subsidiary task should be simple, thus requiring very little learning, and the subject should be given an opportunity to practice on the subsidiary task alone until he reaches steady state on the learning curve. This yields the added benefit of minimizing inter-subject variations as the base performance for each subject can be determined.

4. The subsidiary task information may occupy the channel only in the absence of primary task information. This implies that subsidiary task messages should be very short. This requirement can be met by using discrete stimulus-response units.

5. As mentioned above, the subsidiary task is used as a measurement tool, to determine the operator's reserve capacity and hence the portion of his total capacity which is expended on the primary task. As a measuring device, the scores of a given subsidiary task should be comparable from situation to situation. In addition to providing an average score over an entire run, in many applications it is desirable for the subsidiary task to provide an indication of the instantaneous rate of flow of information continuously throughout the run.

2.4 The Subsidiary Task

As mentioned in Section 2.3, the subsidiary task is characterized by the following features:

1. It is performed only when the subject feels that this will not result in a decrement in his performance on the primary task.
2. It involves psychomotor activity different from the primary task's.
3. It is simple and over-learned
4. It consists of short, discrete message units.
5. It can be scored continuously throughout an entire run, and the information conveyed by the scores is comparable from situation to situation.

Based on these required features, a "warning light" type subsidiary task was selected for this research. It consisted of two small, 1/8" diameter red lights mounted above each other outside the subject's foveal vision and peripheral vision, and a rocker thumb switch mounted on the left horn of the control yoke.

The lights provided the stimuli. They were located 75^{o} to the right of the center of the flight instruments. The intensity

of the lights was very low and was adjusted individually for each subject via a variable resistance to ensure that the subject would not be able to detect the lights in his peripheral vision. The lights were mounted on a matte black background and the two-inch distance between them subtended a relatively large visual angle of 4°, to minimize confusion (see Figure 2.3).

During the run the upper or the lower light, with equal probability, was lit at random times for two seconds. A correct response by the subject to this stimulus consisted of turning the light off by a proper motion of the rocker thumb switch; that is, pushing the switch up if the upper light was on or pushing it down if the lower light was on.

A correct response by the subject caused the light to turn off. A "hit" was scored and the subject's response-time stored. In the absence of a correct response the light stayed on for two seconds, then turned off and a "miss" was scored. An incorrect response by the subject (that is, pushing the switch the wrong way) was also scored as a "miss".

After a light was turned off, a time delay followed, uniformly distributed between 0.5 and 5.0 seconds, and the process was then repeated. The time delay, as well as the selection of the light, was

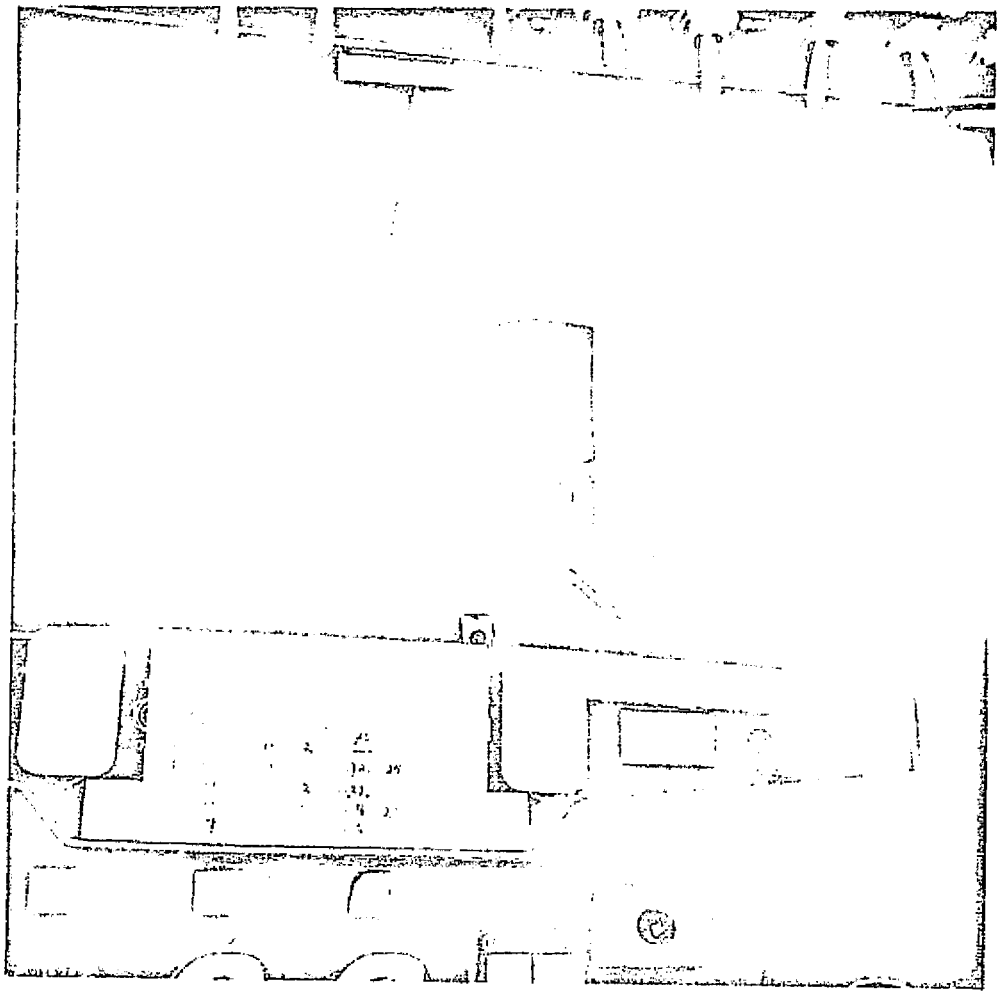

Figure 2.3 Subsidiary Task Warning Lights

controlled by a random number generator in the computer program.

The subject was instructed to consider the piloting task of flying an ILS approach as his major concern at all times (see Appendix B, "Instructions to Pilot - Workload Measurement"). It was emphasized that his primary concern should be to do the best that he could flying the approach, and that he should respond to the lights if and only if he felt that he could do so without sacrificing his piloting performance. To further impress upon the subject the importance of the piloting task he was told that during the workload-measurement runs he did not have the option of executing a missed approach and that each approach had to terminate in a touchdown on the runway on the first trial.

A subsidiary task of this type has been shown to combine sensitivity to workload changes with minimal degredation of primary tracking task performance (Spyker *et al.*, 1971). This point was further substantiated in this study by subjective evaluation (see Appendix C, "Pilot Questionnaire") as well as statistical analysis of RMS tracking errors. These results are reported in detail in Chapters III and IV.

2.5 Apparatus

For the purpose of this thesis, a simulation capability including the ADAGE AGT/30 digital graphics computer and a fixed-base cockpit simulator has been developed.

A mathematical model has been developed of a large transport aircraft in the landing approach flight envelope. The actual flight data of a DC-8 were used in the equations of motion (Teper, 1969), and the various parameters were later refined following a series of flight tests by a senior airline captain with considerable Boeing 707/123 experience. Non-linear phenomena such as ground effect and stalls have also been included. As an added assurance, the simulator had been flown by ex-fighter pilots and airline captains prior to commencement of the actual experimentation and all felt that it was quite adequate.

An integrated-cue flight-director system has been designed for this simulator, providing the capability of landing the simulated aircraft manually in zero-zero conditions in a relatively satisfactory manner. Also, a two-axis auto-pilot has been incorporated into the simulation which is capable of flying ILS coupled approaches, in either axis or in both axes, to touchdown. The autopilot and the

flight-director systems have been tested extensively (see Figures A.11-A.12).

We also had the capability of adding wind disturbances to the simulation to induce different workload levels. The wind modes were:

1. No wind.
2. 5 kt wind, gusting to 15 kt, from 260° (i.e., at 45° to the runway heading. Runway 4R at Logan Airport, whose heading is 35°, was our active runway).
3. 10 kt wind, gusting to 30 kt from 260°.

The gusts were modelled as filtered white noise with a cutoff frequency of $\pi/6$ rad/sec.

The equations of motion of the aircraft, as well as the flight-director and autopilot systems, are described in detail in Appendix A.

The mathematical model was programmed into the AGT/30 computer which was linked via multiplexer channels and sense lines to the cockpit simulator. The cockpit was a mock-up of the captain's crew station in a Boeing transport aircraft (see Figure 2.4). The windows were frosted to eliminate external visual reference.

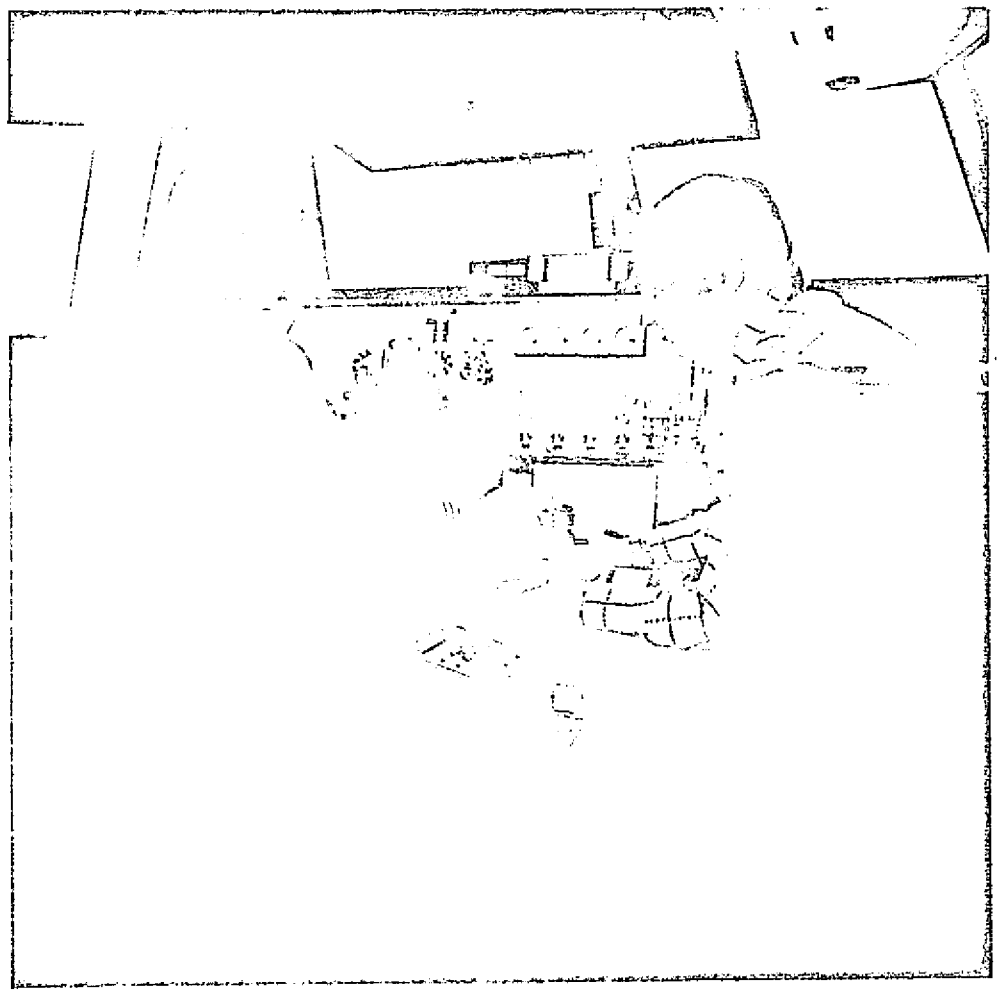

Figure 2.4 Cockpit Simulator -- General View

The controls included an operational, spring-centered control column with a control wheel and rudder pedals, as well as four throttles, flaps, speed-brake and landing gear levers, and flight-director and autopilot controls.

Apart from engine instruments and marker beacon lights, the simulator was equipped with three CRT screens, mounted one each on the main instrument panels at the captain's and the first officer's stations and one in place of the weather radar screen. The screens were driven simultaneously by the ADAGE computer. The screens on the main panels presented six standard flight instruments (see Figure 2.5): air speed, attitude-flight director indicator, altimeter, instantaneous vertical speed indicator, horizontal situation (HSI) and radio magnetic (RMI) indicators, as well as a DME digital readout and a glideslope deviation needle which was repeated on the attitude indicator and the HSI. The HSI included a course deviation line which was tuned to the localizer. The RMI needles were tuned to the outer compass locator and to the Boston VOR station (see also Figure A.3)

One of our goals in this study was to investigate the pilot's failure detection performance based on his internal model of the environment and on his capability of processing raw flight data. Consequently, we did not include any displays of a mode progress

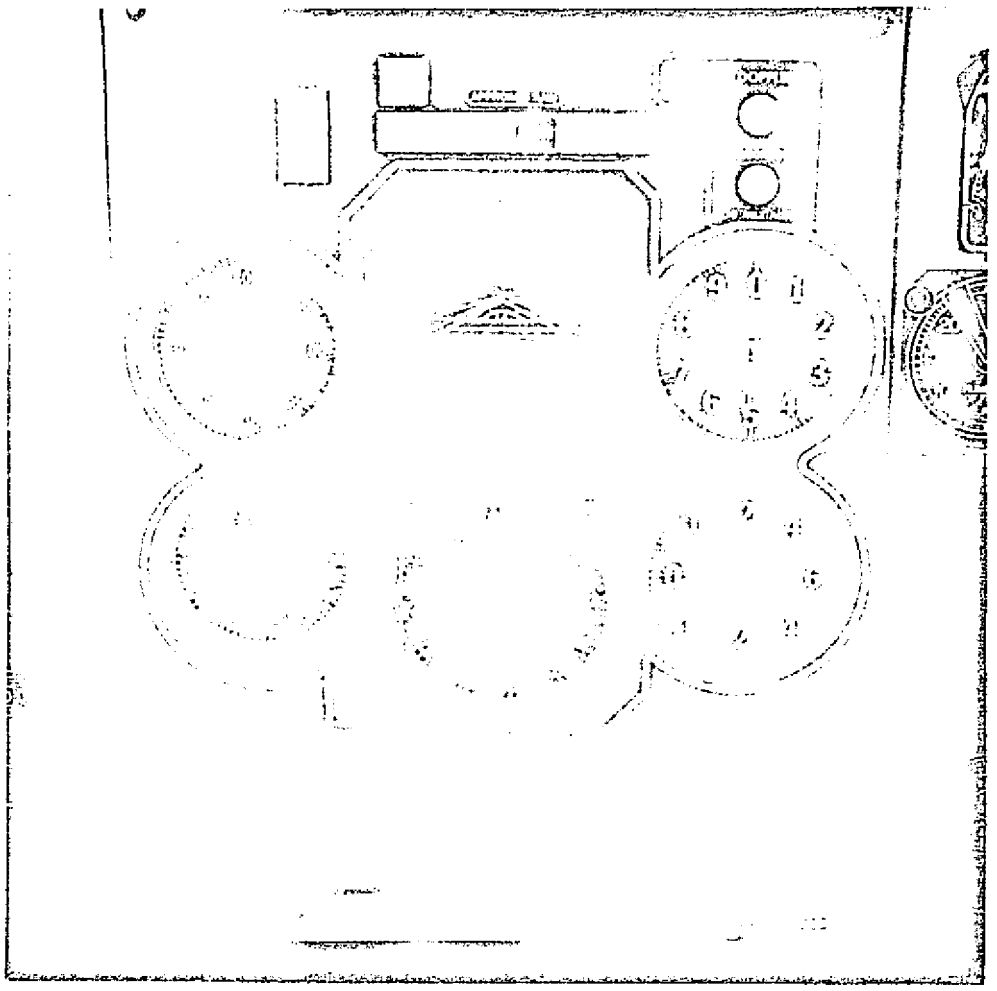

Figure 2.5a Flight Instruments

(For legend, see Figure 2.5b)

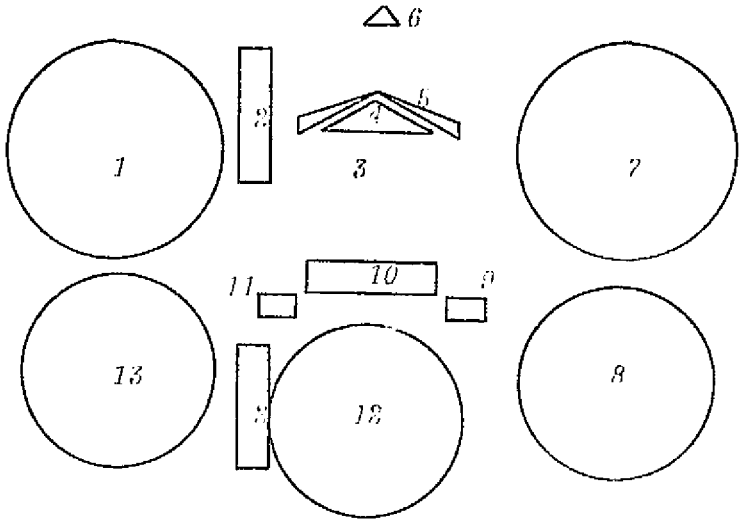

1. Airspeed
2. Glideslope Deviation (GSI)
3. Attitude (Artificial Horizon)
4. Aircraft Reference Symbol
5. Integrated Cue Command Bars
6. Bank Indicator
7. Altimeter
8. Vertical Speed (IVSI)
9. Course Set
10. Localizer Deviation
11. Distance Measuring (DME)
12. Horizontal Situation (HSI) and Course Deviation (CDI)
13. Radio-Magnetic Compass (RMI)

Figure 2.5b Flight Instruments

annunciator, movable bugs or a fault annunciator panel, nor were there any warning flags.

The CRT screens were driven by the computer at a rate of 24 frames per second which was sufficient to produce flicker-free images. The images were updated at a rate of 5/second.

2.6 Measurements

Throughout each run continuous measurements were taken on-line by the computer program. These measurements were stored initially in memory buffers; at the end of the run they were written on disk and on magnetic tape as data files for subsequent off-line analysis.

2.6.1 Flight Data

During an approach, the airplane's spatial coordinates, i.e., the distance from the runway threshold, the distance from the localizer course (runway centerline) and the altitude were sampled at constant time intervals and stored. The sampling intervals were set at 5 seconds initially and at one second at altitudes below 150 feet, where aircraft responses of higher frequencies were expected during the flare or go-around maneuvers. These date enabled us to reconstruct

the flight path and to estimate derivatives, such as velocity and sink rate, which we could not store directly due to memory limitations.

At touchdown (i.e., when altitude equals zero) pertinent quantities were sampled and stored. They are:

1. distance from threshold
2. distance from centerline
3. airspeed
4. sink rate
5. pitch angle
6. bank angle
7. heading
8. crab angle

These data allowed us to assess the acceptability of the landings. A landing was considered successful if it satisfied all of the following requirements (Gainer *et al.*, 1967):

1. range - first 3000 feet of the 7500-foot runway
2. centerline - $\pm$ 75 feet
3. airspeed - less than 135 kt
4. sink rate - less than 360 fpm
5. pitch - between 0^{o} and 9^{o}

6. bank - less than 5^{o} left or right
7. heading - within 4^{o} of runway heading, i.e., between 31^{o} and 39^{o}

There were no penalties for excessive crab, i.e., lateral drift, as the pilot was not presented with any decrab information.

In addition to these, time to detection of failures, when a failure occurred, was also recorded. A detection was indicated by pressing a push-button located on the center console in the cockpit.

2.6.2 Workload Data

When it was activated, the pilot's performance on the subsidiary warning-light task was monitored on-line. Data were recorded in real time throughout the run and stored in memory, to be written on disk and on magnetic tape at the end of the run as data files.

Specifically, the program recorded the number of times that the subject responded correctly to the warning light by activating the thumb switch ("hits"), his response time (latency) and the X^{*}-coordinate of the aircraft, i.e., the distance from the runway threshold at the time of the response. This last measure enabled us to correlate the subject's workload with the altitude via the recorded flight-path data. The distance from threshold was recorded, rather

than the actual altitude, as it was conceivable that the aircraft would fly at a constant altitude or pass through an altitude more than once, while it was improbable that a pilot would be more than once at any given X^*-coordinate, that is, fly a course at an angle of 90° or more from the runway heading.

Incorrect responses by the pilot, that is, not responding to an illuminated light or activating the switch the wrong way, were counted and labelled as "misses". The X^*-coordinates corresponding to the "misses" were also recorded and stored.

A workload index was computed from these data as follows:

1. As each stimulus was presented for 2 seconds, the total response-time ratio, RTR, for both "hits" and "misses" was computed by

$$RTR = \frac{\text{cumulative latency } (\Sigma_i T_i)}{\text{Total number of stimuli x 2 sec}} \qquad (2.2)$$

2. A miss rate MR was computed by

$$MR = \frac{\text{Number of stimuli missed}}{\text{Total number of stimuli}} \qquad (2.3)$$

3. A workload index WLX was then extracted using the best least squares fit weighting coefficients

$$WLX = \frac{0.780\ RTR + 0.626\ MR}{0.780 + 0.626} \times 100 \text{ percent} \qquad (2.4)$$

This measure of workload has been shown (Spyker *et al.*, 1971) to be correlated with physiological predictors of workload with a correlation coefficient $\rho = 0.646$, significant at the $p < 0.005$ level.

For the purpose of correlating failure detection performance with workload levels, subject responses between altitudes of 2000 feet and 800 feet were used in computing the workload index because between these altitudes the aircraft was stabilized on the approach path and because failures occurred only in this region. Also, we wished to eliminate differences between subjects which may have been caused by different subjects assigning different relative priorities to the primary tracking task and the subsidiary task. To this end the workload index of each subject was normalized, that is, a workload index of zero was assigned to the approach which resulted in the lowest workload measure for each subject and a workload index of 100 was assigned to the approach with the highest workload measure for each subject. The normalized workload index on approach i of

subject j was computed by

$$\text{Normalized } WLX_{ij} = \frac{WLX_{ij} - \min_i \{WLX_{ij}\}}{\max_i \{WLX_{ij}\} - \min_i \{WLX_{ij}\}} \times 100 \text{ percent} \quad (2.5)$$

2.7 Experimental Design

The experimental variables to be investigated in this study were the pilot's participation level in the piloting task, the workload induced by the control dynamics and by external disturbances, and the pilot's failure detection performance.

The experiment involved four levels of participation:

1. "Passive monitoring", with autopilot coupling in all axes, including autothrottles.
2. "Control yaw", with autopilot coupling in the pitch axis and autothrottle coupled.
3. "Control pitch", with autopilot coupling in the yaw axis only.
4. "Control both", i.e., a fully-manual approach.

There were three levels of wind disturbance:

1. No wind.
2. A 45° tailwind of five knots, gusting to fifteen knots.
3. A 45° tailwind of ten knots, gusting to thirty knots.

Three failure conditions were used:

1. No failure.
2. Failure in the yaw axis (see Section A.4). In this condition the autopilot, if coupled, or the flight director would steer the airplane away from the localizer course, resulting in a one-dot deviation (1.25° of angular error) about 100 seconds after the failure occurred. This type of failure was chosen, rather than a runaway failure, because it was quite subtle and so provided a good measure of the limits of the pilot's failure-detection capability.
3. Failure in the pitch axis, which resulted in a one-dot deviation (0.35° of angular error) approximately 30 seconds after the occurrence of the failure (see Figure A.11).

Failures were presented only between the altitudes of 1800 and 800 feet. The selection of the failure altitude was randomized, as was the selection of the direction of the failure (left-right in a yaw failure mode, up-down in a pitch failure mode). Workload levels

and failure detection performance were investigated in separate experiments, to avoid possible contamination of failure detection data by the presence of a concomitant subsidiary task. Also, we were interested in measuring workloads at the different participation levels. The occurrence of a failure during the approach would have made this impossible, as the control mode changed following a failure.

2.7.1 Workload

The effects of the level of participation and of the wind disturbance on the pilot's workload were investigated in a 4 x 3 factorial experiment as shown schematically in Figure 2.6.

The order of presentation of the twelve treatments was randomized, and every pilot (replication) flew all twelve approaches indicated by the design. The subject's workload level was measured by the subsidiary task. No failures were presented and go-arounds were not permitted.

2.7.2 Failure Detection

The effects of the level of participation and of the wind disturbance on the pilot's failure detection performance were investigated in a 4 x 3 x 2 factorial experiment as shown schematically in Figure 2.7.

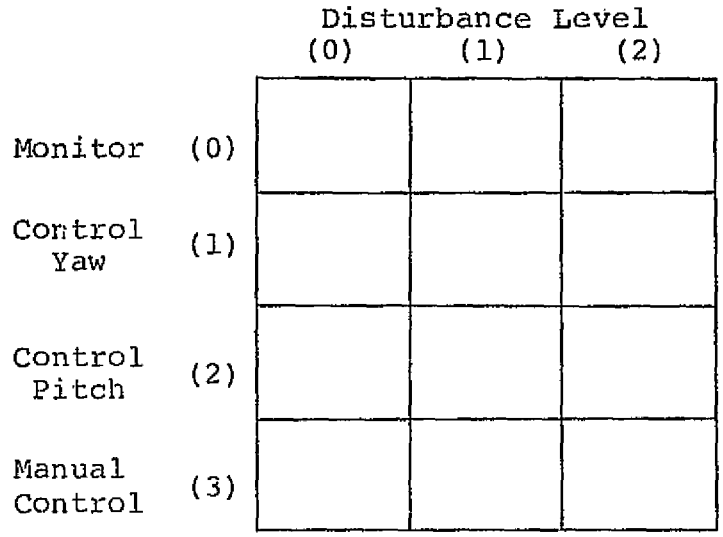

Fig. 2.6 Experimental Design - Workload Measurement

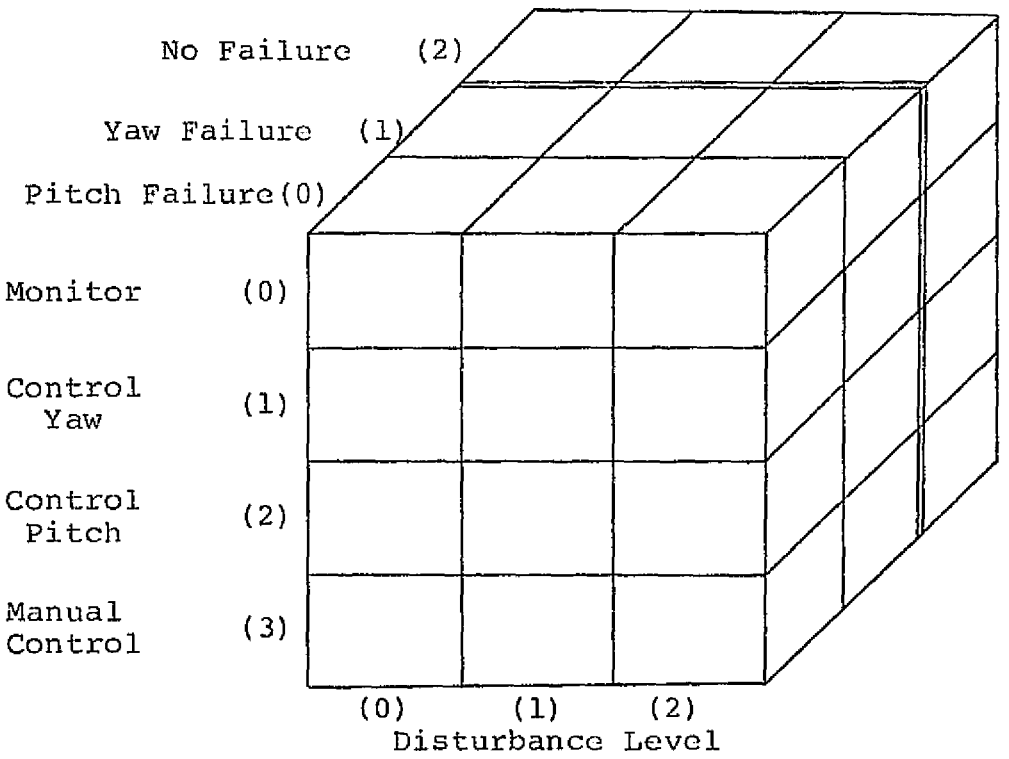

Fig. 2.7 Experimental Design - Failure Detection

The "no failure" condition was also incorporated in the design so that the subject would not anticipate a failure on each and every approach. This, however, resulted in a 4 x 3 x 3 = 36 treatments per replication for this experiment in addition to the twelve treatments of the workload experiment. We felt that such a large number of treatments placed an unacceptable burden on the volunteer subjects. Consequently, some high-level interactions were partially confounded in the failure detection experimental design (Cochran and Cox, 1968; Li, 1955), resulting in eighteen treatments per subject (replication). With the workload index experiment, this meant 30 treatments in all per subject, which we felt was a more manageable load. The interactions which were partially confounded were (participation) x (failure) and (participation) x (disturbance) x (failure). The average loss of information regarding these interactions was 1/27 and 4/27, respectively (Li, 1944), compared to a full rank design; that is, the accuracies of the estimates of these effects were 26/27 and 23/27, respectively, of the accuracy of the estimates of the non-confounded effects. The treatments presented to each subject, excluding the six approaches in which no failures occurred, are shown in Table 2.1. The subsidiary task was not presented in this part of the experiment and go-arounds were permitted.

The order of presentation of the twelve treatments was randomized. Each pilot flew the twelve approaches indicated by the design, failures

Table 2.1 Treatments of Failure Detection Experiment

Treatment {ijk} $\triangleq$ participation mode i
disturbance level j
failure condition k

REPLICATION (SUBJECT)									
2b	3a	3b	4a	4b	5a	5b	6a	6b	7a
001	000	001	001	000	001	000	000	001	000
010	010	011	010	011	010	011	010	011	011
021	021	020	020	021	021	020	021	020	021
101	100	101	100	101	100	101	101	100	101
110	110	111	111	110	111	110	111	110	110
121	121	120	121	120	120	121	120	121	120
200	201	200	200	201	200	201	201	200	200
211	211	210	211	210	211	210	211	210	211
220	220	221	221	220	220	221	220	221	221
300	301	300	301	300	301	300	300	301	301
311	311	310	310	311	310	311	310	311	310
320	320	321	320	321	321	320	321	320	320

Table 2.1 (continued)

REPLICATION (SUBJECT)				
7b	8a	8b	9a	9b
001	000	001	001	000
010	011	010	011	010
020	020	021	020	021
100	101	100	100	101
111	110	111	110	111
121	121	120	121	120
201	200	201	201	200
210	211	210	211	210
220	220	221	220	221
300	301	300	300	301
311	310	311	310	311
321	321	320	321	320

were presented and the pilot's detection performance was monitored. Each pilot flew six additional approaches in which no failure occurred. These approaches were randomly interspersed among the twelve failure approaches. No failure detection data were obtained from these approaches, of course, but records of these runs were kept for identification of possible loading effects of the subsidiary task, when present, by means of analysis of variance of RMS tracking errors.

The data which were obtained in these experiments were processed off-line by a package of statistical computer programs, UCLA BMD. The methods of analysis are described in detail in Chapter IV of this thesis.

2.8 Procedure

2.8.1 Familiarization and Training

Each pilot was first briefed in general terms about the purpose of this research, and after he filled out a personal data questionnaire (Appendix C) he proceeded to the simulator.

The subject was familiarized with the instruments and with the various controls, levers and switches. He was shown an approach plate for runway 4R at Logan on which the initial aircraft position

and heading were indicated by an arrow (Figure 2.8), and the approach procedures were explained to him: the subject was told that all approaches began at the same position, 12 miles from the runway threshold, one mile to the left of the localizer course and heading of 065°, at altitude 2500 feet and airspeed 170 KIAS, with the landing gear up and flaps set at 30°. He was to capture and track the ILS approach path, lower the flaps to 40° when the glideslope deviation indicator needle started moving down and call for the landing gear and for full flaps (50°) when passing through altitude of 2000 feet. It was made clear to the subject that, as pilot-in-command, he could deviate from these guidelines at his own discretion. The experimenter was to act as a co-pilot and operate the flaps and the landing gear.

The autopilot was then coupled, the flight director was turned off and biased out of view, and the subject observed a fully automatic coupled approach to touchdown. The experimenter, in the co-pilot's seat, called out the following events: localizer alive, glideslope alive, 2000 feet, outer marker, 1000 feet, middle marker, and threshold passage (inner marker). These calls were made on all subsequent approaches.

At touchdown the CRT screen blanked out for one second and then a list was displayed (Figure 2.9) indicating to the pilot the parameters at touchdown.

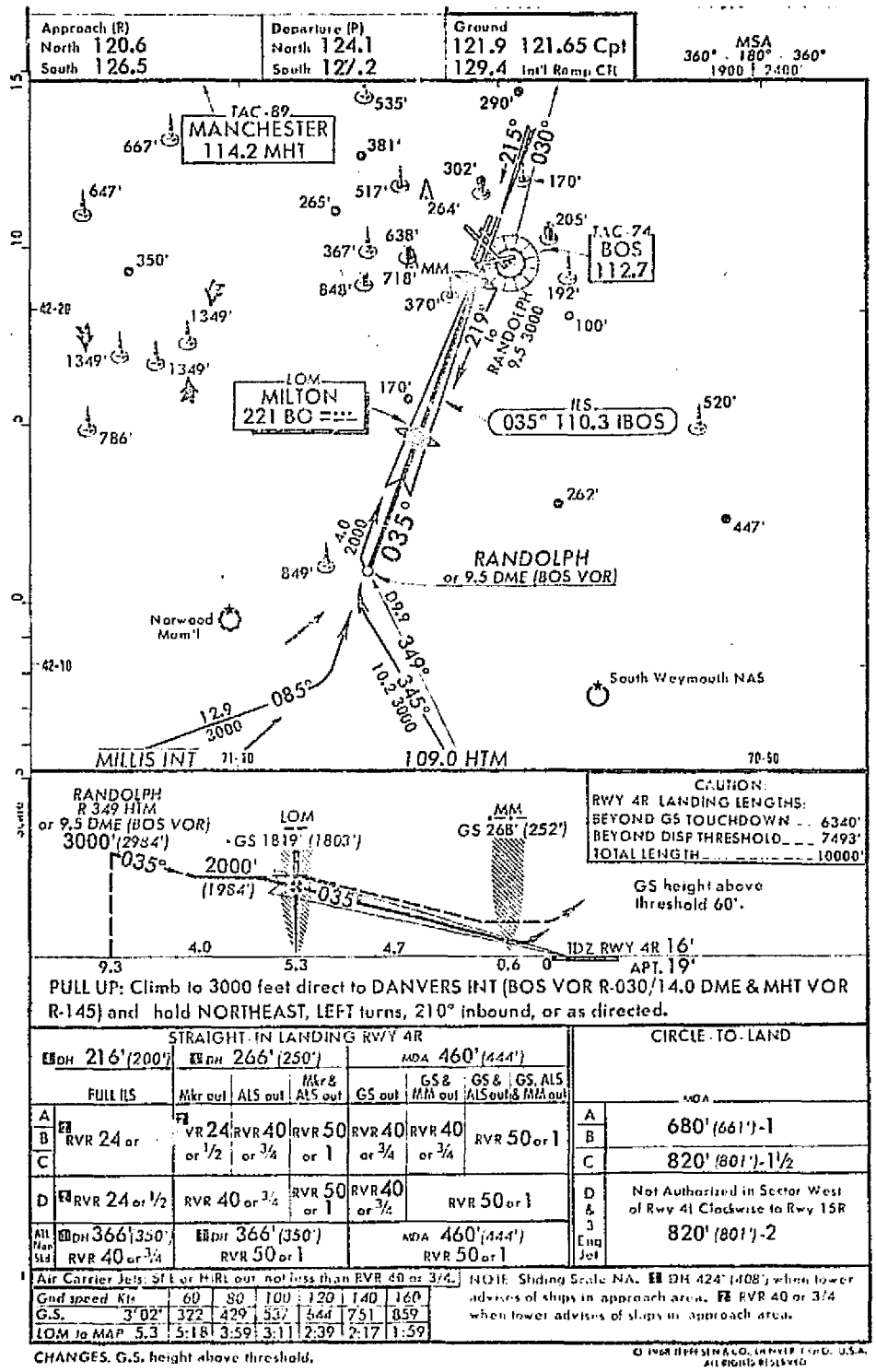

Figure 2.8 Approach Plate -- Runway 4R, Logan Airport

PARAMETERS AT TOUCHDOWN OR AT STOPACTION

DISTANCE FROM THRESHOLD	1707. FT.
DISTANCE FROM CENTERLINE	12. FT.
INDICATED AIRSPEED	127. KNOTS
VERTICAL SPEED	-178. FPM
FLARE COMMANDED AT ALT.	45.9 FT.

PITCH ANGLE	5. DEGS.
BANK ANGLE	-1. DEGS.
HEADING	35. DEGS.
GROUND TRACK	36. DEGS.
CRAB ANGLE	1. DEGS.

DT = 0.2000
DATA UPDATE RATE = 5
LOCD= 67 HITS= 73 MISS= 12

Figure 2.9 CRT Display at Touchdown

Next, the lateral autopilot was uncoupled, the flight director was turned on in the roll (LOC) mode, and the pilot flew a split-axis approach, in which he controlled the aircraft in yaw and in roll, to touchdown. The third familiarization approach was a split-axis control in pitch in which the pilot was, for the first time, in control of the power, followed by a fully manual approach.

The subject continued to fly fully manual approaches until he indicated that he was satisfied with his performance or until he flew at least two approaches which terminated in a successful touchdown, which ever occurred later. This ended the training period.

The actual experimental runs then commenced. The experiment consisted of two separate sessions, with each pilot flying fourteen approaches in the first session and sixteen approaches in the second session. Seven pilots flew the workload approaches first, followed by the failure detection runs; the order was reversed for the other eight subjects. This was done to counter-balance any possible learning effects.

Each approach lasted between five and six minutes; the first session usually lasted for about three hours, including one 20-minute break. The second session was conducted about a week or two weeks after the first, and also started with a re-training

period. Generally less practice was required, however, to reach a plateau on the learning curve and the second session lasted for about two hours, including the 20-minute break.

2.8.2 Workload Experiment

The subject was instructed in the use of the subsidiary task (see Appendix B.1), and it was emphasized to him that his primary concern at all times should be to do the best that he could on the primary task (flying the approach). To further impress upon the subject the priority of the primary task he was told that he could not elect to execute a missed approach and that each and every approach should terminate in a touchdown on the first trial. The brightness of the subsidiary task's warning lights was then adjusted by the experimenter with the subject looking at the attitude indicator, until the subject reported that he could not detect the lights in his peripheral vision. The twelve experimental runs for the record then commenced. At the end of this session, the subject was asked to answer a subjective evaluation questionnaire (see Appendix C).

2.8.3 Failure Detection

Instructions concerning the general characteristics of this experiment were read to the pilot (Appendix B.2). He was told that as soon as he detected conflicting readings or discrepancies between instruments he should call it out as a failure and specify the axis

in which he suspected the failure occurred, such as "roll failure", "lateral malfunction", "drifting off the localizer" and the like. This was done to assure that the pilot detected an actual failure and was not reporting a false alarm which may have resulted from a sudden gust or a vertical draft.

The pilot was told that his reaction time would be recorded by way of the experimenter pressing a button on the center console. The experimenter held his hand over the button throughout the approach on every approach, including the ones in which no failure was to occur, to minimize delay-times and to avoid cueing the subject inadvertently.

The pilot was told that following a correct identification, the malfunctioning system would be disconnected by the experimenter and it would be up to him to decide whether to continue the landing or to execute a missed approach, which consisted of calling for a go-around and establishing a positive rate-of-climb, at which point the run was terminated by the experimenter.

FAA regulations or company policy concerning the termination of an approach were not to be adhered to. The pilots were to use their own judgement, the decision-criterion being the probability of an acceptable landing. If they thought that they could complete the landing following a malfunction, the pilots were to do so;

if, in their judgement, an acceptable touchdown was precluded, they were to initiate a go-around.

The flight-director operated only in the axes which were controlled manually. The matrix of control modes following a failure is given in Table 2.2.

2.9 Pilot Subjects

A total of twenty qualified pilots participated in this research. Of these, four pilots - two airline captains and two MIT personnel - assisted in the preliminary phases of simulator validation, flight parameters adjustment, and experimental procedures shakedown runs. Of the remaining sixteen pilots, one dropped out of the program after one session for personal reasons and fifteen pilots from Delta Airlines and Eastern Airlines - seven captains, six first officers and two second officers - flew 450 approaches for the formal experiments. These pilots' personal data are summarized in Table 2.3.

All of the pilots were volunteers who had an interest in the program and who participated in the experiments in their free time. They did not receive any payment for their participation.

Table 2.2 Control Modes Following a Failure

	FAILURE	
	Autopilot	Flight Director
Fully Automatic	Autopilot disconnected, flight-director coupled in failed axis	---
Split Axis	Autopilot disconnected, flight-director coupled in failed axis	Flight-director disconnected, pilot reverts to raw data in failed axis
Fully Manual	---	Flight-director disconnected, pilot reverts to raw data in failed axis

Table 2.3 Pilot Background Data

PILOT	AGE	POSITION	CURRENT EQUIP.	FLIGHT EXPERIENCE, HOURS					FLIGHT DIRECTORS*		
				COMMERCIAL		MILITARY		OTHER			
				JET	RECIP.	JET	RECIP.		CP	RB	O
2b	38	F/O	DC-9	5000	1500			1500	✓	✓	
3a	56	Captain	B727	5000	15000		2000	550	✓	✓	
3b	32	Captain	B727	4000	1000			2000	✓	✓	
4a	33	F/O	B727	2200	300			550	✓	✓	
4b	39	Captain	DC-9	5000	5000				✓	✓	
5a	41	F/O	B727	3300				250	✓	✓	
5b	62	Capt(ret)	DC-9#	7000	18000		5000	1200	✓	✓	
6a	55	Captain	B727	9500	16500		1500	850	✓	✓	
6b	35	S/O	B727	400		1500	150	500	✓		
7a	32	F/O	Electra	300	2000	1000		250		✓	
7b	40	Captain	DC-9	5500				3500	✓	✓	
8a	30	S/O	B727	1000		1500	300	400	✓	✓	✓
8b	32	Captain	B727	5000				3000	✓	✓	
9a	28	F/O	B727	300			600	3100		✓	
9b	31	F/O	B727	4000				350	✓	✓	
Mean	39			3800	7400	1300	1600	1800			

*CP=cross-pointers (Sperry); RB=roll-bars (Collins); O=other (Litton)
#equipment flown prior to retirement

The total flight experience of the pilots who participated in the experimental phase of the research ranged from 2,550 hours to 31,200 hours, with a median of 6,000 hours. Twelve pilots had accumulated 10,000 hours or less, with a median of 4,200 hours; three pilots had more than 22,000 hours each, with a median of 28,350 hours.

This experience had been accumulated in commercial jets such as B707, B727, DC8, DC9, FH227 and CV880; reciprocating commercial aircraft such as DC3, DC4, DC5, DC6, DC7, CV240, CV340 and CV440; military jets such as F4, A6, T33 and T37; military propellor-driven aircraft such as O-1, T41, T42 and an assortment of World War II aircraft; and various light fixed- and rotary-wing airplanes.

All pilots, with one exception, had had experience with integrated-cue flight directors such as the Collins FD105 and FD109. With the exception of subject 5b, all pilots had flown numerous ILS approaches in the six-month period immediately preceeding the first experimental session, the most recent ILS approach having been within two weeks or less.

CHAPTER III

DATA AND RESULTS

3.1 Description of the Records

Data were accumulated during each run and throughout the run. They were initially stored in arrays in the computer's memory; at touchdown, which automatically terminated the run, or when the experimenter manually terminated the run after initiation of a missed approach, all the data of that run were copied into data files and stored on a disk. At the end of a session, all the data files of that session were also copied onto magnetic tapes. In all, about 1500 data files were accumulated.

The measurements which were taken on-line are reported in Section 2.6 of this thesis. A sample output record is shown in Figure 3.1.

3.2 Workload

Both raw and normalized workload scores (Section 2.6.2) were analyzed. The frequency distribution of the raw workload scores of

```
RUN CODE: JH113
PARAMETERS AT TOUCHDOWN OR AT STOPACTION:


DISTANCE FROM THRESHOLD          1936. FT.
DISTANCE FROM CENTERLINE          -88. FT.
INDICATED AIRSPEED                127. KNOTS
VERTICAL SPEED                   -143. FPM.


PITCH ANGLE          6. DEGS.
BANK ANGLE           1. DEGS.
HEADING             36. DEGS.
CRAB ANGLE           0. DEGS.

TIME TO DETECT       0.00 SECS.
TIME TO IDENTIFY     0.00 SECS.
```

Figure 3.1 Sample Output Record

(Continued on next 4 pages)

75 SAMPLES OF SPATIAL COORDINATES FOLLOW:

ELAPSED TIME,SECS.	X,FEET	A, FEET	Y, FEET
0.008	-71807.	2500.	-6079.
5.208	-70505.	2496.	-5318.
10.008	-69297.	2495.	-4616.
15.058	-68032.	2494.	-3878.
20.108	-66757.	2494.	-3120.
25.008	-65513.	2495.	-2379.
30.058	-64204.	2492.	-1681.
35.108	-62862.	2489.	-1080.
40.158	-61492.	2488.	-547.
45.009	-60138.	2488.	-93.
50.059	-58701.	2485.	274.
55.109	-57248.	2481.	492.
60.159	-55796.	2475.	548.
65.009	-54440.	2475.	501.
70.059	-53114.	2471.	440.
75.110	-51806.	2469.	405.
80.210	-50473.	2472.	386.
85.060	-49202.	2464.	348.
90.160	-47874.	2426.	289.
95.010	-46612.	2371.	243.
100.060	-45297.	2318.	224.
105.161	-43959.	2275.	267.
110.011	-42689.	2242.	318.
115.011	-41386.	2192.	350.
120.111	-40066.	2120.	349.
125.161	-38769.	2046.	312.
130.011	-37522.	1983.	269.
135.110	-36207.	1934.	216.
140.210	-34983.	1890.	152.
145.009	-33897.	1819.	99.
150.109	-32768.	1735.	42.
155.058	-31676.	1669.	-15.
160.157	-30556.	1619.	-54.
165.007	-29474.	1582.	-37.
170.106	-28319.	1554.	-9.
175.006	-27205.	1518.	16.
180.105	-26044.	1458.	44.
185.204	-24875.	1382.	92.
190.054	-23754.	1315.	156.
195.203	-22556.	1261.	203.
200.052	-21445.	1210.	197.
205.152	-20286.	1149.	167.
210.051	-19191.	1079.	121.
215.151	-18058.	1000.	74.
220.200	-16930.	933.	41.
225.099	-15830.	885.	23.
230.199	-14690.	841.	11.
235.048	-13607.	791.	11.
240.147	-12470.	727.	12.
245.197	-11348.	659.	0.

250.046	-10274.	592.	-6.
255.145	-9142.	529.	-11.
260.245	-8013.	474.	-15.
265.094	-6939.	424.	-13.
270.144	-5818.	370.	-1.
275.243	-4681.	314.	11.
280.092	-3599.	259.	15.
285.192	-2467.	197.	-2.
289.191	-1583.	149.	-27.
290.091	-1384.	138.	-33.
291.191	-1141.	126.	-41.
292.091	-942.	115.	-48.
293.191	-699.	102.	-57.
294.091	-500.	92.	-64.
295.190	-258.	79.	-73.
296.090	-60.	69.	-80.
297.190	182.	56.	-89.
298.090	380.	45.	-94.
299.190	622.	33.	-99.
300.090	820.	25.	-102.
301.190	1062.	16.	-102.
302.090	1260.	10.	-101.
303.189	1501.	5.	-99.
304.089	1699.	2.	-94.
305.189	1936.	0.	-88.

28 CORRECT RESPONSES FOLLOW:

X,FEET	RESPONSE T, SEC.
-70013.940	1.950
-68357.560	2.000
-67100.440	0.850
-66200.750	1.100
-63210.030	1.750
-57939.340	1.750
-54917.410	1.350
-54266.280	1.300
-50538.250	1.300
-47704.720	0.900
-37689.845	1.550
-36321.315	1.300
-35192.125	1.100
-32514.126	1.350
-30212.923	1.100
-27512.360	1.750
-25082.032	1.550
-23695.469	1.600
-20488.969	1.750
-15729.657	1.800
-14500.133	1.750
-12325.117	0.650
-9929.036	1.550
-7625.890	1.350
-6251.277	1.800
-5327.676	1.750
-3989.508	1.350
-2654.590	0.900

38 INCORRECT RESPONSES FOLLOW:

X,FEET
-64947.3
-61422.9
-59699.7
-56355.6
-54561.9
-53114.0
-52027.2
-48745.5
-46729.0
-45518.7
-44248.4
-43264.7
-41840.9
-40919.0
-39782.0
-38371.1
-33897.2
-31335.8
-29417.8
-28318.8
-26852.9
-25689.9
-24471.2
-22154.6
-21090.9
-19592.0
-18946.7
-17768.4
-16424.7
-13462.3
-11591.8
-10805.4
-8456.3
-4580.6
-1726.4
-302.1
622.0
1259.7

the 15 subjects, segregated by participation level, are shown in Figures 3.2-3.5; those of the normalized workload scores are shown in Figures 3.6-3.9.

The non-normalized workload scores ranged from 28.6 to 100.0; the normalized scores ranged from 0.0 to 100.0. Normalized workload scores as a function of the gusts' strength are shown in Figure 3.10, and as a function of the participation mode - in Figure 3.11.

We were also interested in the time-variations in the instantaneous workload levels. To this end, workload data were segregated by participation modes; mean scores were extracted at 300-feet altitude intervals between the altitudes of 2000 and 500 feet, and at 100-feet intervals between 500 feet and touchdown. The results, averaged over all pilots, are shown in Figures 3.12 through 3.15.

A measurement of each subject's evaluation of the primary and secondary task difficulty was included in our study. The questionnaire which was used (Appendix C) had four multiple-choice questions related to the overall difficulty of the primary task and two questions on the difficulty of the secondary task. Points were assigned for each answer on a zero-to-ten Cooper rating scale (Figure 3.16), with 10 indicating the greatest difficulty (Cooper and Harper, 1969). This was the same type of questionnaire that had been used in a pilot-

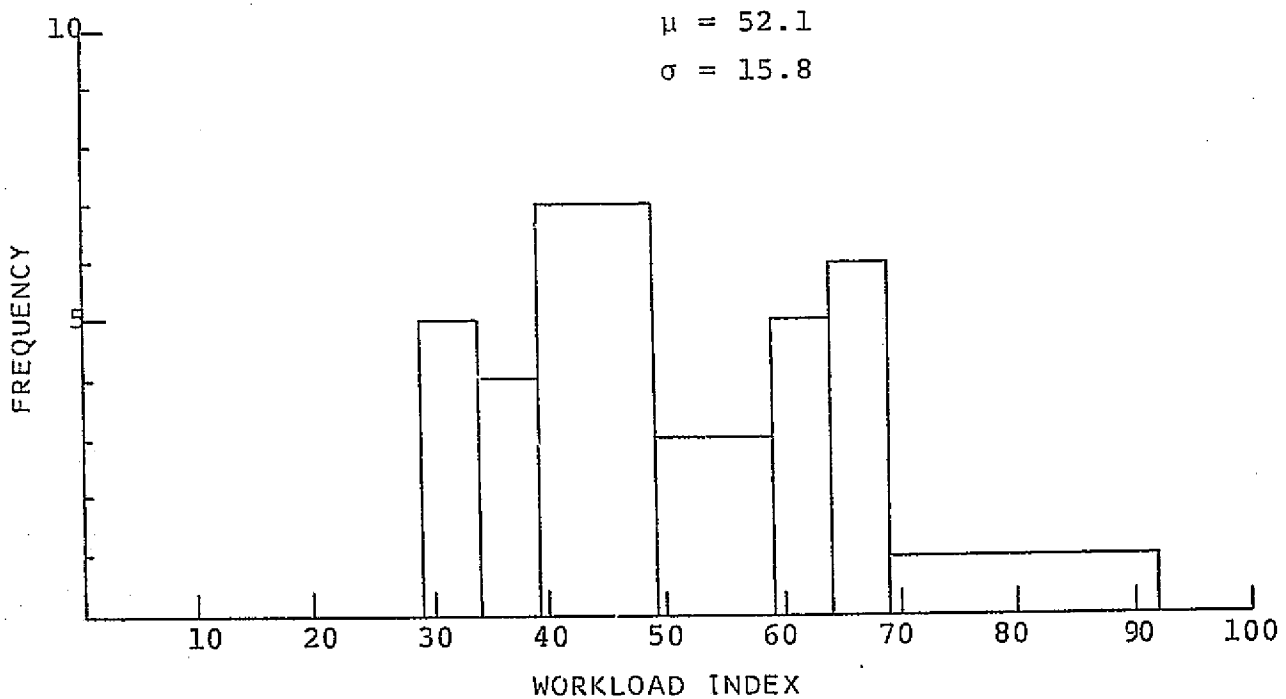

Fig. 3.2 Non-Normalized Workload Scores - Monitor

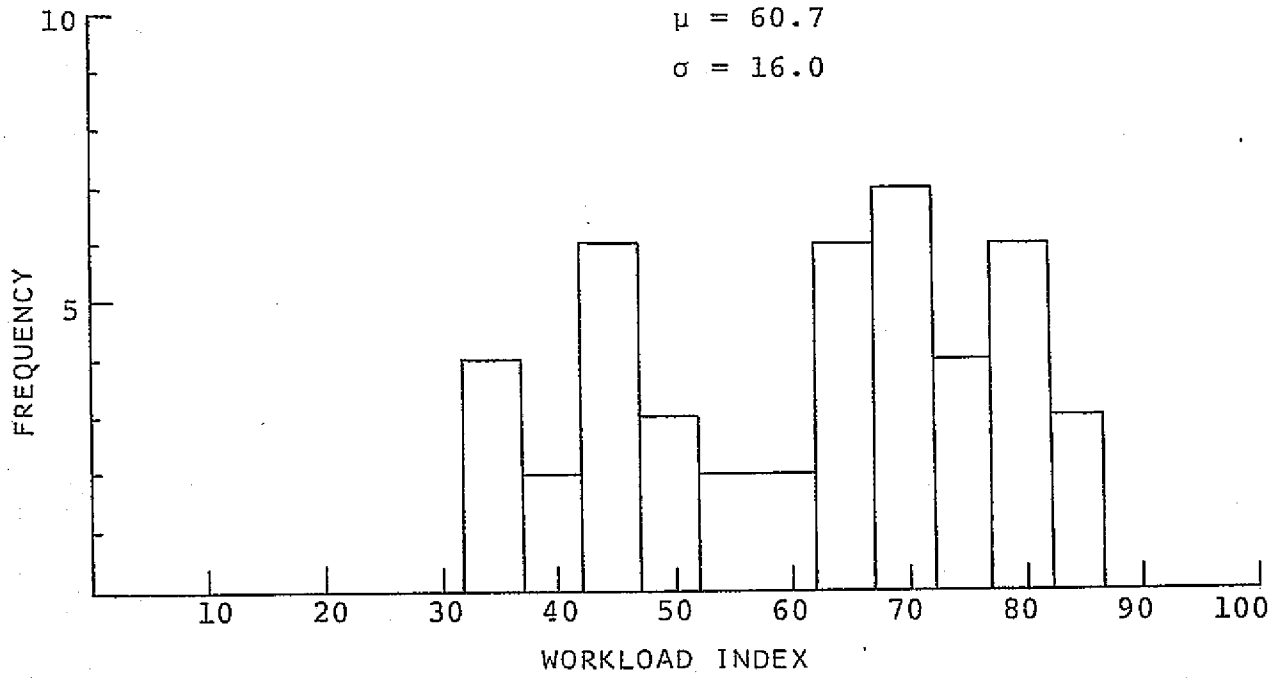

Fig. 3.3 Non-Normalized Workload Scores - Lateral Control

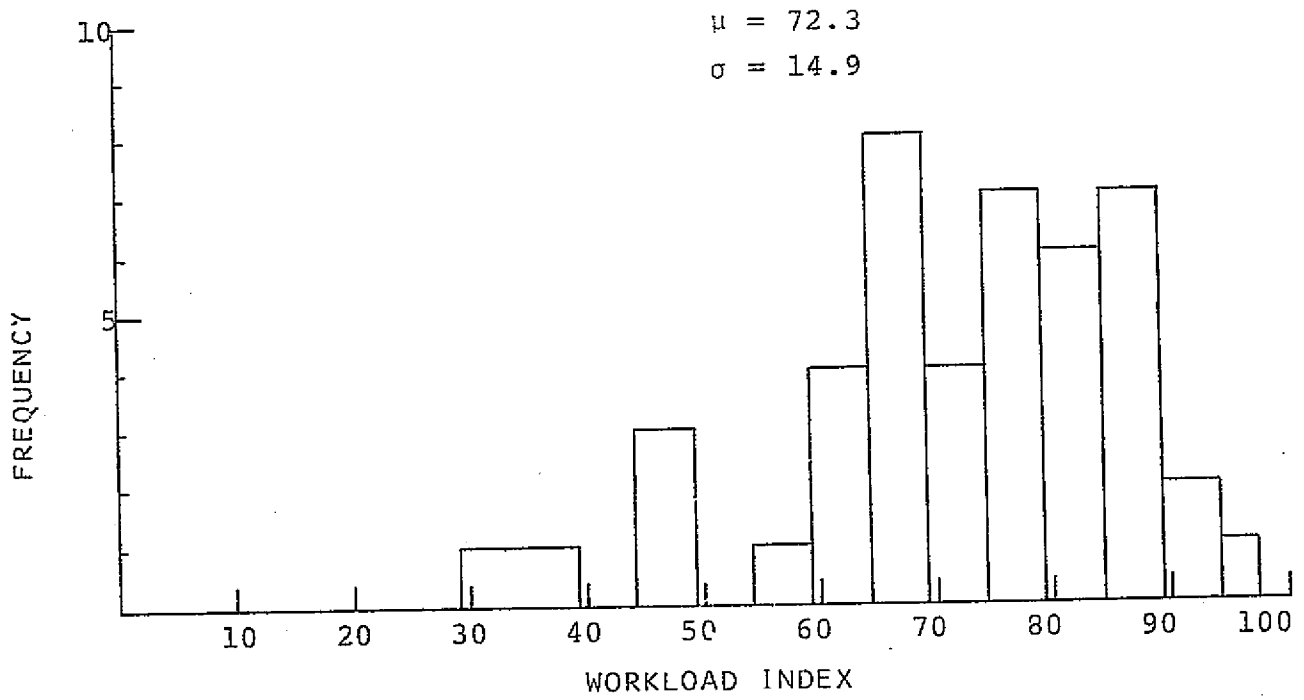

Fig. 3.4 Non-Normalized Workload Scores - Longitudinal Control

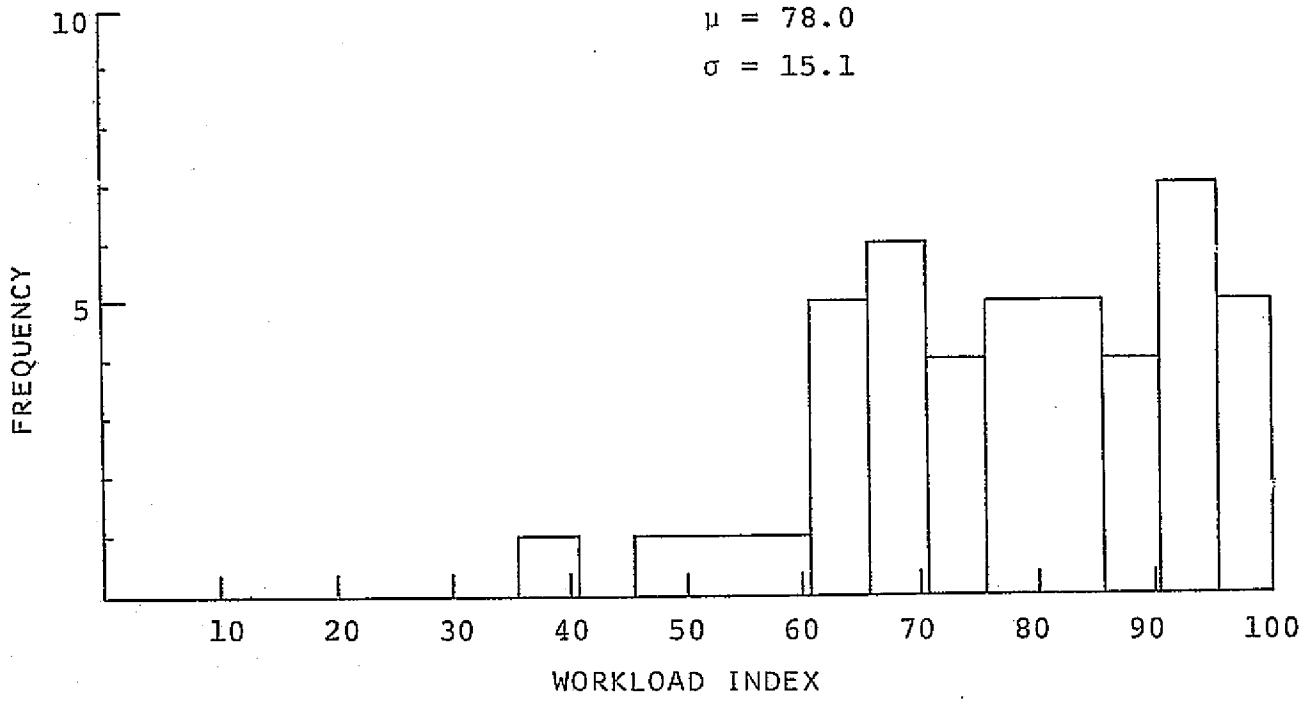

Fig. 3.5 Non-Normalized Workload Scores - Manual Control

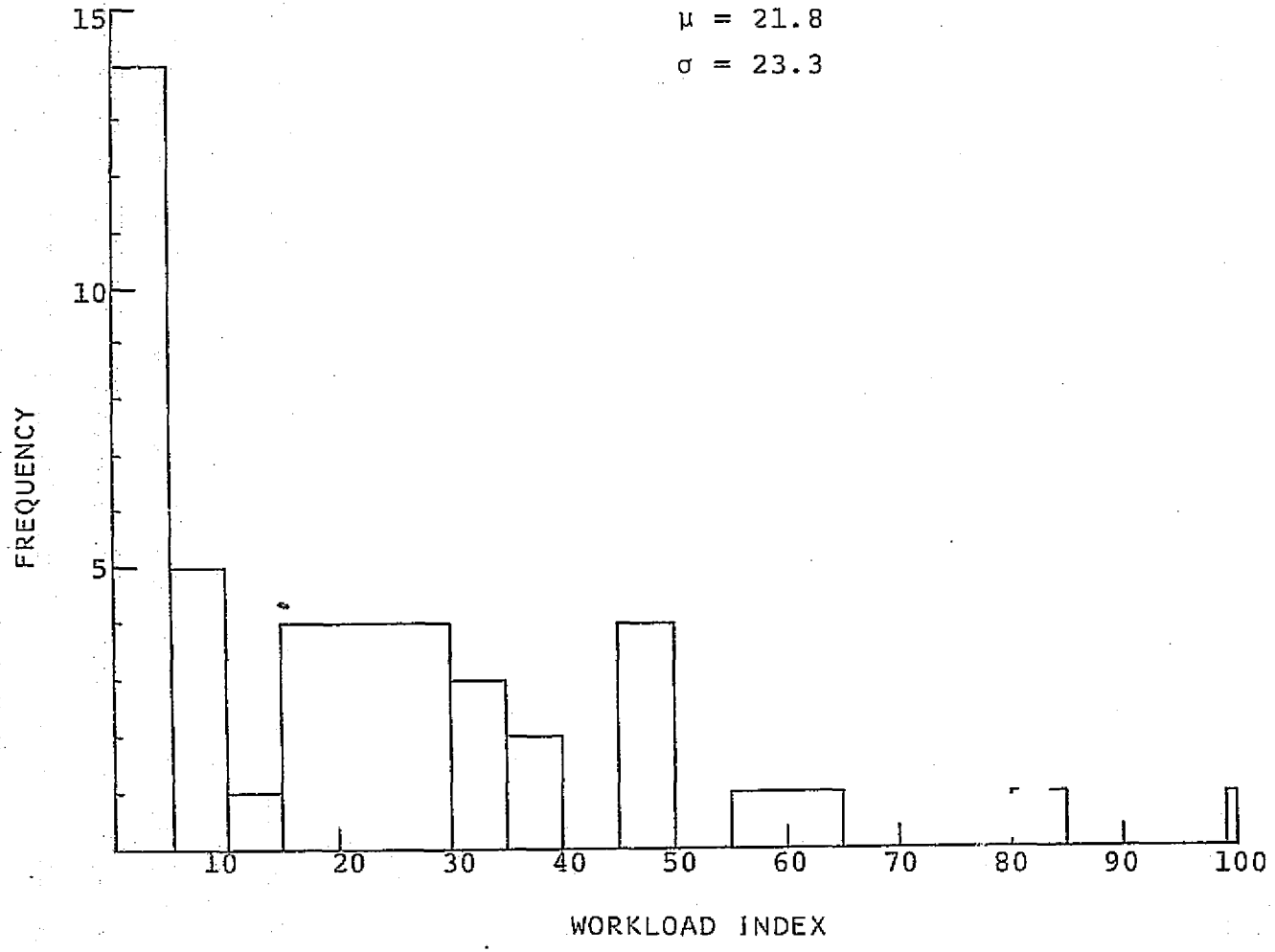

Fig. 3.6 Normalized Workload Scores - Monitor

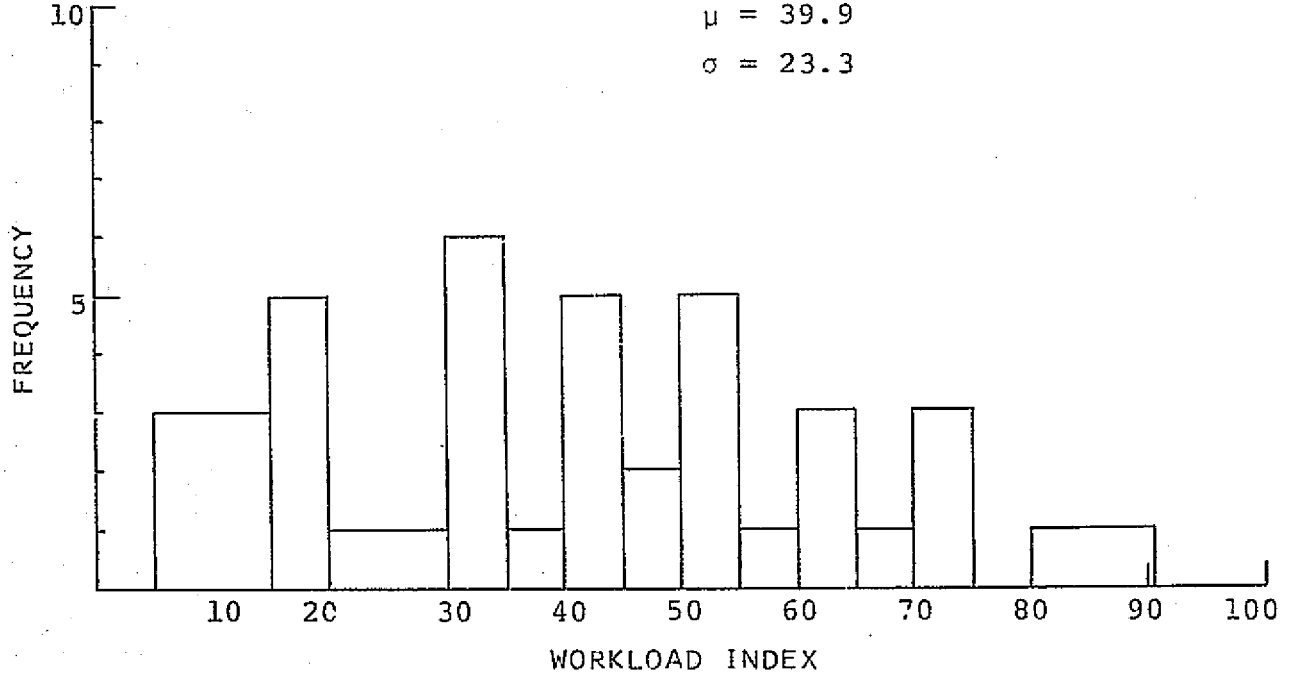

Fig. 3.7 Normalized Workload Scores - Lateral Control

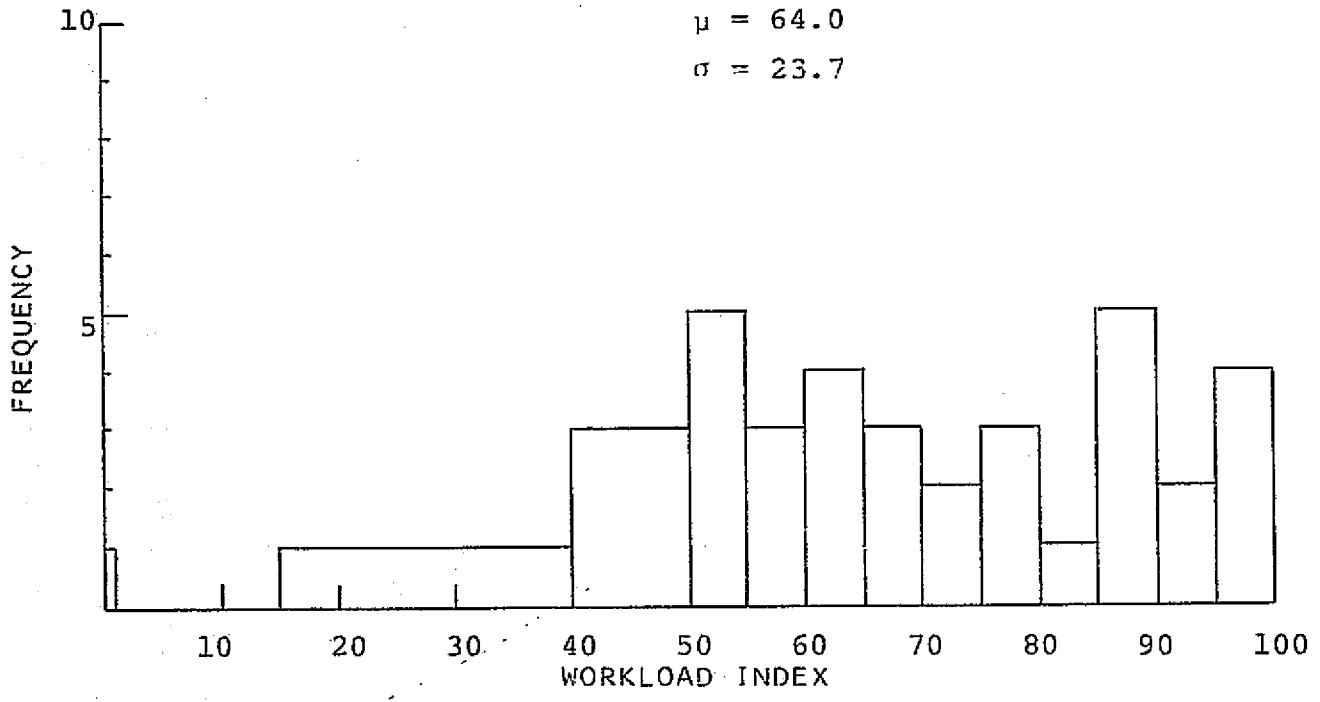

Fig. 3.8 Normalized Workload Scores - Longitudinal Control

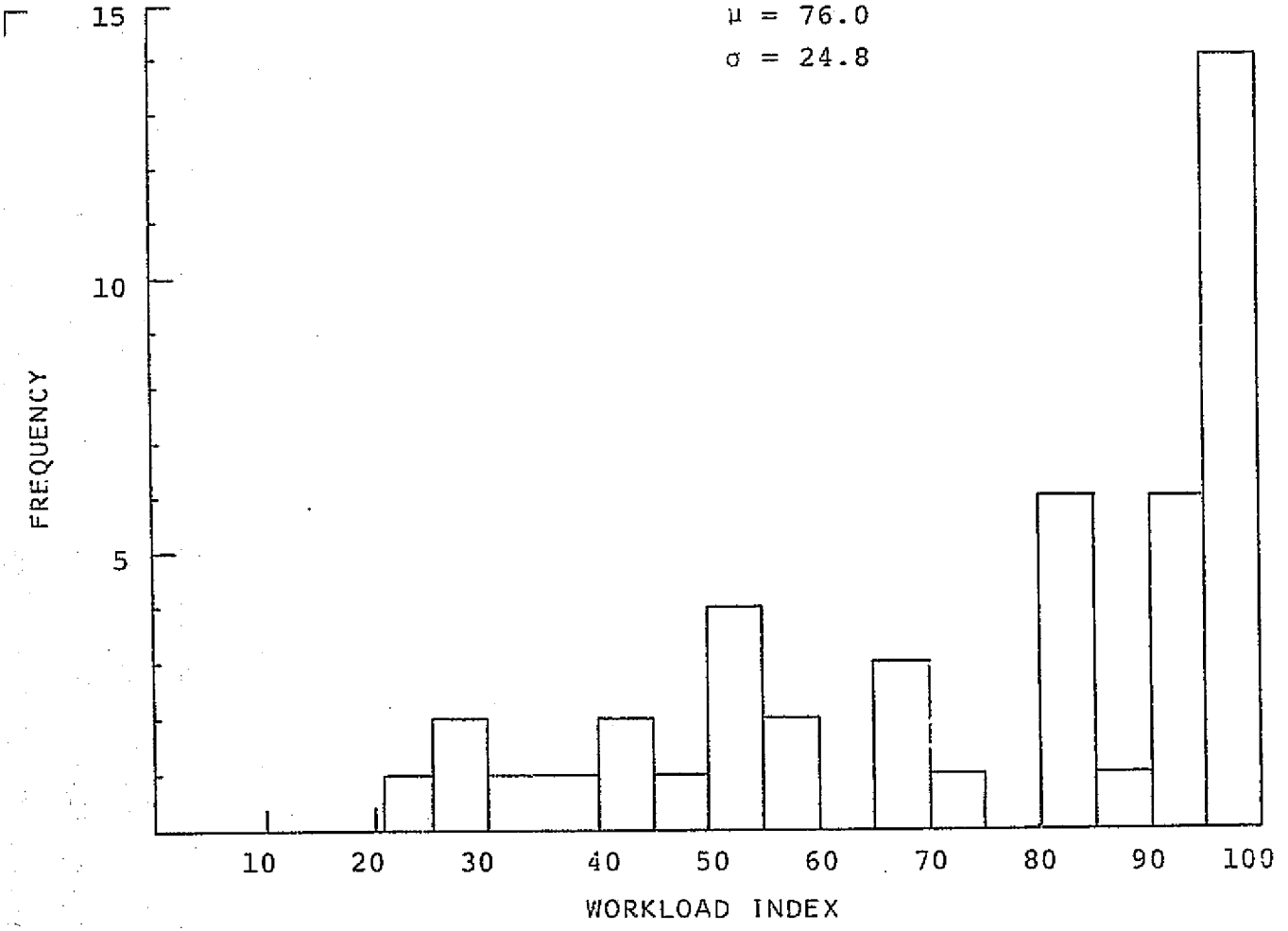

Fig. 3.9 Normalized Workload Scores - Manual Control

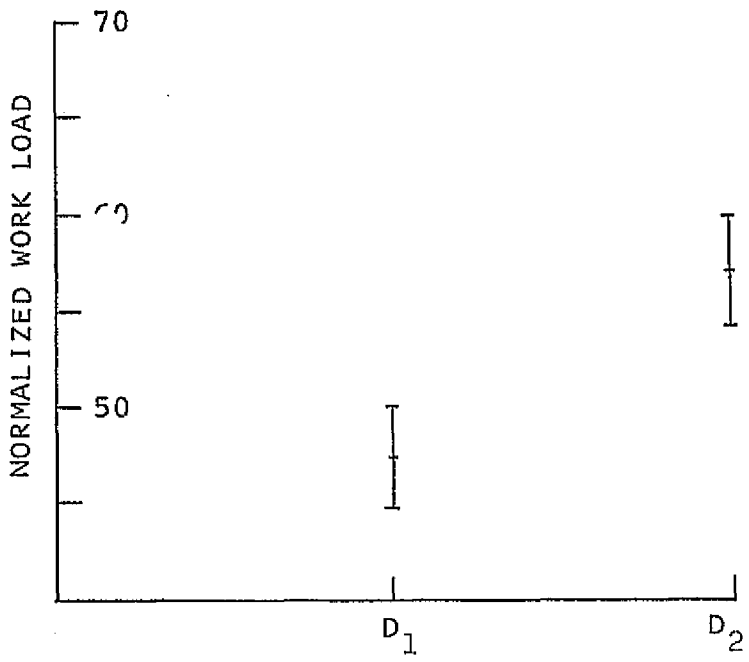

Figure 3.10

Normalized Workload Index at Two Disturbance Levels

D1 - Calm Air

D2 - 10 kt. Wind, Gusting to 30 kt.

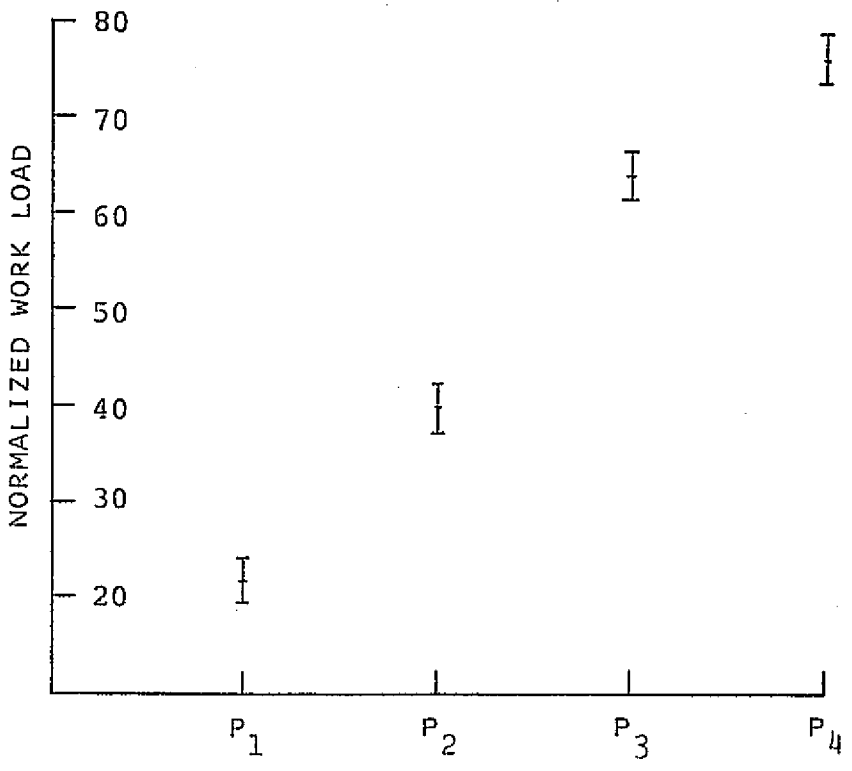

Figure 3.11

Normalized Workload Index at Four Participation Modes

P1 - Fully Automatic

P2 - Split Axis, Yaw Manual

P3 - Split Axis, Pitch Manual

P4 - Fully Manual

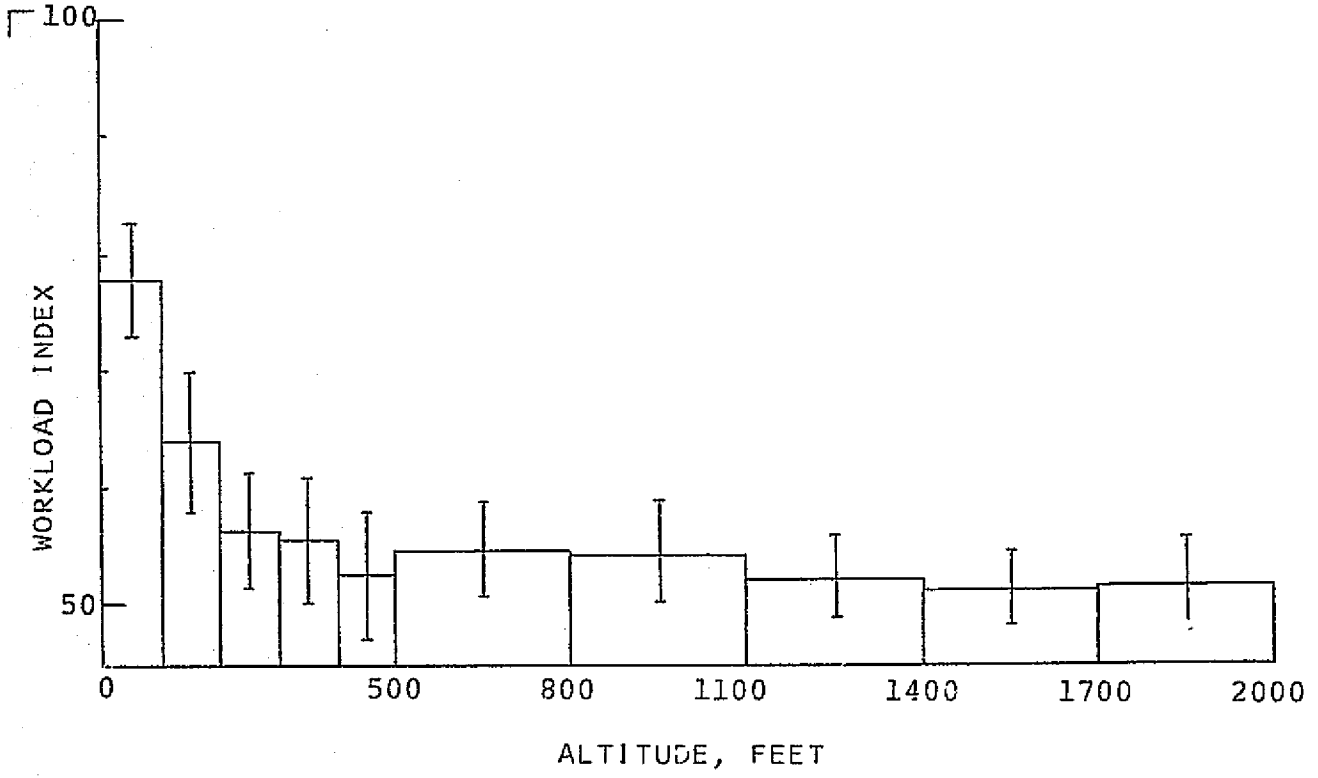

Fig. 3.12 Non-Normalized Workload Scores vs. Altitude - Monitoring

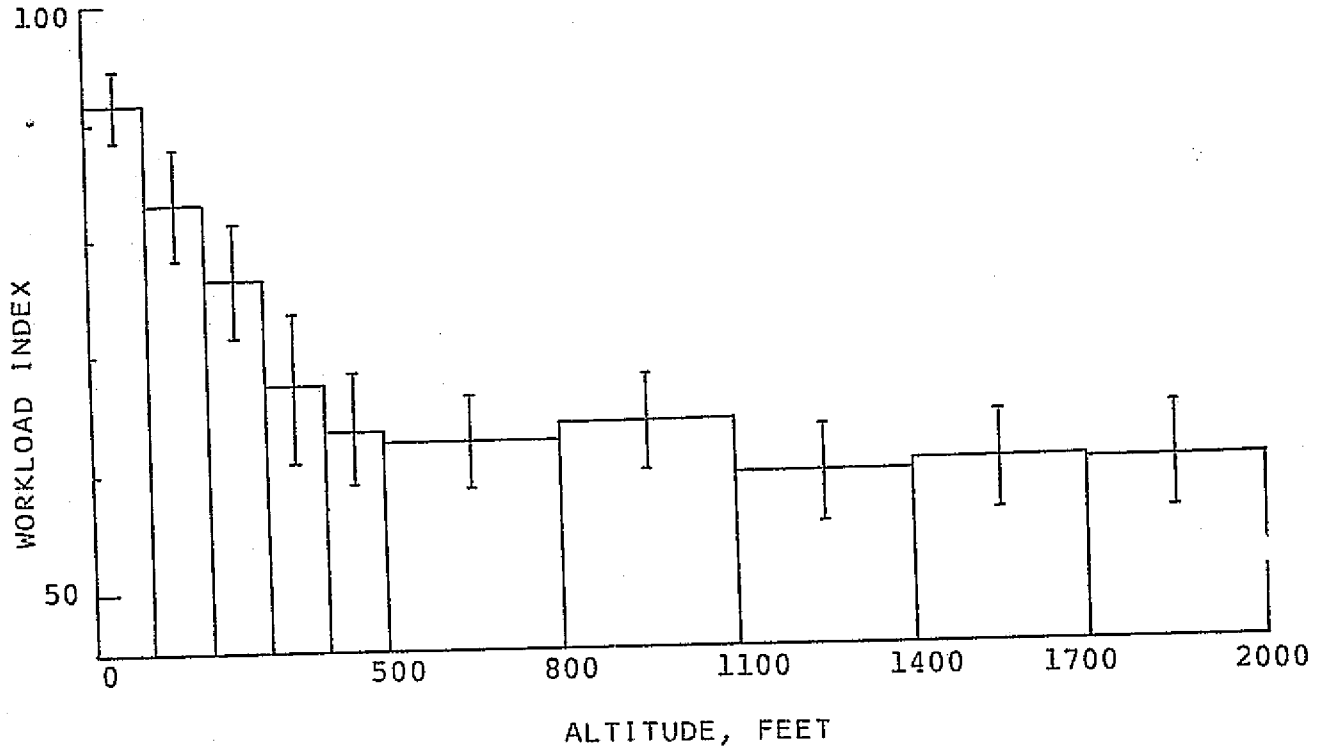

Fig. 3.13 Non-Normalized Workload Score vs. Altitude - Lateral Control

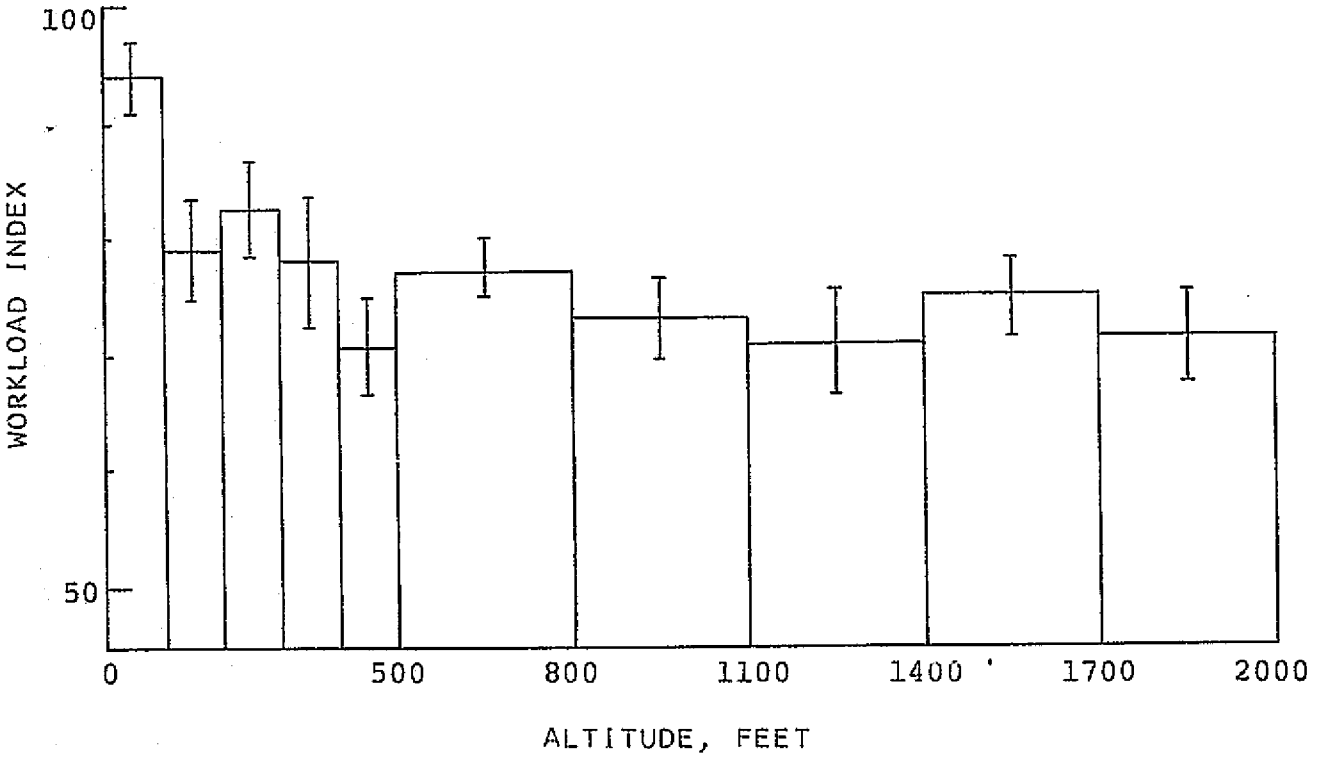

Fig. 3.14 Non-Normalized Workload Scores vs. Altitude - Longitudinal Control

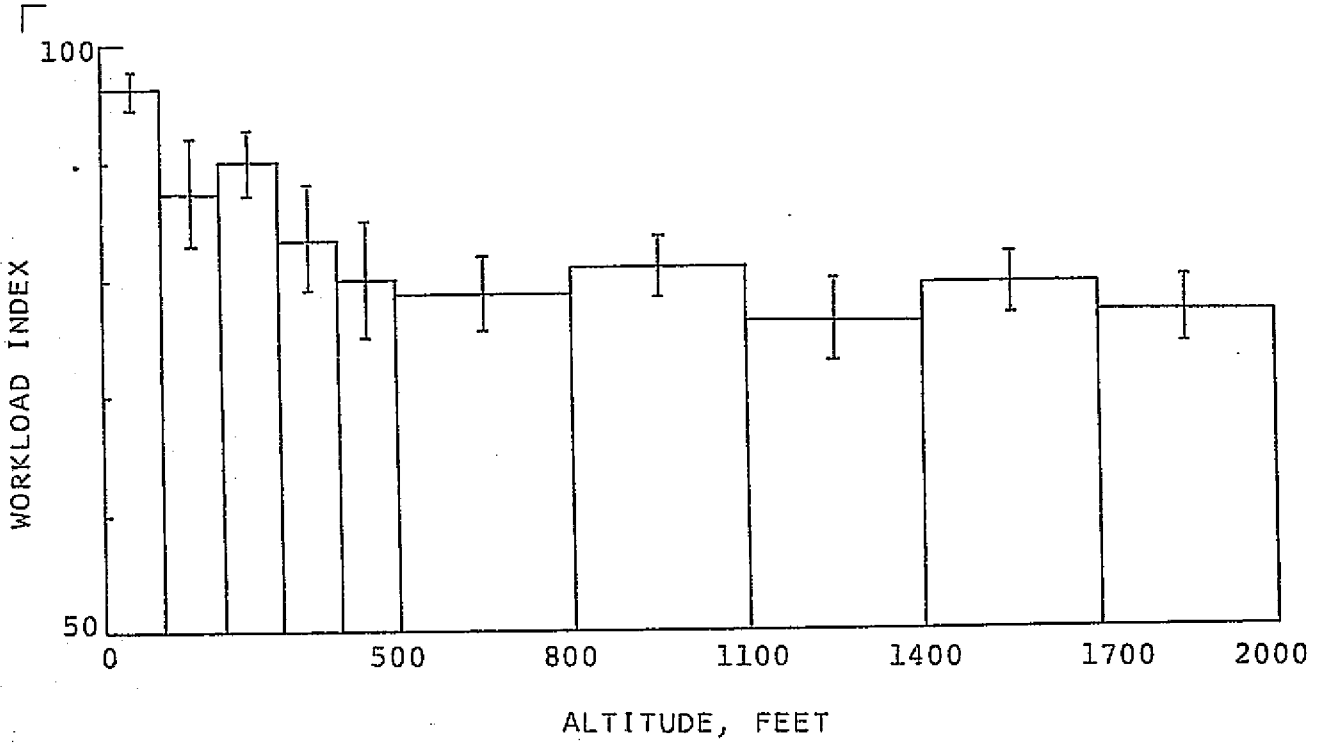

Fig. 3.15 Non-Normalized Workload Scores vs. Altitude - Manual Control

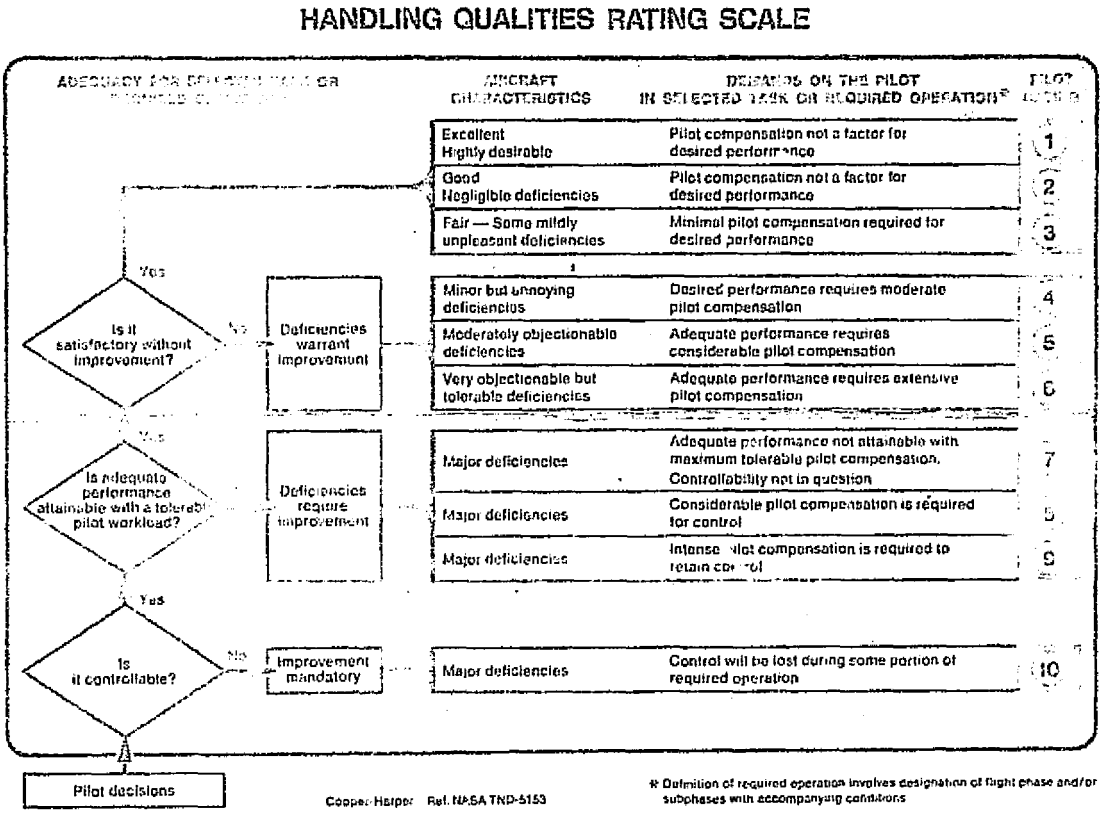

Figure 3.16 The Cooper-Harper Rating Scale

workload study conducted by Spyker *et al.* (1971). The results are shown in Figures 3.17-3.22.

3.3 Detection Performance

Detection performance was analyzed in terms of detection-time and accuracy. Detection-time was defined as the elapsed time between the occurrence of a failure and the verbal report by the subject that the failure has been detected; the subject also reported the failure-axis to insure that he reported a bona-fide failure and not a false alarm. Detection-time results are presented in Figures 3.23-3.25 for longitudinal failures and in Figures 3.26-3.28 for lateral failures.

Accuracy was measured by the fraction of failures that were missed altogether. We differentiated between approaches in which a failure went unreported but which resulted in a successful touchdown or in an error at touchdown which was unrelated to the failure (such as excessive bank, following a longitudinal failure), and approaches in which a failure was missed and which did not terminate in a successful landing because of a gross error in the failed axis. The latter are shown in Table 3.1 and 3.2; the numbers in parentheses represent the fraction of all missed failures, whether or not they resulted in a successful landing.

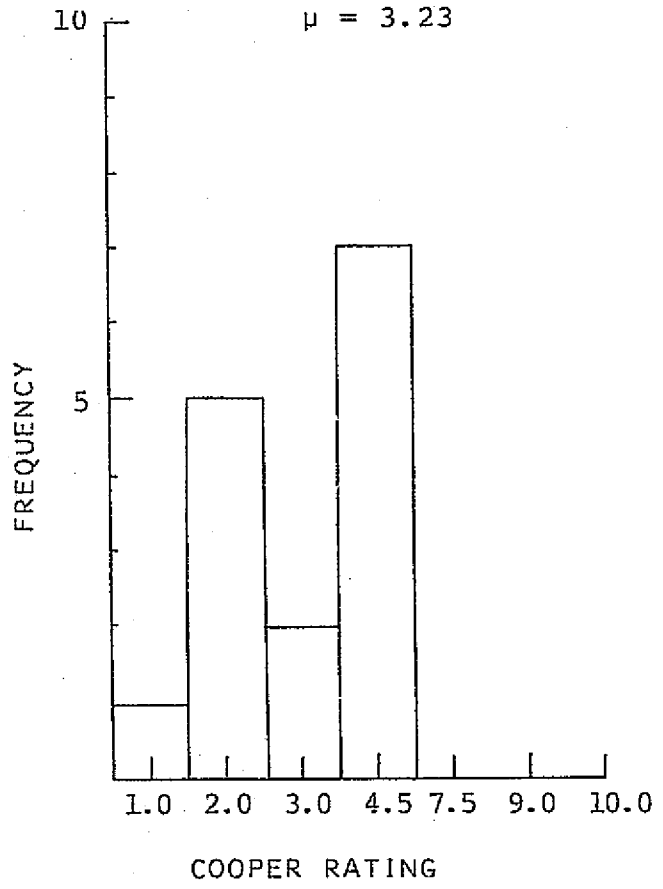

Fig. 3.17 Subjective Evaluation - Question 1

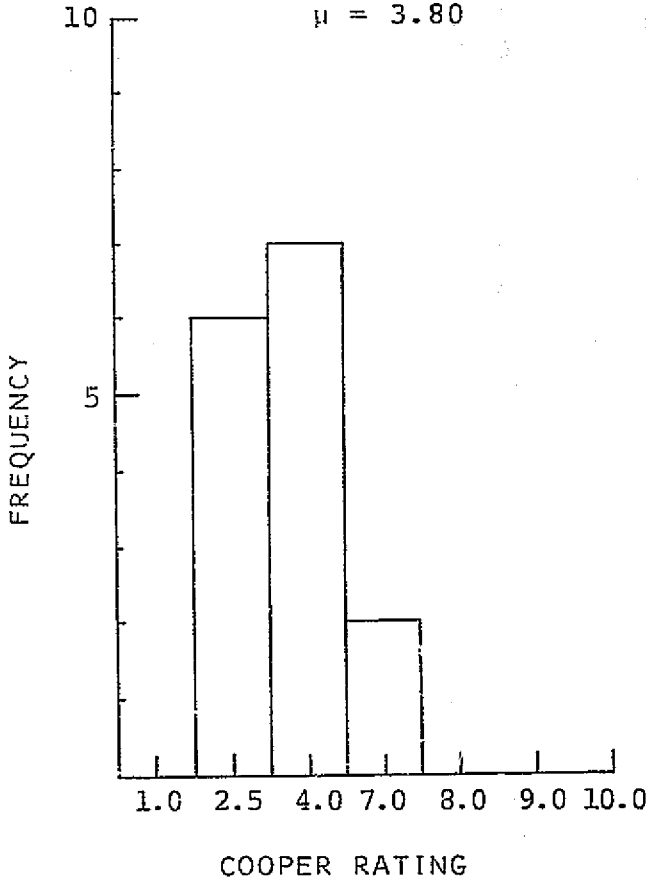

Fig. 3.18 Subjective Evaluation - Question 2

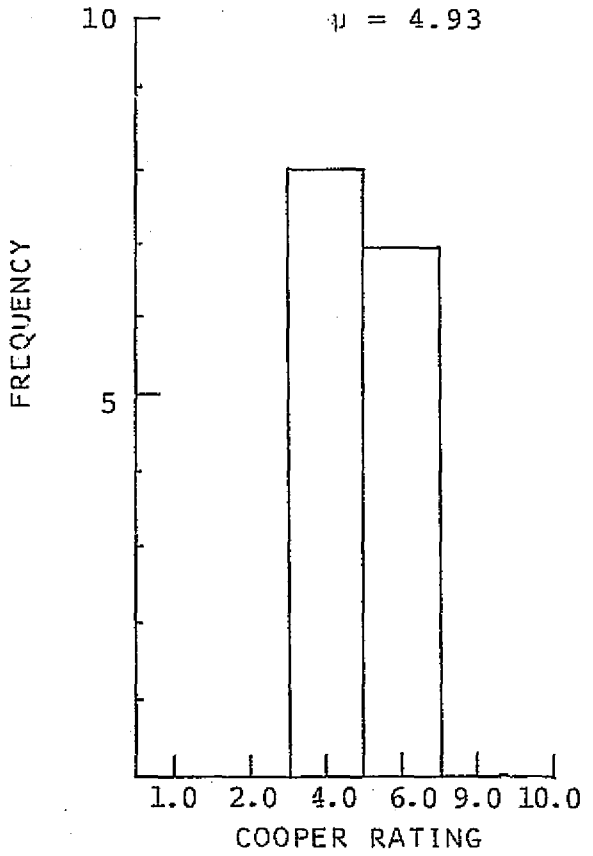

Fig. 3.19 Subjective Evaluation - Question 3

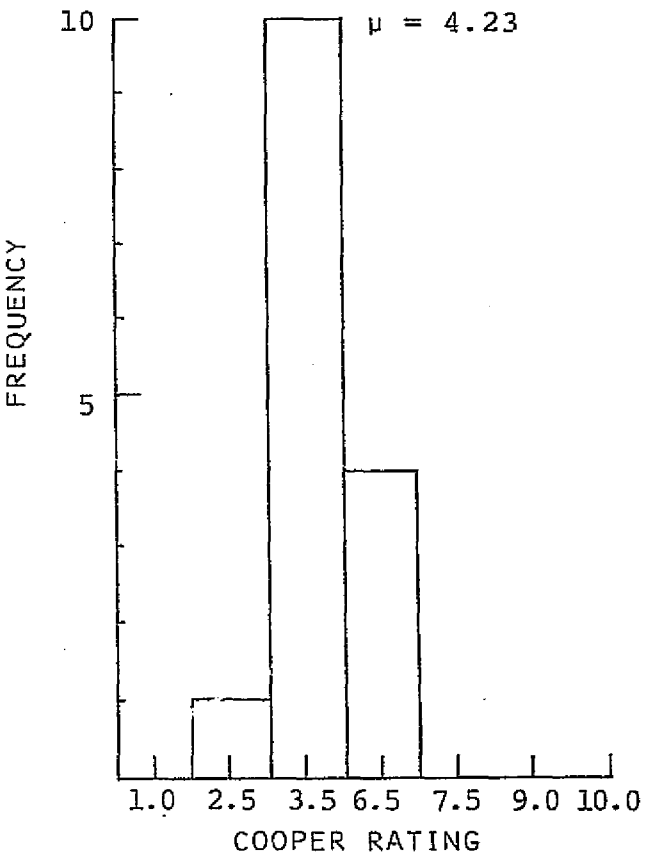

Fig. 3.20 Subjective Evaluation - Question 4

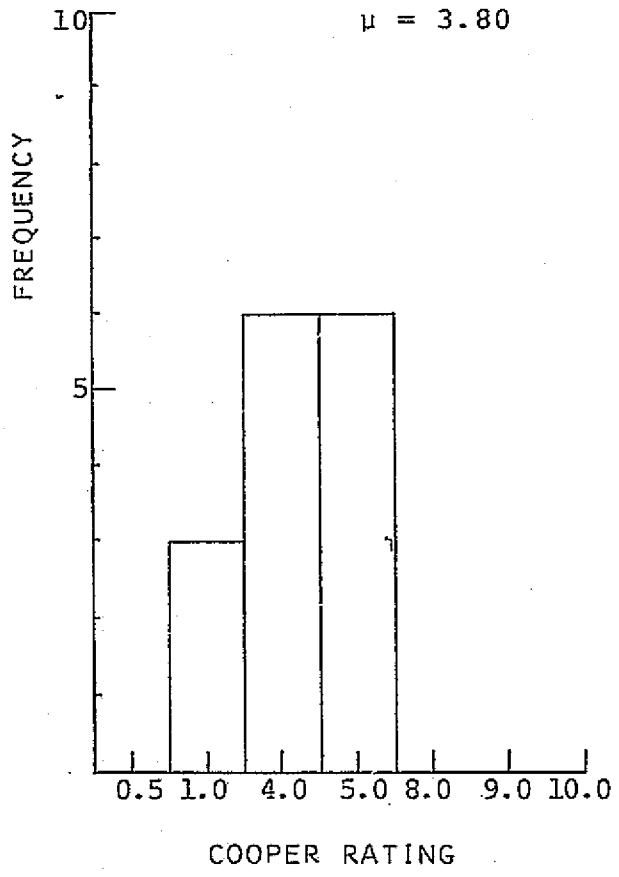

Fig. 3.21 Subjective Evaluation - Question 5

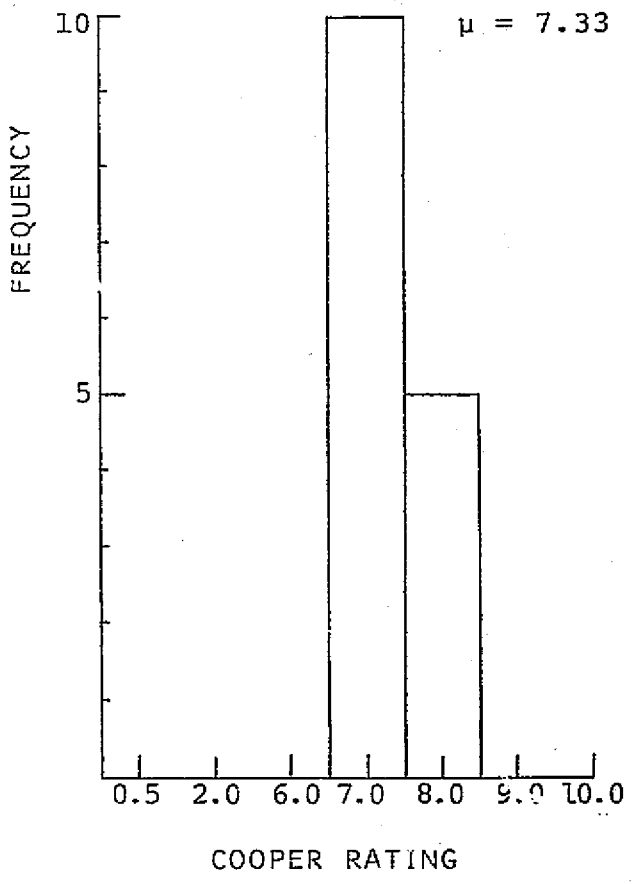

Fig. 3.22 Subjective Evaluation - Question 6

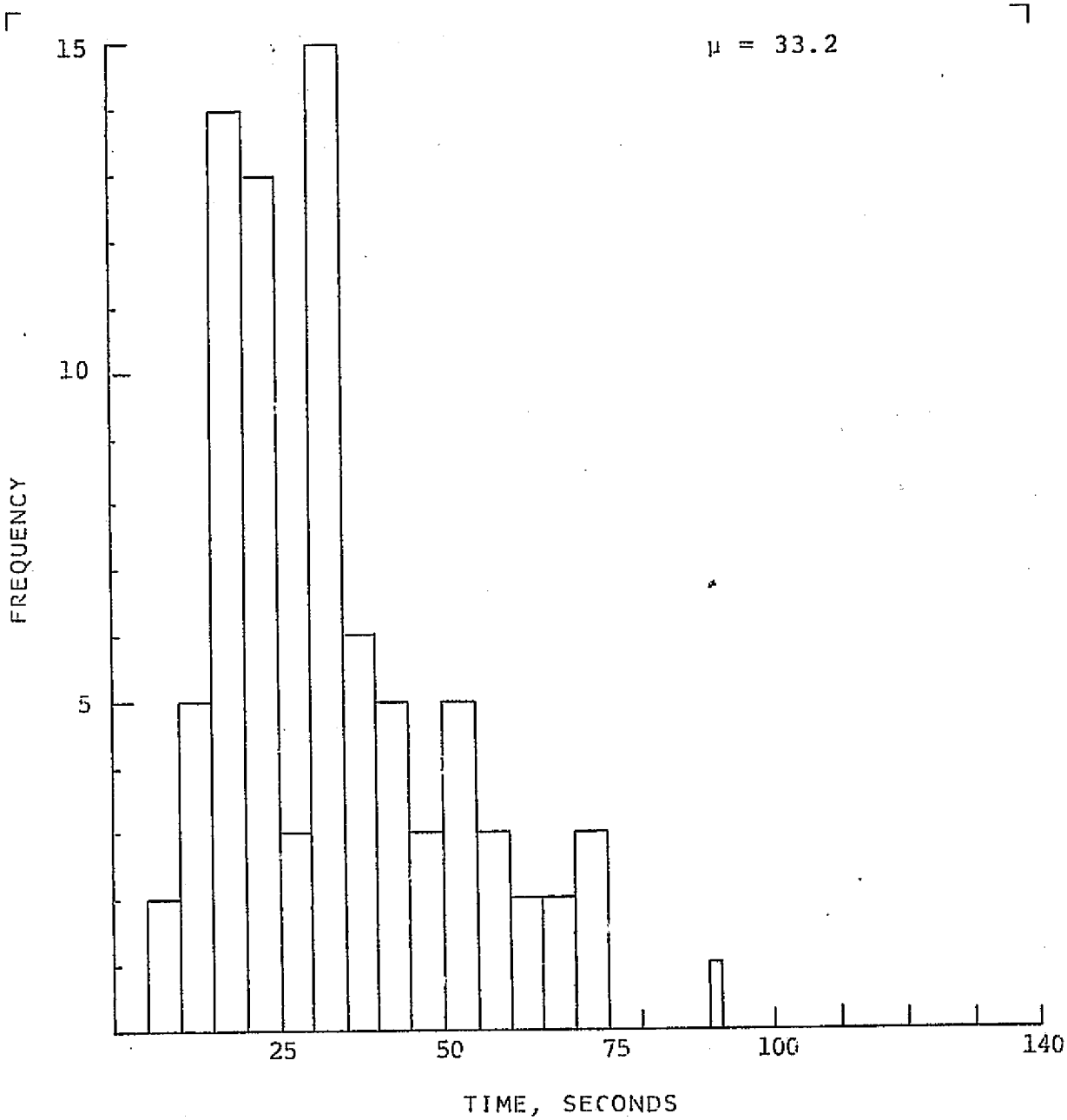

Fig. 3.23 Detection Times - Longitudinal Failures

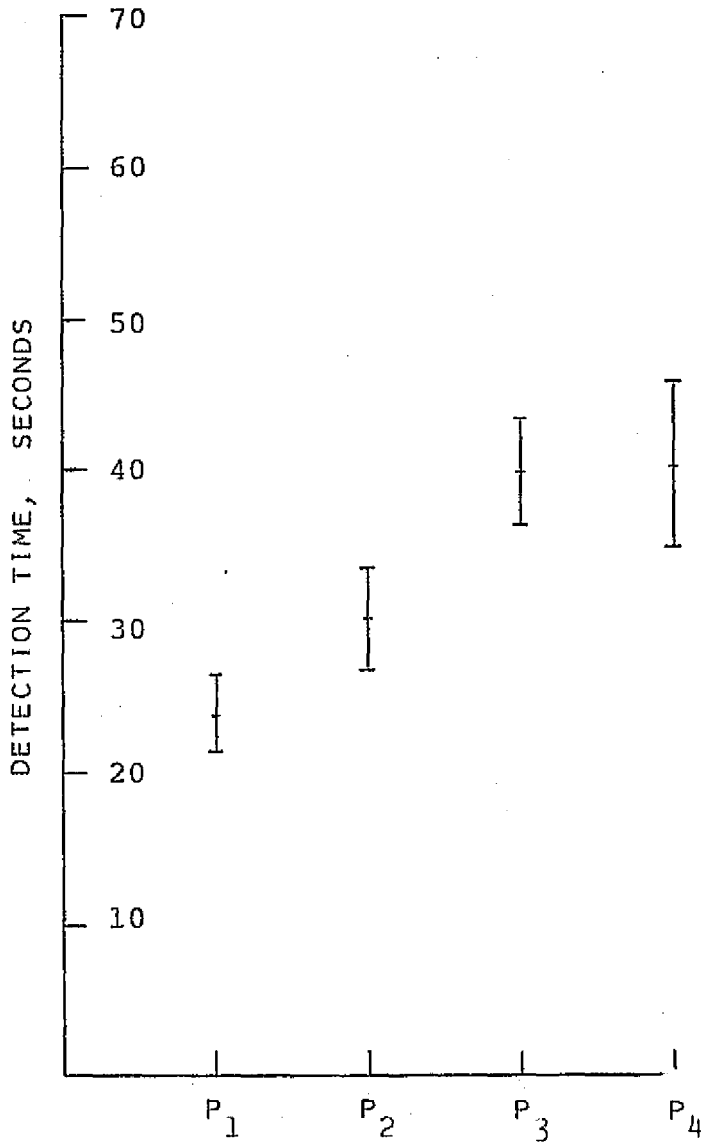

Figure 3.24

Pitch Failure Detection Times at Four Participation Modes

(See Fig. 3.11)

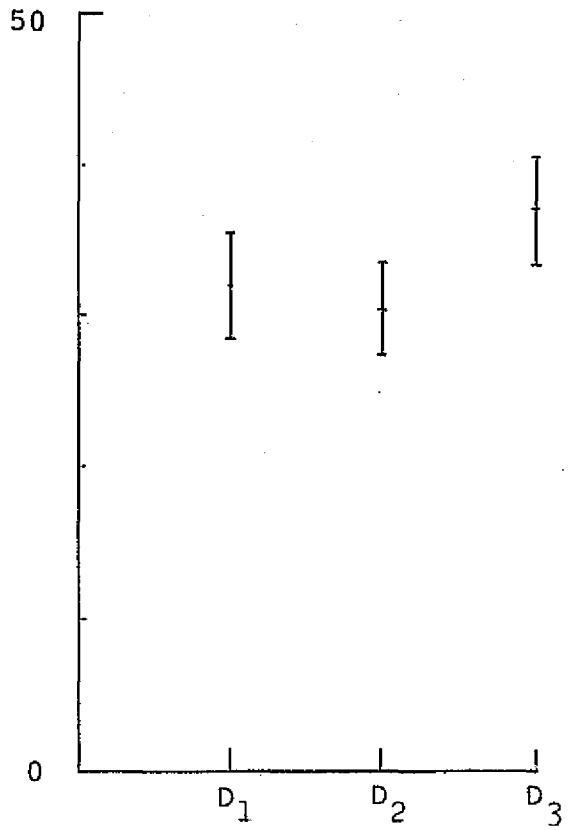

Fig. 3.25 Pitch Failure Detection Times at Three Disturbance Levels

D1 - Calm Air

D2 - 5 kt. Wind, Gusting to 15 kt.

D3 - 10 kt. Wind, Gusting to 30 kt.

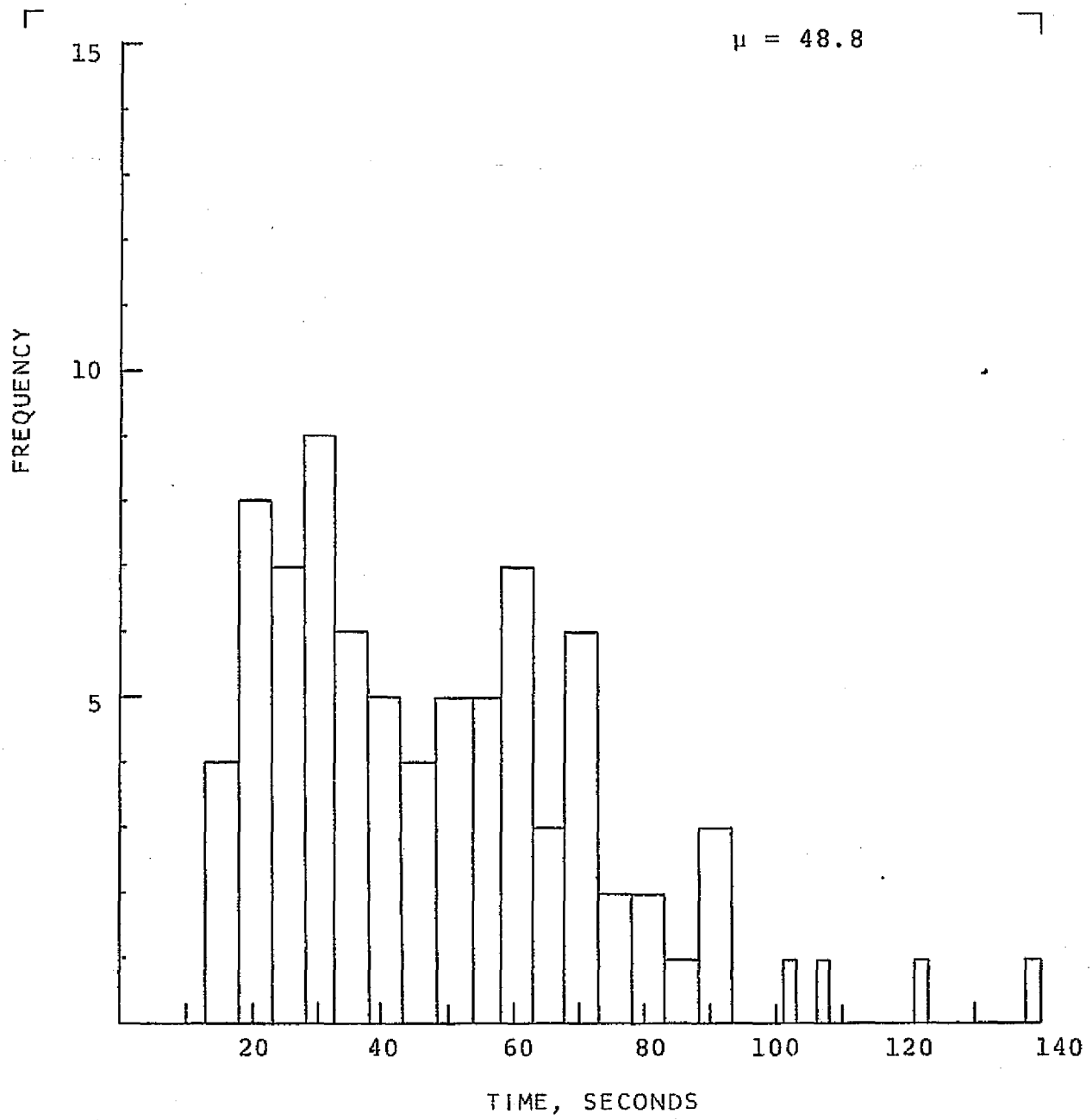

Fig. 3.26 Detection Times - Lateral Failures

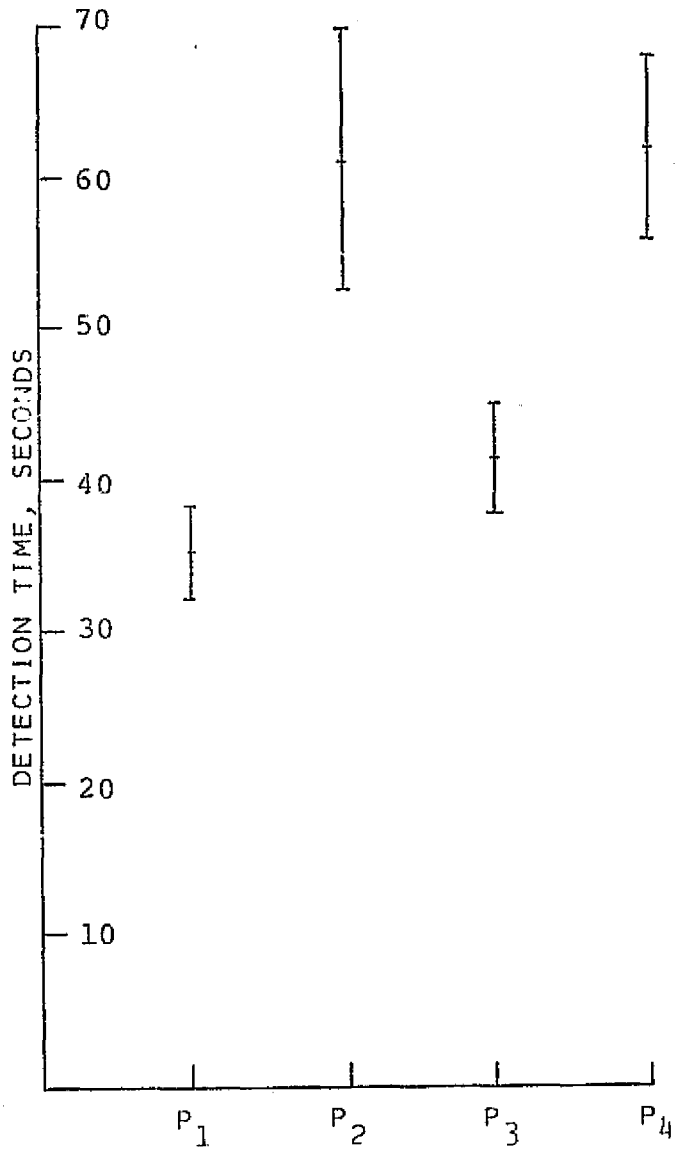

Figure 3.27

Yaw Failure Detection Times at Four Participation Modes

(See Fig. 3.11)

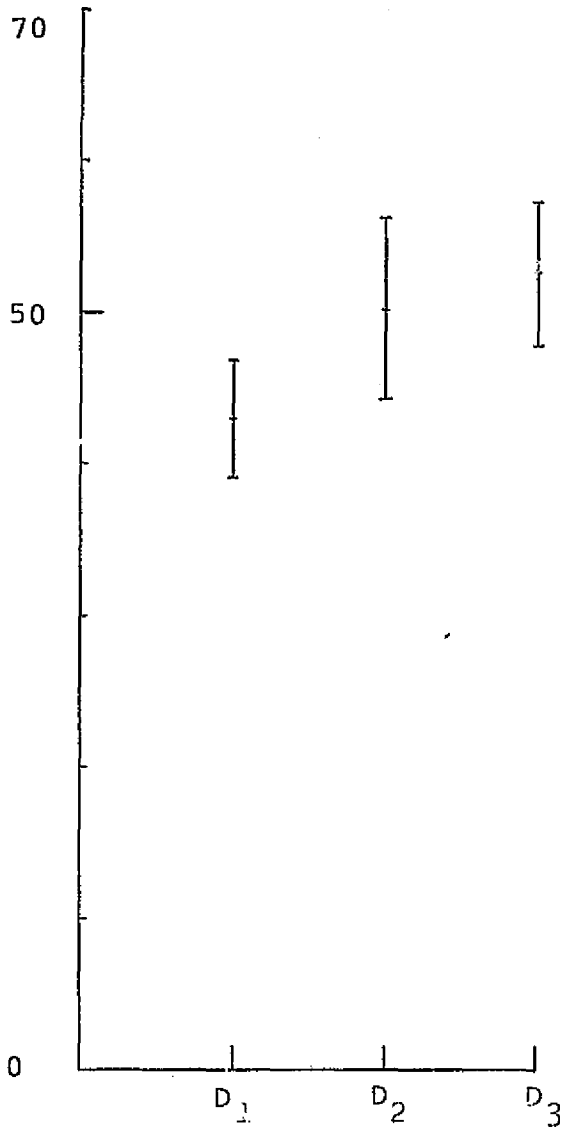

Fig. 3.28 Yaw Failure Detection Times at Three Disturbance Levels

(See Fig. 3.25)

Table 3.1

Fraction of Missed Longitudinal Failures

in percent of all longitudinal failures (in parentheses) and in percent of missed alarms resulting in gross deviations in failed axis

Participation Mode	disturbance Level			Overall
	1	2	3	
Monitor	0.	0.	0.	0.
Control Yaw	0.	0.	0.	0.
Control Pitch	12.5 (12.5)	0. (14.3)	12.5 (12.5)	8.7 (13.0)
Manual Control	0. (12.5)	14.3 (14.3)	37.5 (37.5)	17.4 (21.7)
Overall	3.3 (6.7)	3.3 (6.7)	13.3 (13.3)	6.7 (8.9)

Table 3.2

Fraction of Missed Lateral Failures

in percent of all lateral failures (in parentheses)

and in percent of missed alarms resulting in gross deviations in failed axis

Participation Mode	Disturbance Level			Overall
	1	2	3	
Monitor	0.	0.	0.	0.
Control Yaw	25.0 (37.5)	14.3 (14.3)	12.5 (37.5)	17.4 (30.4)
Control Pitch	0.	0.	0.	0.
Manual Control	14.3 (14.3)	0.	14.3 (14.3)	9.1 (9.1)
Overall	10.0 (13.3)	3.3 (3.3)	6.7 (13.3)	6.7 (10.0)

In all, 90 approaches were flown in which a longitudinal failure occurred; of these, eight went unreported, six of which did not terminate in a successful landing. Of the 90 lateral failures presented, nine were missed; of these, six did not terminate in a successful touchdown.

3.4 Touchdowns

Of the 450 approaches flown by the fifteen subjects, 389 terminated in an attempted landing. Go-arounds were initiated in 59 approaches, and data of two approaches (both fully-automatic, no-failure cases) were discarded as simulator malfunctions occurred during these approaches.

Figures 3.29 through 3.35 summarize the touchdown data. When the criteria discussed in Section 2.6 were applied to the data, only 193 landings, or about 50%, were judged as acceptable. These criteria are marked on Figures 3.29-3.35 by arrows.

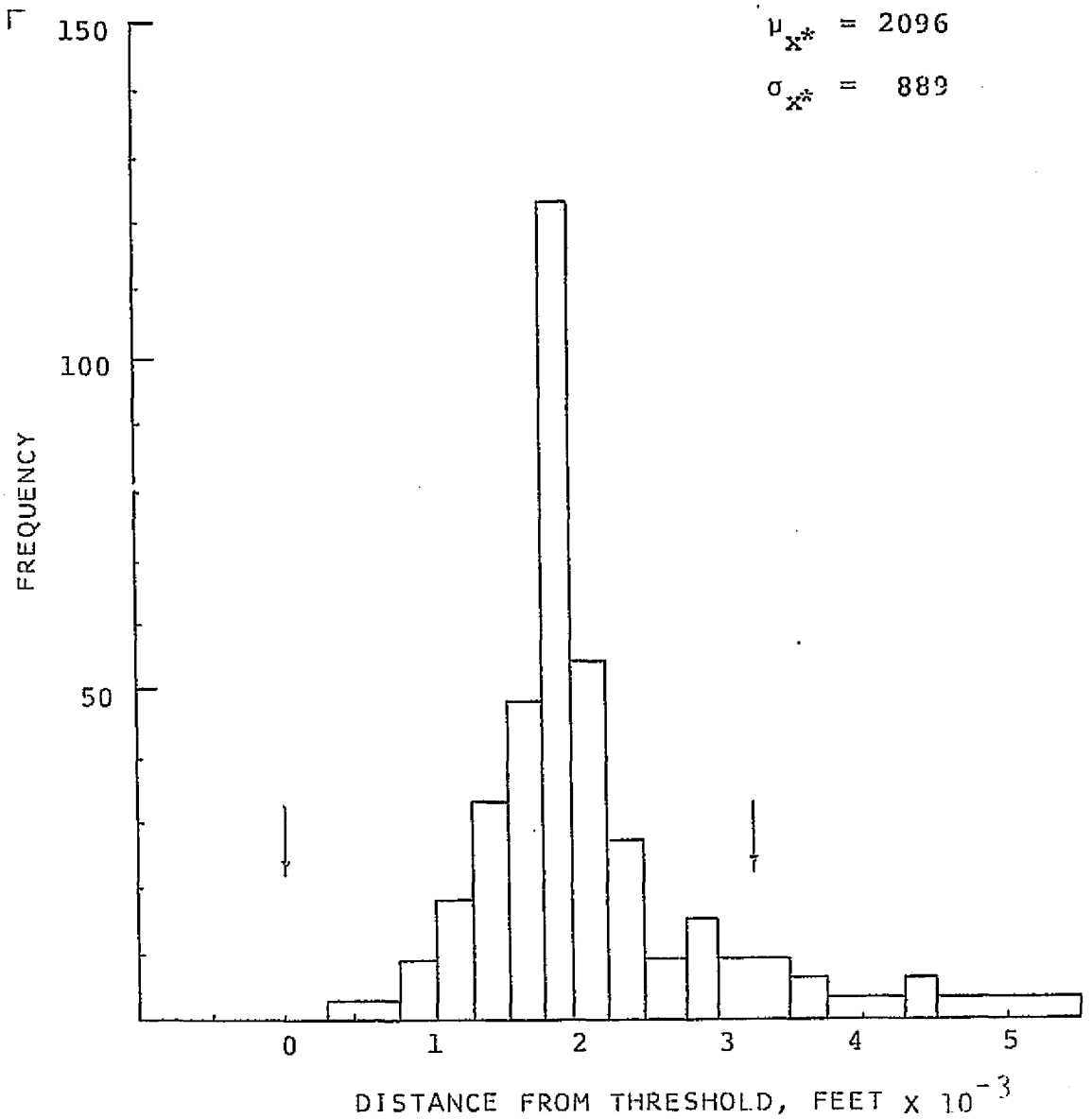

Fig. 3.29 Distance From Threshold at Touchdown

(Frequency is shown in quantum steps of 3)

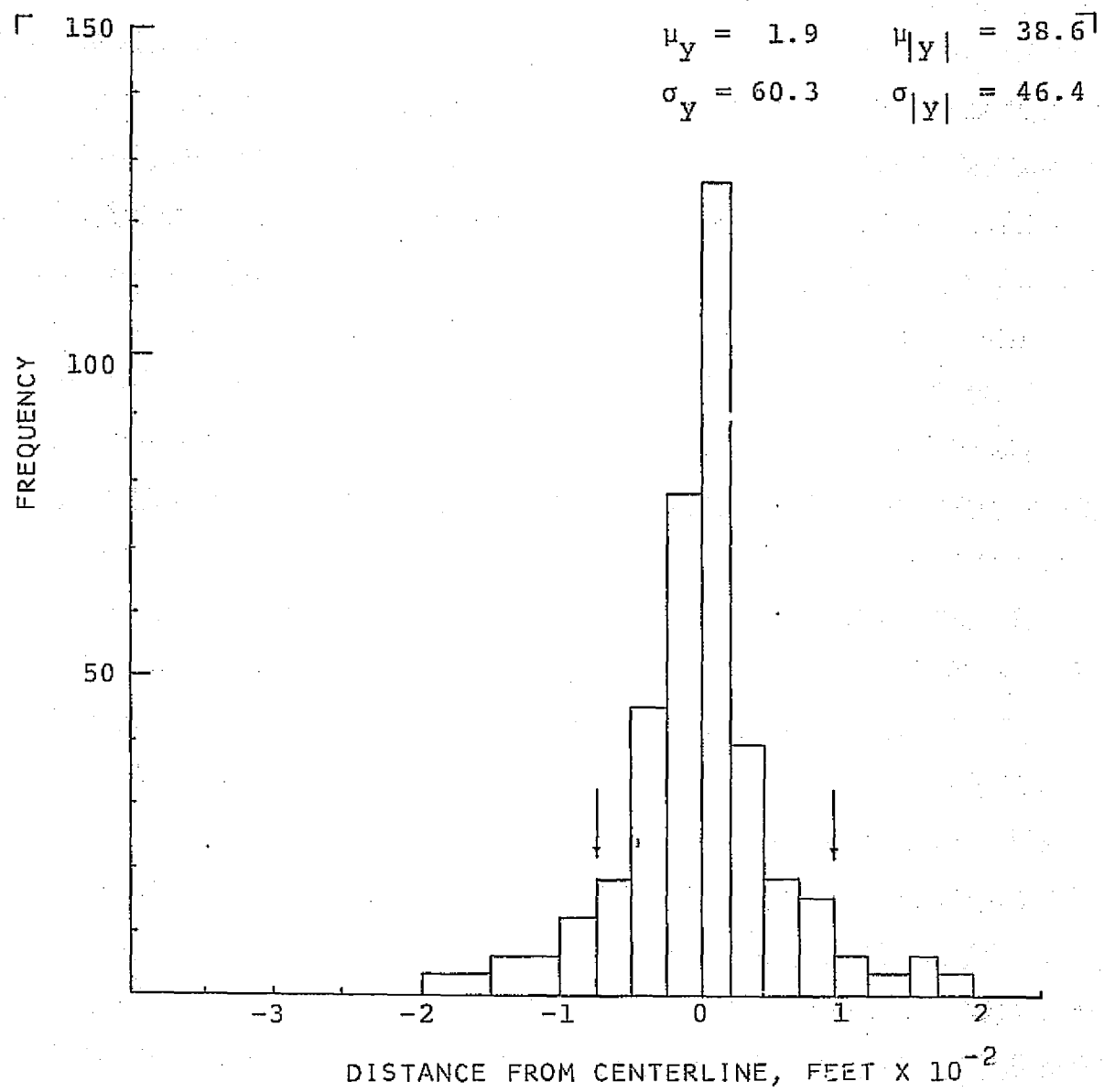

Fig. 3.30 Distance From Centerline at Touchdown

(Frequency is shown in quantum steps of 3)

C-2

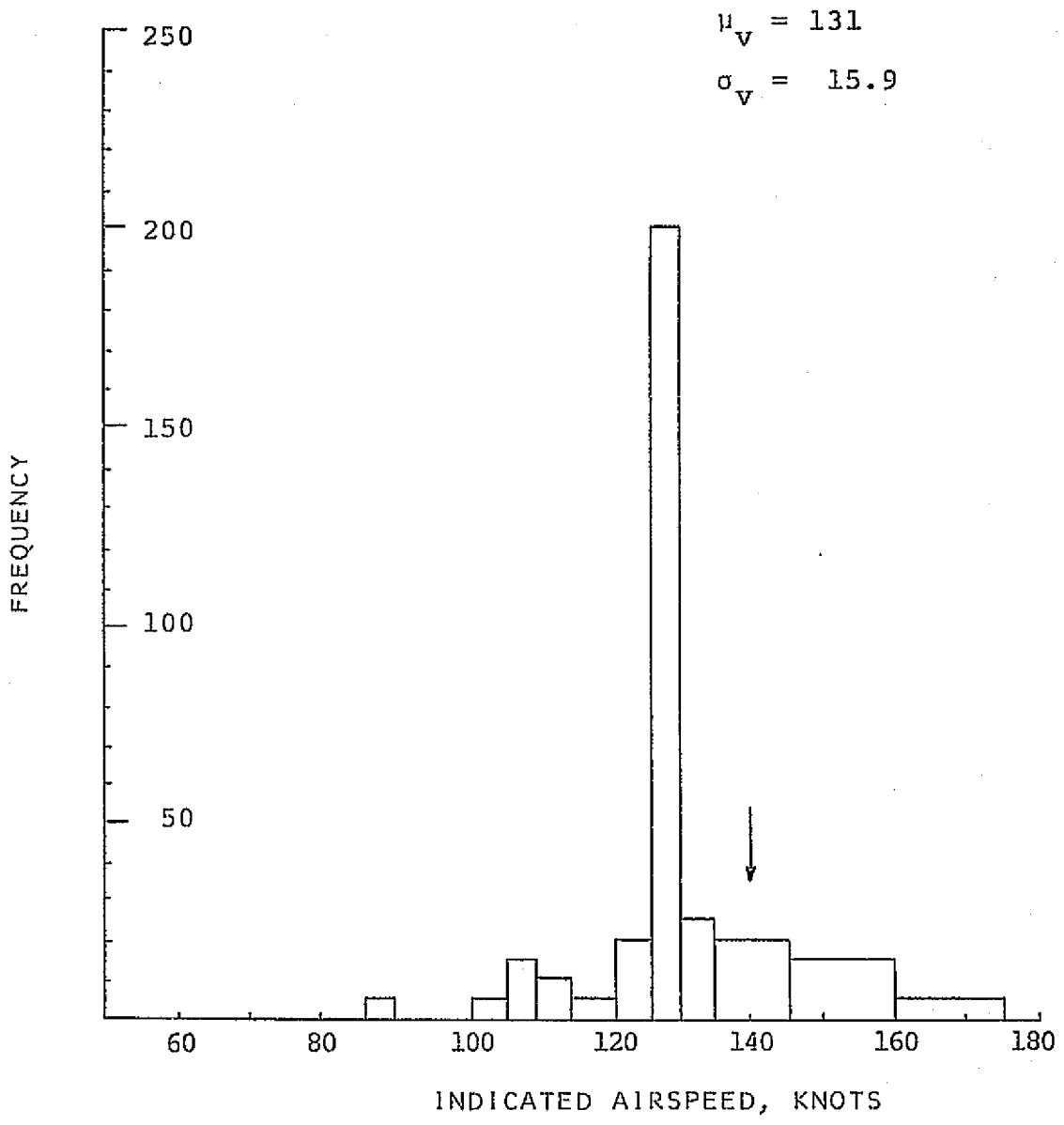

Fig. 3.31 Indicated Airspeed at Touchdown

(Frequency is shown in quantum steps of 5)

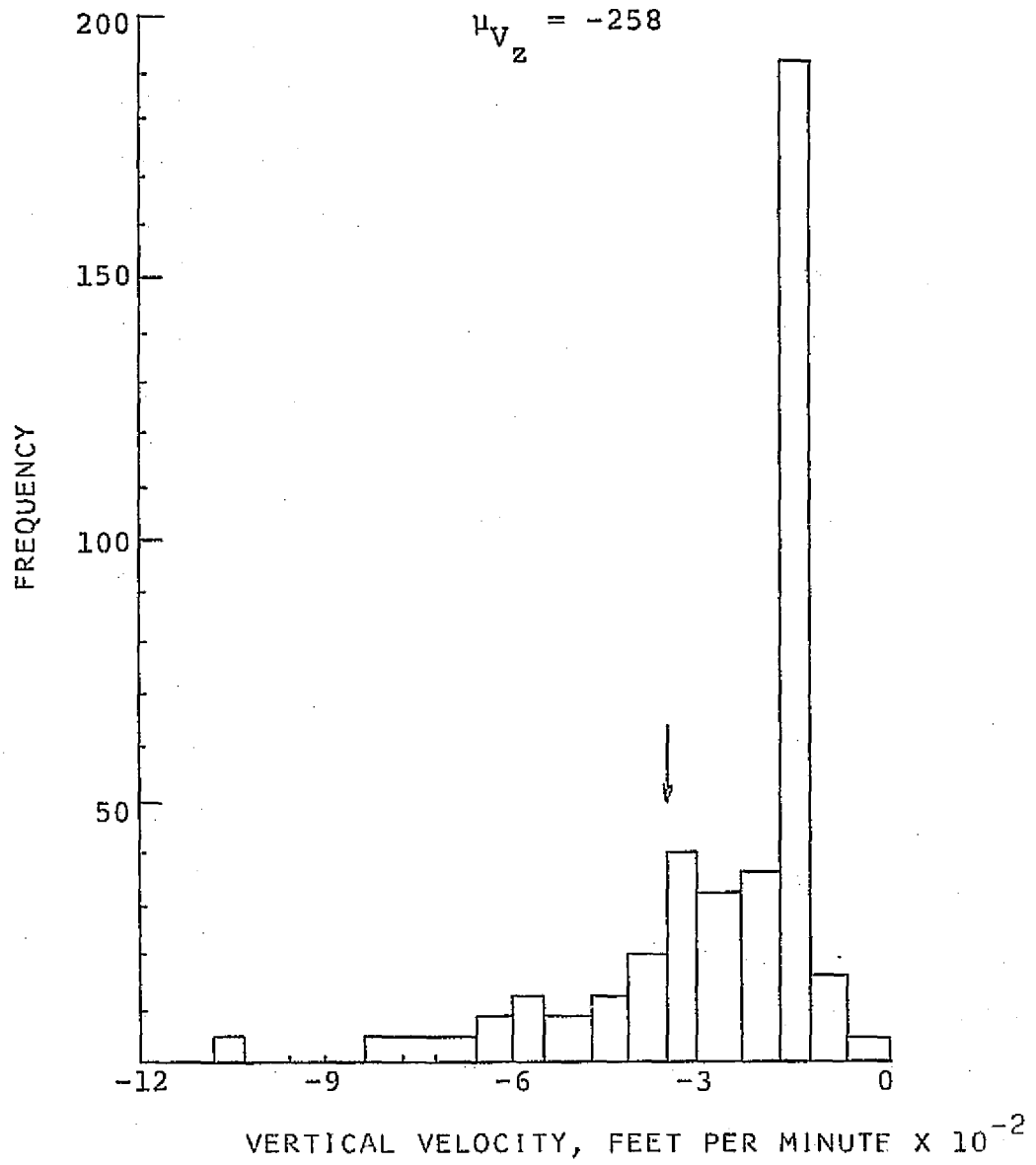

Fig. 3.32 Vertical Velocity at Touchdown

(Frequency is shown in quantum steps of 4)

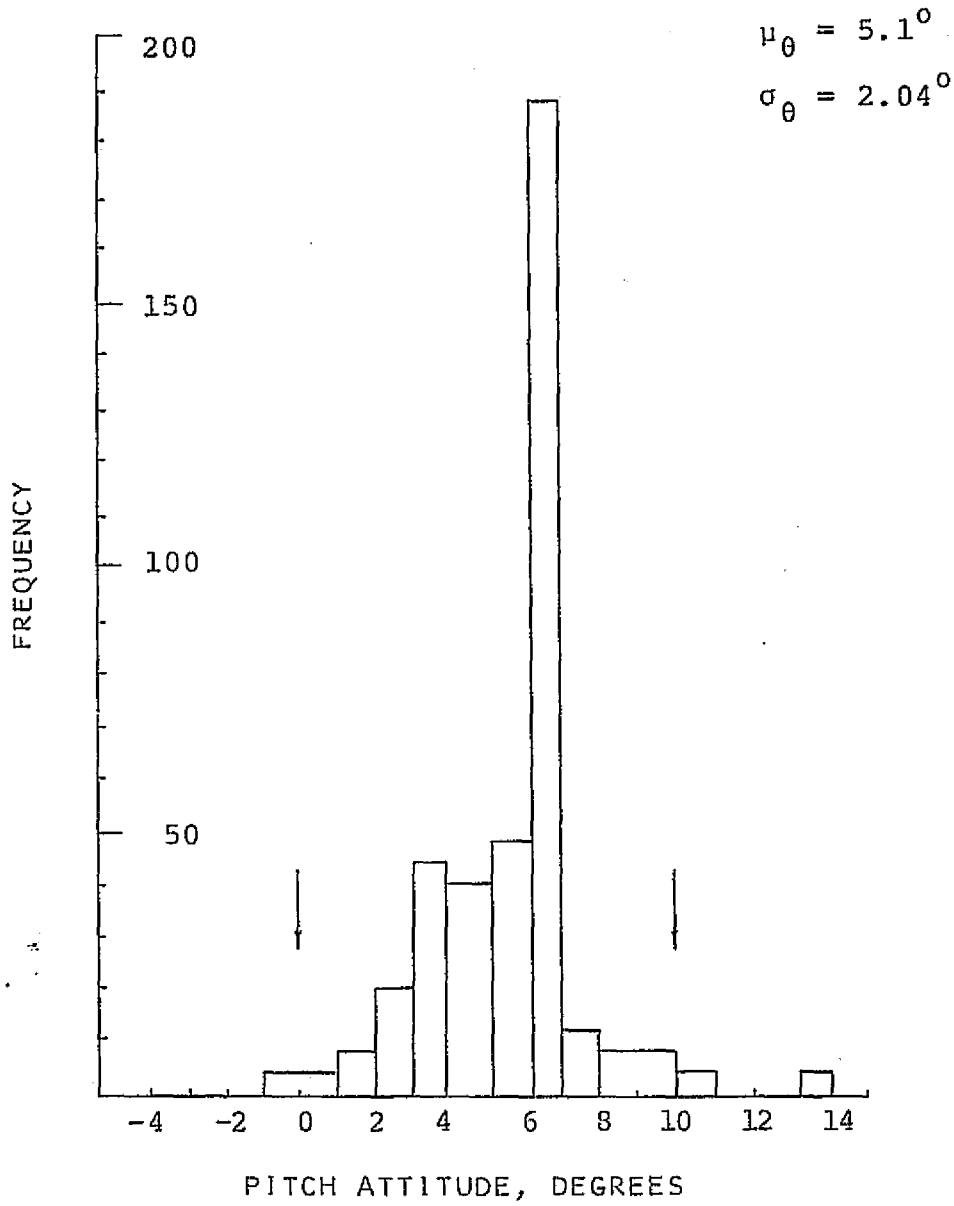

Fig. 3.33 Pitch Attitude at Touchdown

(Frequency is shown in quantum steps of 4)

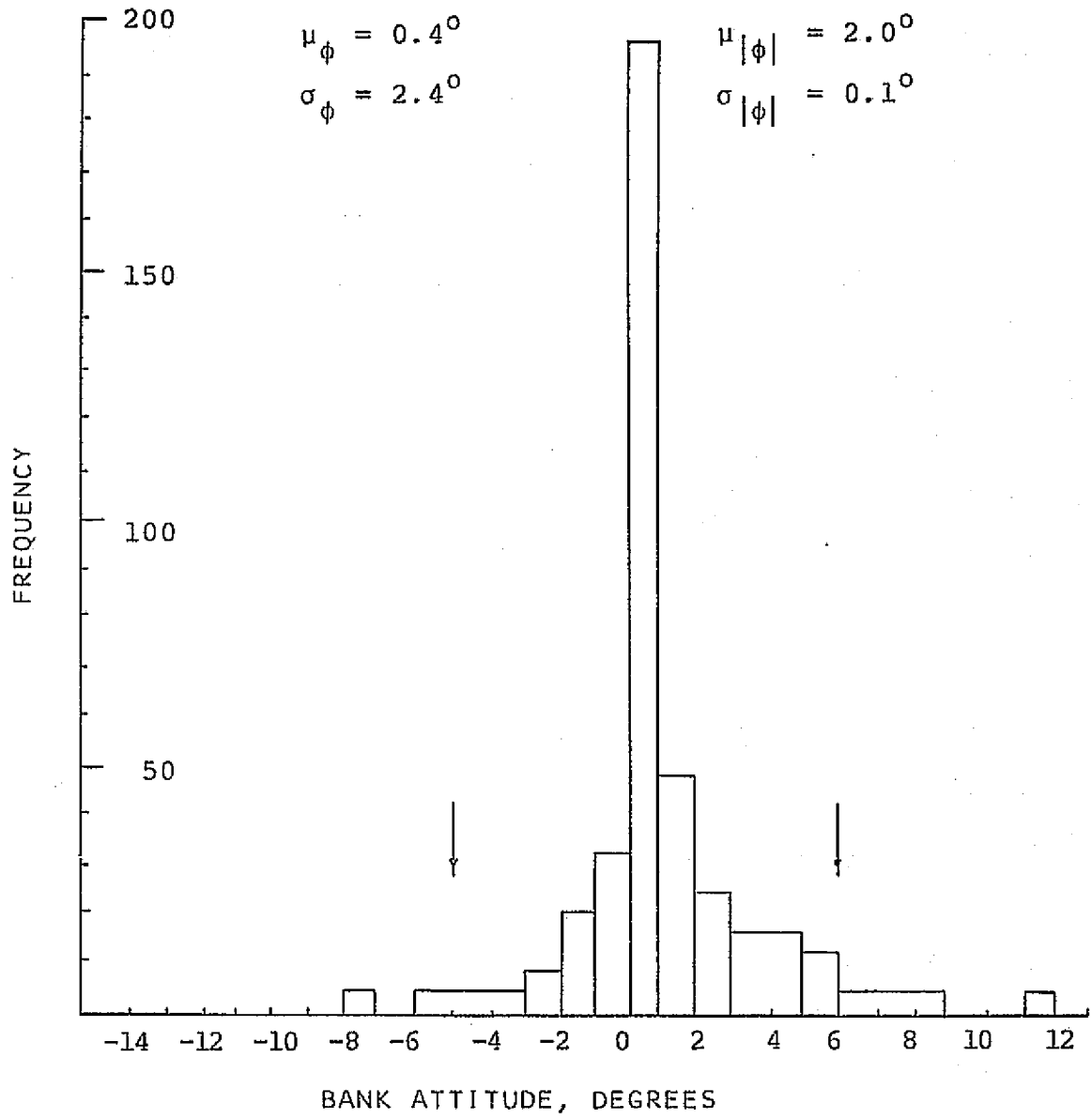

Fig. 3.34 Bank Attitude at Touchdown

(Frequency is shown in quantum steps of 4)

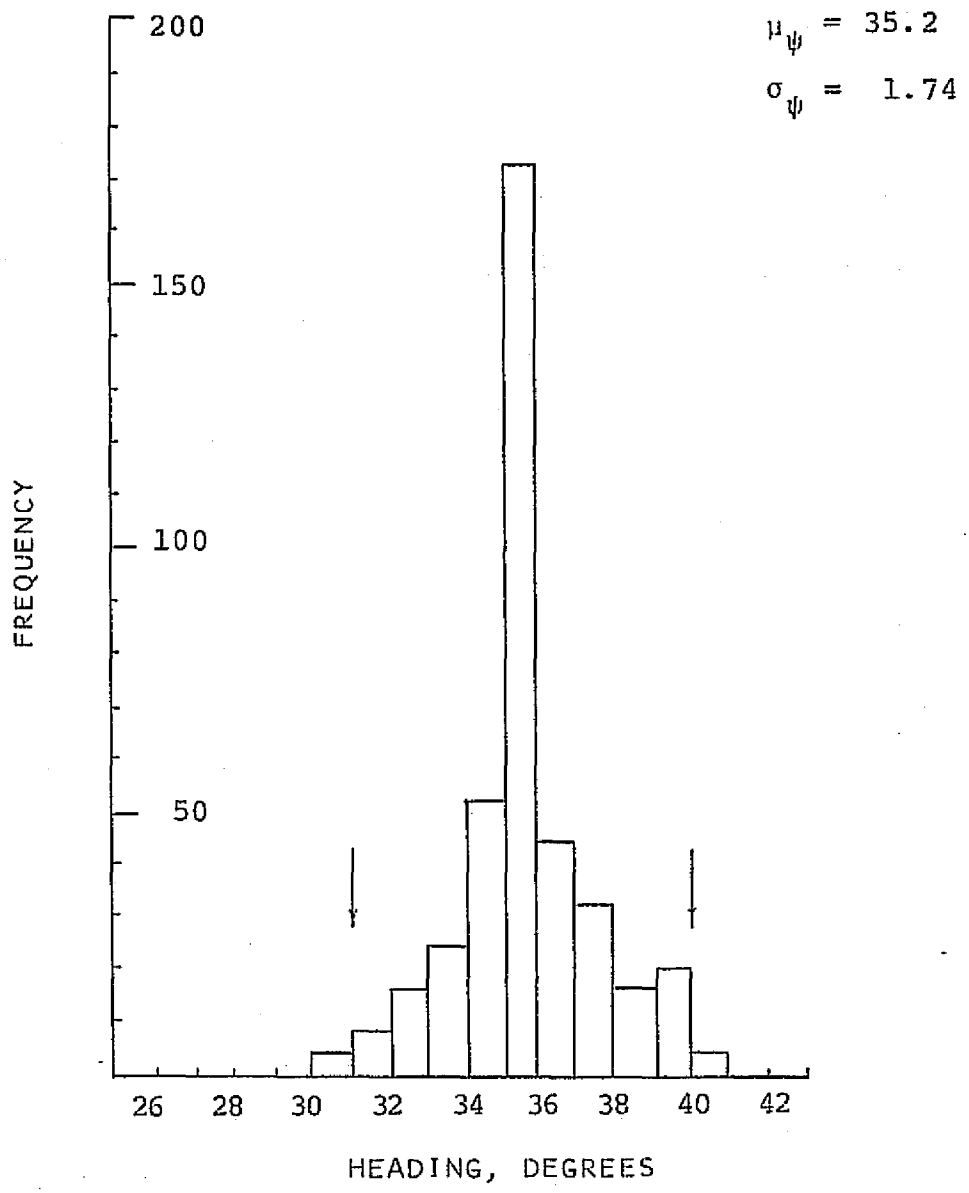

Fig. 3.35 Heading at Touchdown

(Frequency is shown in quantum steps of 4)

3.5 Tracking Performance

As the time-histories of the spatial coordinates of the simulated aircraft during each approach were available (Section 3.1), it was possible to compute angular root-mean-square vector tracking errors. We chose to document tracking performance in angular, rather than linear, RMS errors as only angular information was available to the pilot from the localizer- and glideslope-deviation indicators.

The data of RMS errors were computed between the altitudes of 2000 and 900 feet for the approaches in which no failure occurred. When a failure was simulated, RMS errors were computed between 2000 feet and the point of failure occurrence. Cross-track angular RMS errors are shown in Figure 3.36 as fractions of a full-scale deviation (5°); angular RMS errors in the vertical plane are shown as fractions of a full-scale deviation (1.4°) in Figure 3.37.

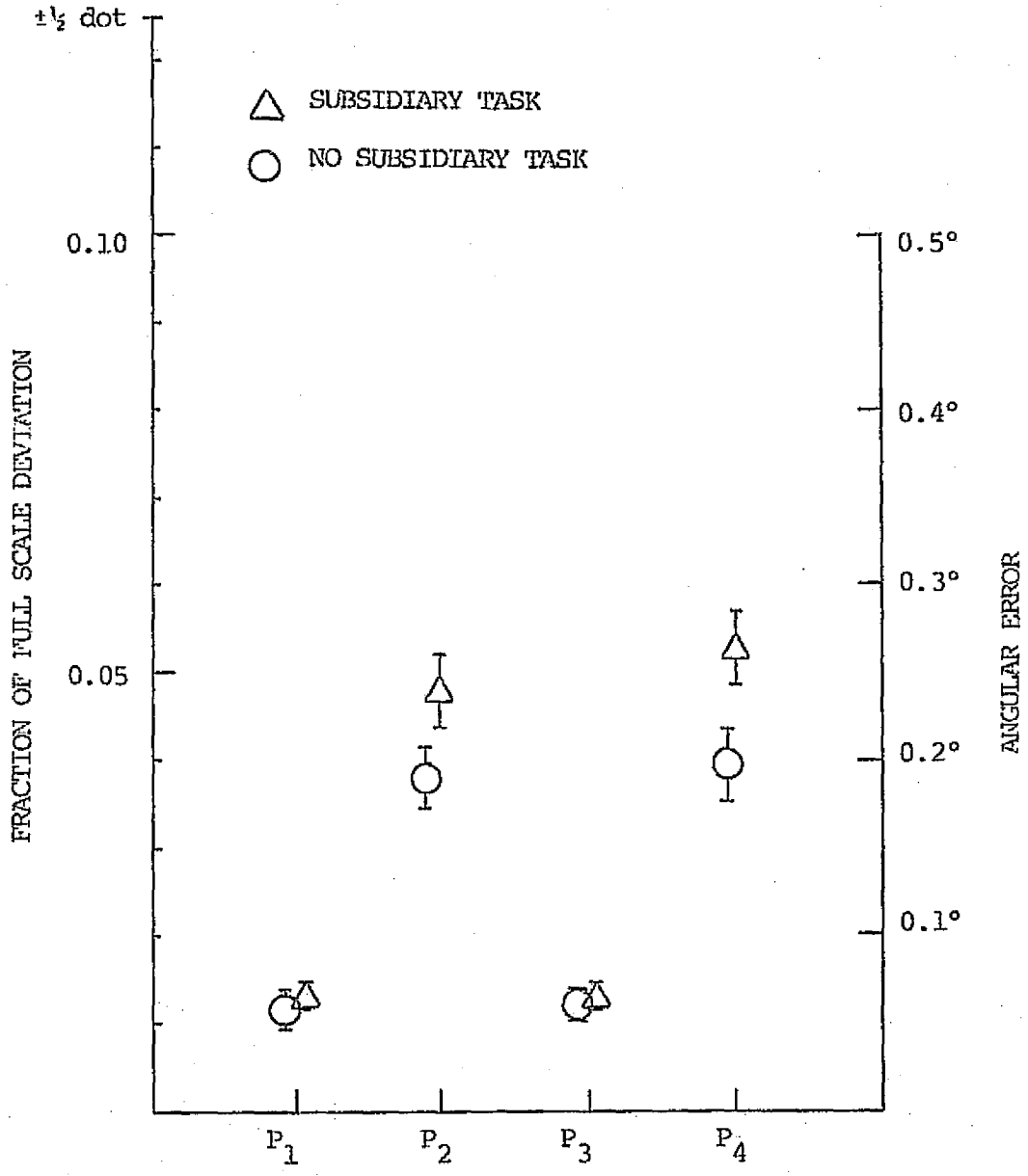

Figure 3.36 Cross-Track Angular RMS Tracking Errors

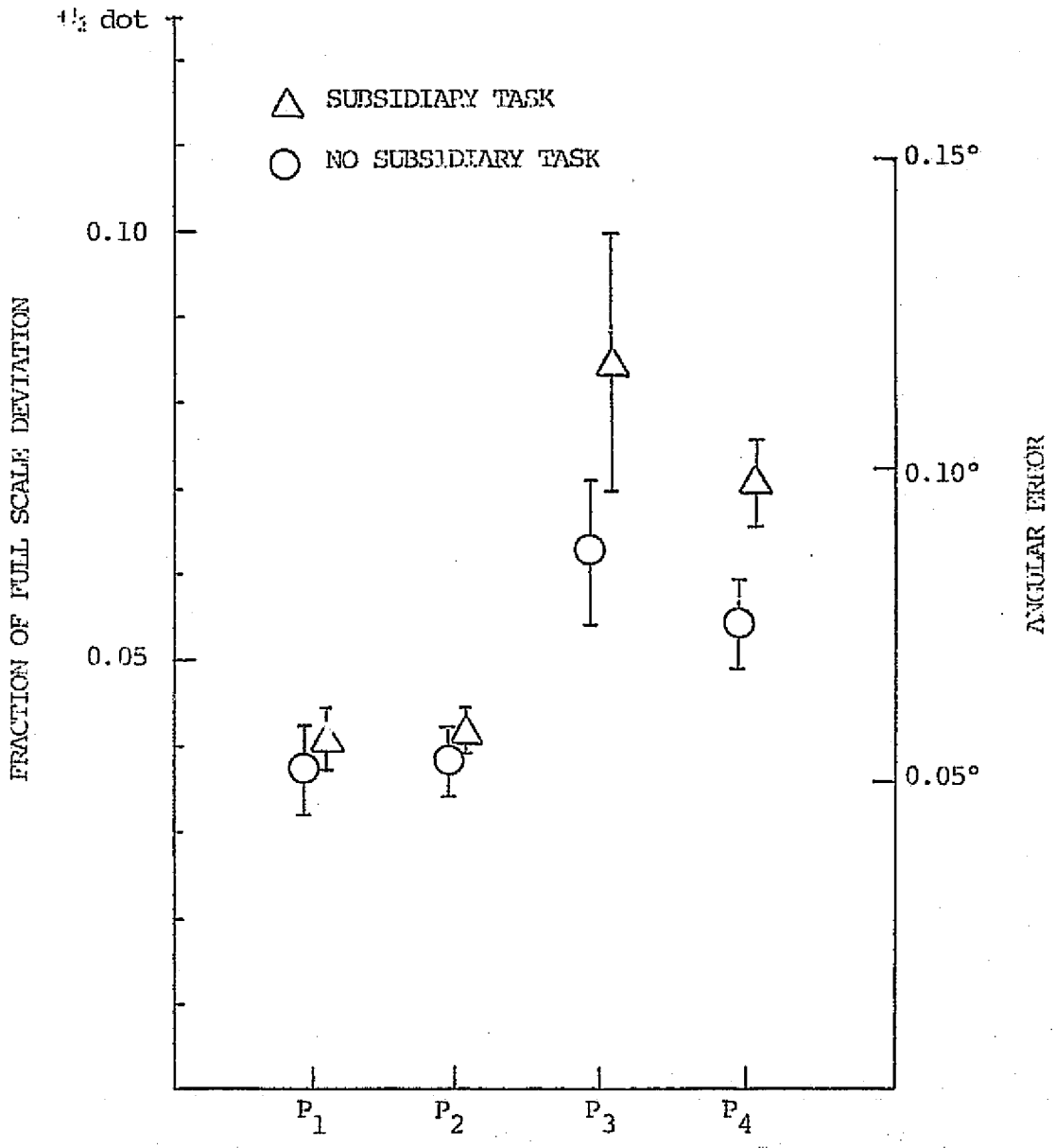

Figure 3.37 Glideslope Angular RMS Tracking Errors

CHAPTER IV

DISCUSSION

Various statistical analyses were performed on the data reported in Chapter III. The University of California at Los Angeles' School of Medicine Biomedical Computer Programs Package (UCLA BMD) was used extensively in the analysis. Particularly, advantage was taken of the following routines:

1. BMD01D, for computation of means, standard deviations and standard errors.
2. BMD05D, for plotting histograms.
3. BMD02D and BMD03D, for computation of cross-correlation and covariance matrices.
4. BMD10V, for analysis of variance and regression analysis.

Excellent documentation of the routines in this package is available (Dixon, 1973; also Afifi and Azen, 1972).

4.1 Workload

We were cognizant of the fact that our workload-measuring side-task may have caused undesired loading of the subjects, and hence, that the piloting performance results obtained in the workload measurement experiment and the data obtained in the runs when the side-task was not present came from different populations. This possibility was carefully investigated. It has been shown (Kelley, 1966) that the most precise piloting performance measure is RMS tracking error; consequently, RMS tracking-error data of the workload measuring experiment were compared with RMS data obtained from the failure detection experiment, on approaches in which no failure occurred. Analysis of variance revealed that the hypothesis that the data represented the same population could not be rejected (Table 4.1). It was concluded, therefore, that the side-task did not cause any significant loading of the pilots and that the workload scores which were obtained during the workload measurement runs were applicable to the failure detection, no-side-task approaches.

It seemed clear from Figures 3.10 and 3.11 that the side-task scores were sensitive to variations both in the disturbance level and in the participation mode. Indeed, analysis of variance under the hypothesis that the effects were additive revealed that the variations

Table 4.1 ANOVA of RMS Tracking Errors

Source	s.s.	d.f.	m.s.	F
Mean	45974.99	1	45974.99	459.3*
Replications	2791.99	14	199.43	2.0
Treatments:				
Participation Mode	4201.48	3	1400.49	14.0*
Disturbance Level	6197.88	1	6197.88	61.9*
Presence or Absence of side-task	318.20	1	318.20	3.2
Error	25023.09	250	100.09	

* - Significance at the 1% level

Table 4.2 ANOVA of Normalized Workload Scores

Source	s.s.	d.f.	m.s.	F
Mean	457561.50	1	457561.50	893.2*
Replications	15019.85	14	1072.85	2.1
Treatments:				
Participation Mode	79507.92	3	26502.64	51.7*
Disturbance Level	3868.10	2	1934.05	3.8
Error	81966.42	160	512.29	

in workload scores as a function of participation mode were significant at the $P << 0.01$ level, and as a function of the severity of the disturbance - at the $P < 0.05$ level (Table 4.2).

There was, however, no significant difference between workloads at the two low disturbance levels, namely, calm air and a quartering wind of 5 knots, gusting to 15 knots. It was assumed, and it was verified by pilots' comments, that the components of the wind normal and parallel to the final approach flight-path (3.5 knots gusting to 10.6 knots) were not strong enough to induce workloads significantly higher than those induced by piloting the simulated aircraft in calm air. Consequently, these two disturbance levels were combined in the analysis and the data were treated as if there were only two distinct disturbance levels, "low" and "high".

An additive model was used in the regression of workload scores on disturbance levels and participation modes:

$$W(P,D) = W_1(P) + W_2(D) = W_0 + W_p(P) + W_d(D) \qquad (4.1.a)$$

where W is the workload score

P is the participation mode

D is the disturbance level

W_p and W_d are the partial derivatives $\partial W/\partial P$ and $\partial W/\partial D$, respectively

and W_0 is the baseline workload score.

Using this model, $W_1(P)$ and $W_2(D)$ were found to be

$$W_1(P) = \begin{cases} 18.7 & \text{for the fully-automatic mode} \\ 36.6 & \text{for the split-axis, yaw-manual mode} \\ 61.0 & \text{for the split-axis, pitch-manual mode} \\ 72.9 & \text{for the fully-manual mode} \end{cases} \qquad (4.1.b)$$

$$W_2(D) = \begin{cases} 0.0 & \text{for the low disturbance level} \\ 9.8 & \text{for the high disturbance level} \end{cases}$$

These values yielded workload-participation mode correlation significant at $P < 0.001$ and workload-disturbance level correlation significant at $P < 0.05$.

Figures 3.12 through 3.15 reveal the asymptotic altitude behavior of the pilot's workload: The workload is essentially constant at altitudes higher than approximately 500 feet, but there is a very marked increase in the workload at lower altitudes. Undoubtedly, this increase is at least partially due to the non-linear increase in display sensitivity with decreasing distance-to-go. However, this increase in pilot workload was observed even when the pilot acted as

a monitor and the autopilot controlled the aircraft, which seems to indicate the effect of other factors as well; such as, possibly, the pilot's mental state arising from his awareness of the proximity of the ground. It is conceivable that optimal display design may reduce the additional workloads imposed on the pilot as a result of the increased display sensitivity; further studies are necessary, however, to find out whether these other factors, if any, are inherent in the situation or whether a reduction is possible in the pilot's workload during the last phase of a landing approach.

4.2 Tracking Performance

Figures 3.36 and 3.37 show the vertical and lateral RMS tracking errors, respectively, averaged over all subjects and over all wind-disturbance levels. It is clear that our subjects were capable of tracking the ILS glide-path within less than 10% of full-scale GSI deflection. Localizer tracking performance was even better, and the largest mean RMS error is approximately 5% of full-scale CDI deflection. The difference between lateral and longitudinal tracking performance may be due partially to the larger size of the course deviation indicator instrument, as compared to the glide-slope deviation indicator, and partially to the difference in the difficulty of controlling the

simulated aircraft in the longitudinal and lateral axes: Longitudinal control, requiring the coordination of power and pitch attitude, impose on the pilot higher demands than does lateral control. This point is further substantiated by the evidence of the higher workload levels which are induced by longitudinal control (Figure 3.11).

We wished to eliminate any learning effects from our experiments. To this end, the order of presentation of the experimental treatments to each subject was randomized. In addition, each experimental session began with a training period designed to bring the subject to a steady-state level on the learning curve (Section 2.8). Indeed, an analysis of variance of the tracking errors, treating the order of presentation as an independent variable, showed that the null hypothesis could not be rejected (Table 4.3).

4.3 Detection Performance

As Tables 3.1 and 3.2 show, about 10% of all failures were not reported by the subjects; about 7% were obviously not detected at all, as evidenced by the fact that these approaches did not terminate in a successful landing because of gross deviations in the failed axis.

Table 4.3 ANOVA of RMS Tracking Errors by Order of Presentation

Source	s.s.	d.f.	m.s.	F
Mean	13649.57	1	13649.57	510.7*
Replications	547.72	14	39.12	1.5
Treatments:				
Participation Mode	278.56	3	92.85	3.5
Disturbance Level	1218.43	1	1218.43	45.6*
Order of presentation	627.92	29	21.65	0.8
Error	3527.73	132	26.73	

A very interesting pattern is obvious from Tables 3.1 and 3.2 and from Figures 3.23 and 3.26: All failures in an automatically-controlled axis were detected in consistently short times; between 9% and 17% of the failures which occurred in a manually-controlled axis were not detected at all, and the ones that were required considerably longer detection times. A t-test revealed the difference between the mean detection times in the automatic and manual modes to be highly significant, at the $P < 0.001$ level.

Our first hypothesis (Section 2.1) attempted to explain this difference in detection performance as being due, in part, to the increased involvement of the pilot in the control task in the manual mode and, in part, to the increased workload levels associated with manual control. We set out, therefore, to separate the individual effects of these factors, participation mode and disturbance level, on the failure detection performance.

In Figures 4.1 and 4.2, the mean detection times of longitudinal and lateral failures, respectively, are plotted as functions of the corresponding mean workload levels for the four participation modes. The following relationships are evident:

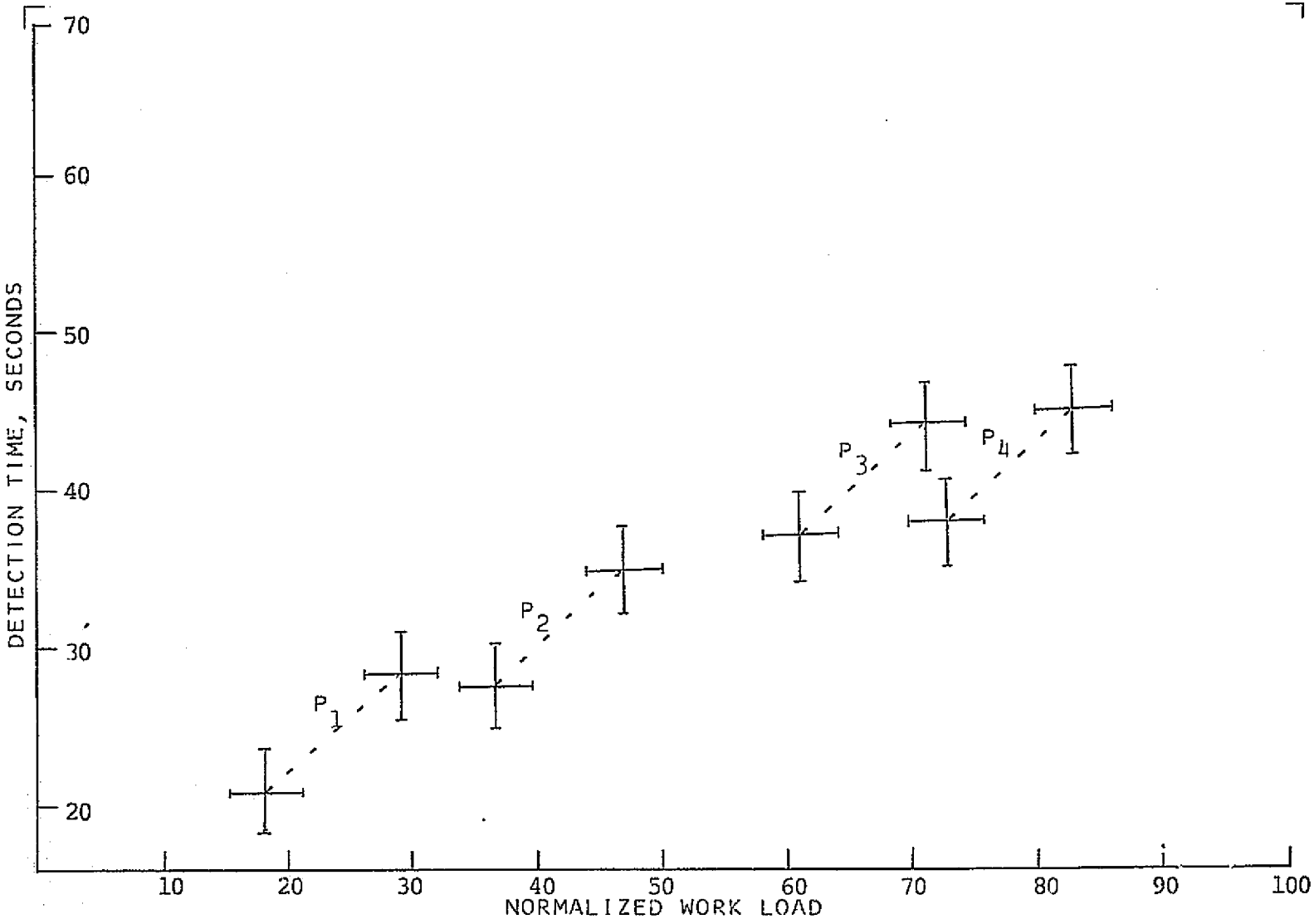

Fig. 4.1 Mean Detection Times of Longitudinal Failures

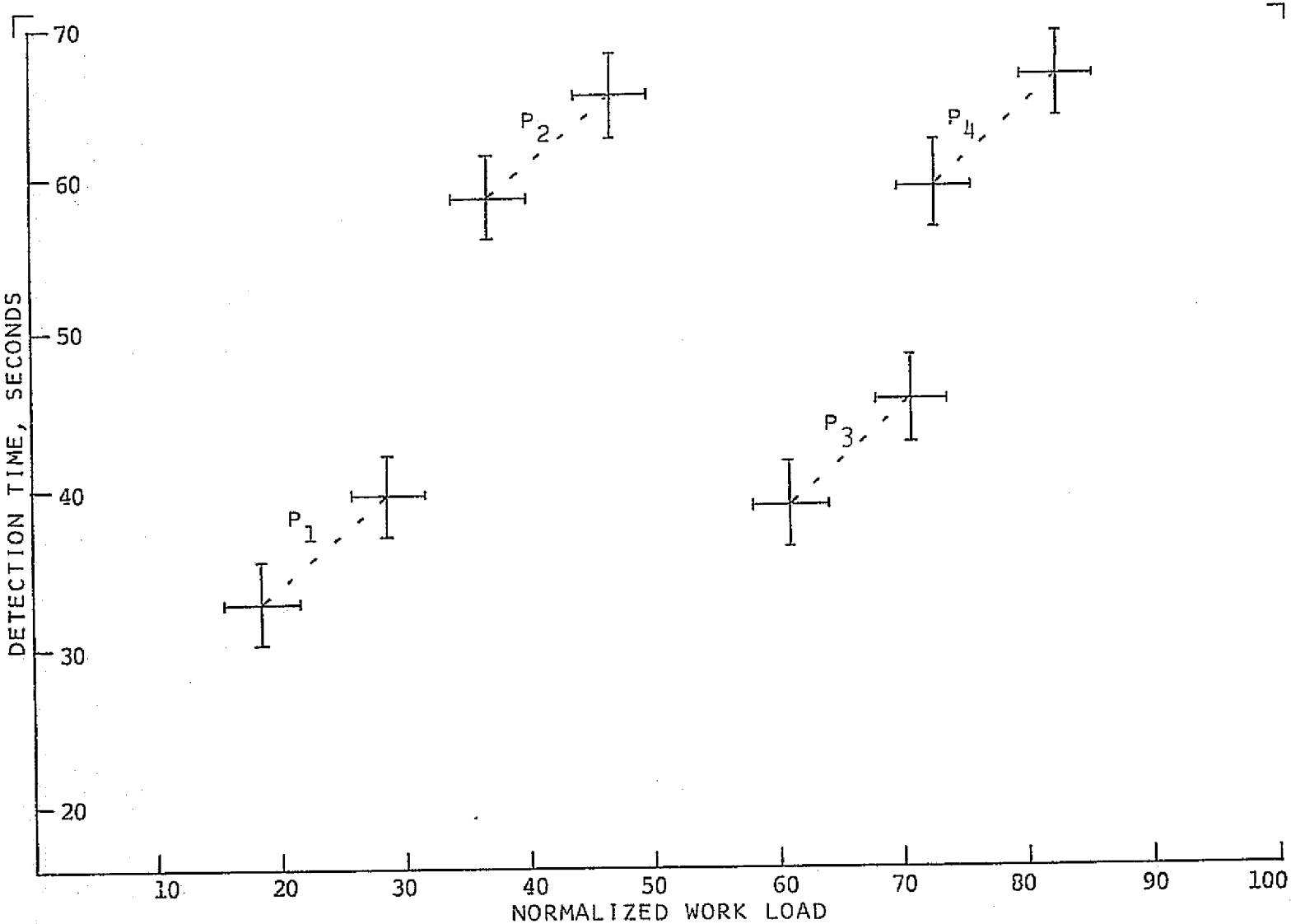

Fig. 4.2 Mean Detection Times of Lateral Failures

1. Detection times in a manually-controlled axis are significantly longer than detection times in an automatically-controlled axis ($P < 0.001$).

2. Detection times for lateral failures are significantly longer than detection times for longitudinal failures at comparable workload levels (Table 4.4).

3. Detection times increase in direct relationship to workload ($\rho_{n=163} = 0.322$).

The apparent similarities between Figures 3.23 and 3.26 and Figures 3.36 and 3.37, respectively, suggest an attractive theory to explain the shorter detection times in the automatic-control modes: The lower angular RMS errors in the automatic modes effect higher signal-to-noise ratios of the displayed tracking error which, in turn, result in better detection performance.

This hypothesis was tested by analysis of variance of the failure detection times, with the angular RMS tracking errors in the failed axis as a covariate (Table 4.5). The F-test rejected the hypothesis, as the RMS errors did not show a significant effect on the failure detection times. A linear correlation analysis yielded the same result, as the RMS-detection time correlation coefficient fell short of significance at the $P < 0.01$ level ($\rho_{n=163} = 0.215$). In addition, under the SNR theory, the tracking errors on the approaches in which a failure was missed altogether should be larger than on other approaches

Table 4.4 ANOVA of Failure Detection Times by Failure Axis

source	s.s.	d.f.	m.s.	F
Mean	279457.71	1	279547.71	648.2*
Participation Mode	10613.87	3	3537.96	8.2*
Disturbance Level	1601.05	2	800.53	1.9
Failure Axis	10017.42	1	10017.42	23.2*
Error	67258.33	156	431.14	

Table 4.5 ANOVA of Failure Detection Times with RMS as Covariate

source	s.s.	d.f.	m.s.	F
Mean	110966.97	1	110966.97	314.6*
Participation Mode	13556.86	1	13556.86	38.4*
Failure Axis	10298.17	1	10298.17	29.2*
Mode x Axis	1053.07	1	1053.07	2.9
RMS	100.91	1	100.91	0.3
Error	50785.94	144	352.68	

with comparable participation and disturbance conditions. A paired-difference Student-t test, however, failed to reveal any difference. Consequently, RMS tracking errors were excluded from further consideration and the failure detection performance was assumed to be a function of the control mode, of the failed axis and of the workload level, but not a function of the RMS tracking error.

A disparity is obvious, however, between Figures 4.1 and 4.2. The longitudinal failure detection data, shown in Figure 4.1 seem to suggest that the increased detection times in the manual control modes P_3 and P_4 are due mainly to the associated increase in workload and that, had the subjects operated at a constant workload level (that is, along a line normal to the abscissa), their detection performance would have, in fact, improved in the manual control modes, compared to the automatic control modes.

The lateral failure detection data of Figure 4.2, on the other hand, exhibit a very different behavior. They imply that the dominant factor in detection performance is the control mode, not the workload (as suggested by Figure 4.1); furthermore, there seems to be an inherent contradiction in the data, as they indicate that, assuming that the extrapolation is valid, the detection performance at a constant workload would be better in a fully automatic mode (P_1) than in the yaw - manual split-axis mode (P_2), but not as good as in the fully-manual (P_4) control mode.

It should be noted that both Figure 4.1 and Figure 4.2 are plots of two dependent variables, as the workload level was controlled in the experiment only indirectly. Consequently, there were measurement errors in both coordinates and therefore, the slopes of the straight lines in Figures 4.1 and 4.2 could, in reality, be quite different than those shown; one possibility is plotted in Figure 4.3. Our statistical tests (t and r) did not have sufficient power to reject either possibility with any degree of confidence.

To resolve the ambiguity, we assumed that the failure detection mechanism of the human operator acts similarly in both lateral and longitudinal axes; any difference in performance between these axes is due to differences in the plant dynamics and in display variables only, not to differences in processes internal to the operator.

This assumption of equivalence between the lateral and longitudinal axes has been made, either explicitly or implicitly, by many investigators. It is based on the theory that the human operator behaves optimally with respect to his task (*cf.* Smallwood, 1967) in all axes, and that the operator adjusts his describing function to match the task (Young, 1969).

Longitudinal and lateral failure data were thus pooled;

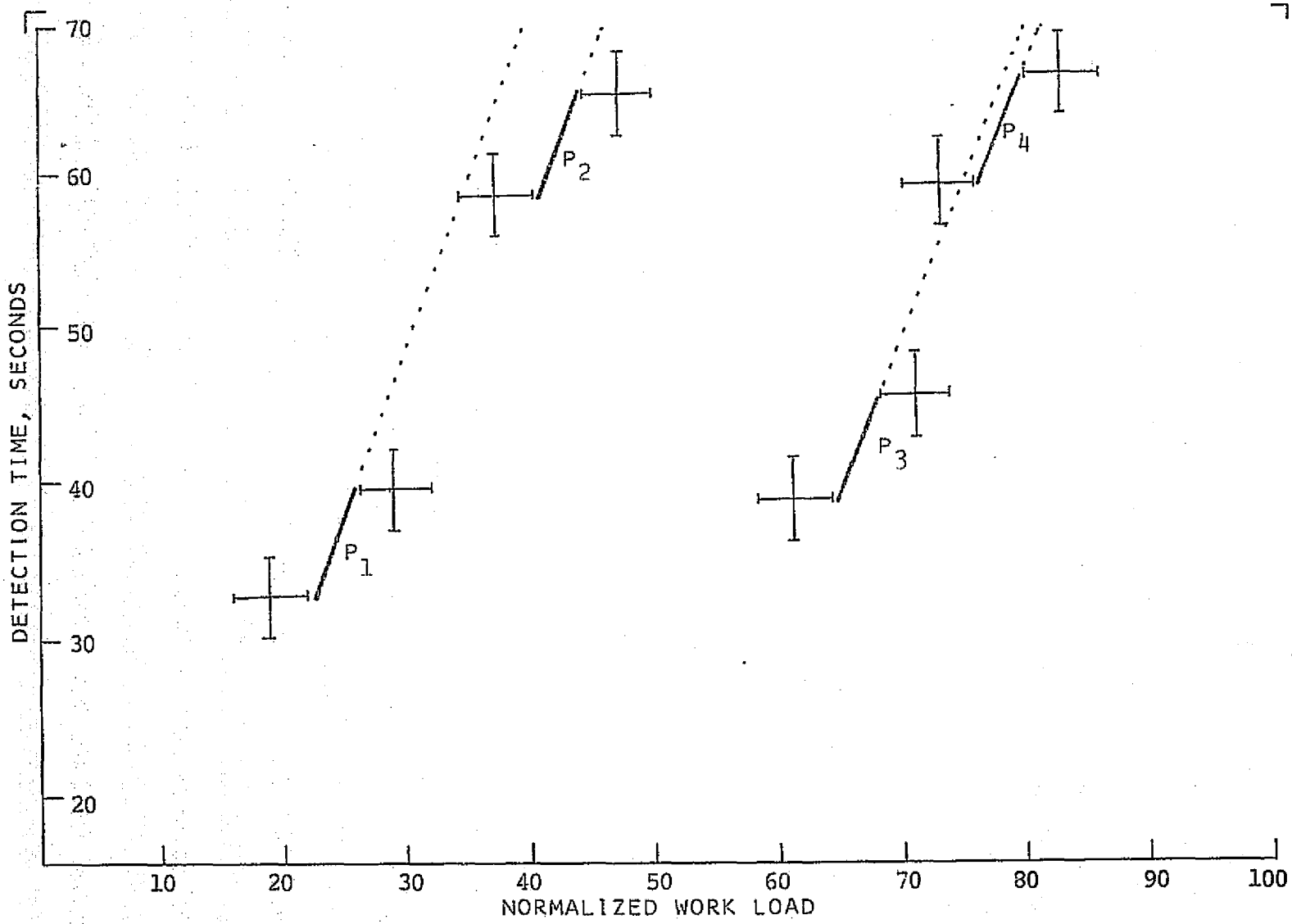

Fig. 4.3 Possible Workload/Detection Relationship, Lateral Failures

detection times were regressed on the type of failure (longitudinal or lateral) and on the control mode in the failed axis, with the workload index as a covariate, based on the following additive model:

$$T_{detection} = T_0 + \alpha(\text{control mode}) + \beta(\text{failed axis}) + \gamma(\text{workload}) \quad (4.2a)$$

A solution was obtained for the regression coefficients α, β and γ:

$$T_{detection} = 20.9 + 16.5\underline{M} + 15.4\underline{A} + 0.10WL \quad (4.2b)$$

where $\underline{M} = \begin{cases} 1 & \text{if the failed axis is controlled manually} \\ 0 & \text{otherwise} \end{cases}$

$\underline{A} = \begin{cases} 1 & \text{if the failure occurs in the lateral axis} \\ 0 & \text{if the failure occurs in the longitudinal axis} \end{cases}$

WL = the normalized workload index

and $T_{detection}$ is measured in seconds.

The relationship is plotted in Figures 4.4 and 4.5 for longitudinal and lateral failures, respectively. Mean detection times at the corresponding mean workload levels are also shown for comparison. The model correlates well with the data, with $\rho_{n=163} = 0.531$, significant at the $P << 0.001$ level.

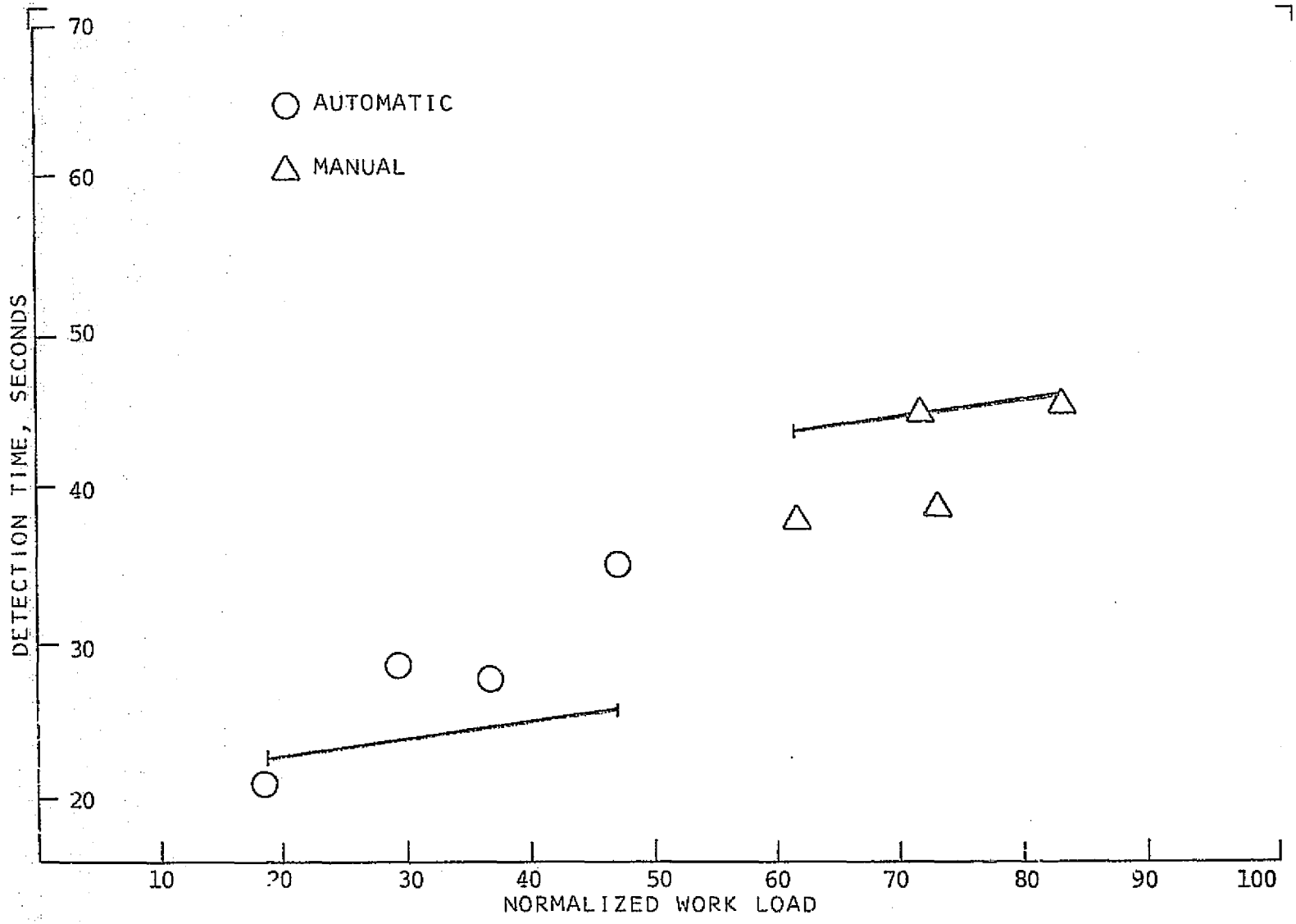

Fig. 4.4 Additive Model, Longitudinal Failures

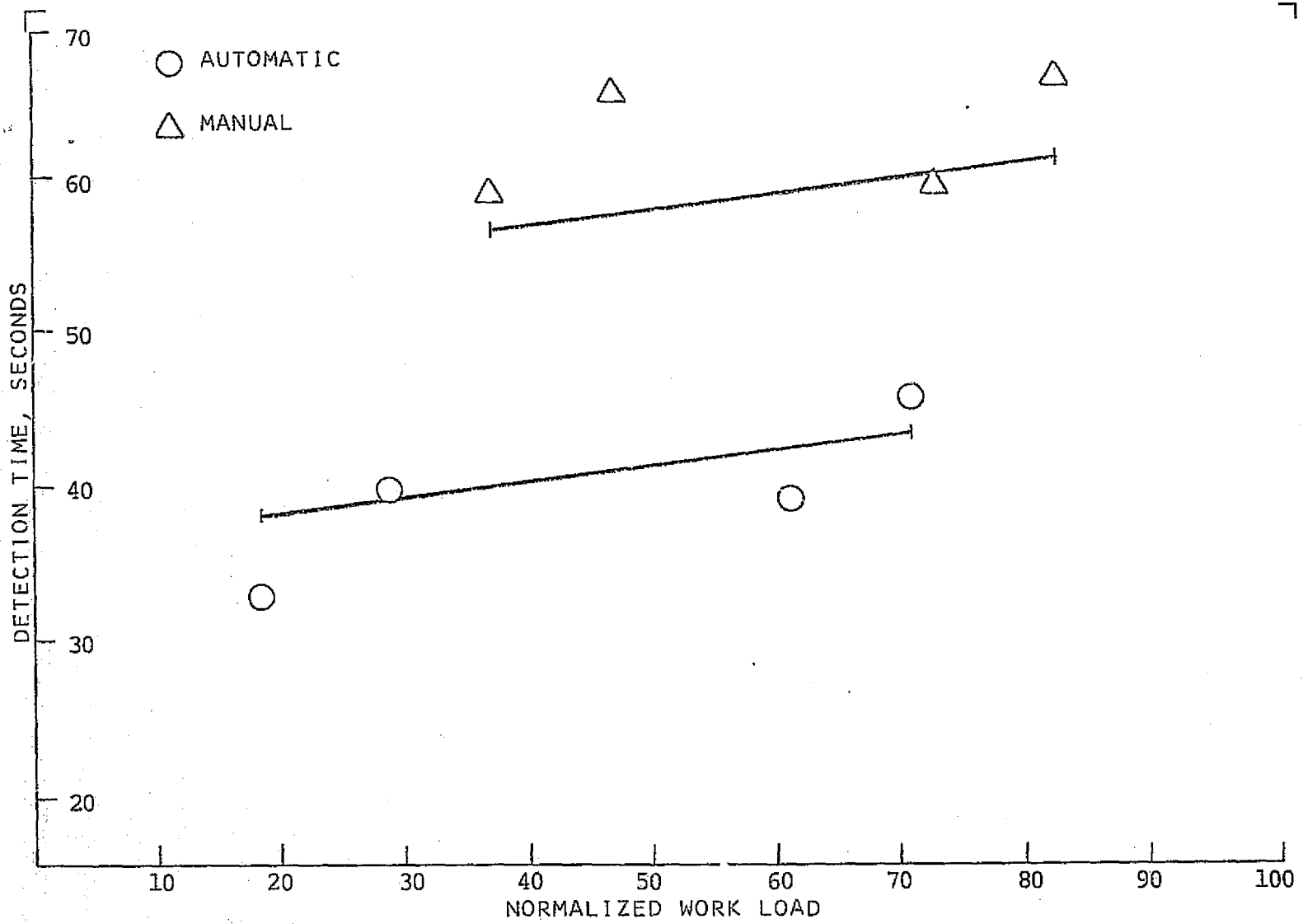

Fig. 4.5 Additive Model - Lateral Failures

4.4 Touchdowns

As mentioned in Section 3.4, 389 of the 450 approaches flown terminated in attempted landings, 59 terminated in a missed approach and two were discarded because of equipment malfunctions. The breakdown of landings and go-arounds by failure type is shown in Table 4.6.

When the "acceptable landing" criteria (Section 2.6) were applied to the data, 193 landings were considered successful and 196 (or approximately 50%) were judged unsuccessful. Of these, 106 were rejected because of an excessive deviation in any one parameter, 61 were rejected because of excessive deviations in two parameters simultaneously, twenty-two - in three parameters, six - in four parameters and one attempted landing was rejected because of simultaneous deviations in five of the seven parameters. Tables 4.7, 4.8 and 4.9 summarize the touchdown performance as a function of the manually-controlled axis and the presence or absence of flight-director information (see also Table 2.2).

It seems clear from Tables 4.7-4.9 that the landing performance was quite poor under all but fully automatic conditions. Longitudinal control presented a more severe problem to the pilot, as evidenced by the difference in the percentage of successful landings which is

Table 4.6 Breakdown of Landings by Failure Conditions

	FAILED AXIS			TOTAL
	NONE*	PITCH	YAW	
ATTEMPTED LANDINGS	257	68	64	389
GO-AROUNDS	11	22	26	59
TOTAL	268	90	90	448

*Including 178 workload-measurement runs in which no failures were presented and go-arounds were not permitted (see Section 2.8.2)

Table 4.7 Touchdown Performance, Pitch Manual

	PERCENT OF LANDINGS, PARAMETER OUT OF TOLERANCE							SUCCESSFUL (ATTEMPTS)
	X	Y	SPEED	SINKRATE	PITCH	BANK	HEADING	
WITH FLIGHT-DIRECTOR	22.0	17.7	46.2	31.7	6.4	4.3	0.5	27.4(186)
WITHOUT FLIGHT-DIRECTOR*	24.2	9.1	48.5	42.4	6.1	3.0	0.	21.2(33)
TOTAL	22.4	16.4	46.6	33.3	6.4	4.1	0.5	26.5(219)

*See Table 2.2

Table 4.8 Touchdown Performance, Yaw Manual

	PERCENT OF LANDINGS, PARAMETER OUT OF TOLERANCE							SUCCESSFUL (ATTEMPTS)
	X	Y	SPEED	SINKRATE	PITCH	BANK	HEADING	
WITH FLIGHT-DIRECTOR	11.9	24.3	27.5	22.8	3.1	8.8	2.6	43.0(193)
WITHOUT FLIGHT-DIRECTOR*	0.	51.7	17.2	6.9	6.9	0.	3.4	37.9(29)
TOTAL	10.4	27.9	26.1	20.7	3.6	7.7	2.7	42.3(222)

*See Table 2.2

Table 4.9 Touchdown Performance, Split-Axis Control

	PERCENT OF LANDINGS, PARAMETER OUT OF TOLERANCE							SUCCESSFUL (ATTEMPTS)
	X	Y	SPEED	SINKRATE	PITCH	BANK	HEADING	
LATERAL	0.	24.5	0.	0.	0.	7.5	4.7	67.0(106)
LONGITUDINAL	27.2	0.	42.7	26.2	5.8	0.	0.	34.0(103)
MANUAL CONTROL, ALL AXES	22.4	31.0	47.4	39.7	5.2	7.8	0.9	19.8(116)

significant at the $P < 0.01$ level. Table 4.9 separates the effects of manual control in the yaw and the pitch axes.

We cannot ascertain from the available data whether the poor landing performance was due to insufficient information presented by the displays, overloading of the pilot in the final stages of the landing, deficiencies in the simulation or some other causes. Some of our subjects executed consistently good landings, which seemed to indicate that the simulator could be landed successfully; some subjects, experienced pilots as they were, did not, however. Further study of the factors affecting pilots' performance in the final phases of the approach and during the flare maneuver is clearly necessary.

4.5 Applicability of the Results

We wished our findings to be applicable to the general population of pilots who fly low-visibility approaches in commercial jet transport aircraft. Great care was taken, therefore, in designing the experiments, in the development of the simulator system and in the selection of subjects. These will be discussed in the following sections.

4.5.1 Experimental Design

The research consisted of two factorial experiments, a 4 x 3 workload measurement test and a 4 x 3 x 3 failure detection experiment. Two full-rank factorial experiments would have resulted in a total of 4x3 + 4x3x3 = 48 treatments per subject. This number was considered to be unrealistically large and, consequently, some high level interactions were partially confounded in the failure detection experiment: Each subject was presented only 18 of the 36 treatments, resulting in a total of 30 experimental treatments per subject. The particular treatments were assigned to individual subjects in a way that resulted in each pair of subjects being presented all the experimental treatments and thus each pair of subjects represented one experimental block.

We wished to estimate the accuracy of the significant differences found in these experiments. Following standard procedures (Cochran and Cox, 1968, pp. 17-23) the *a posteriori* probability of significant differences being detected was calculated for the worst case, namely, the difference in detection times between the lateral and longitudinal axes. This case was considered worst as the mean difference (15.4 seconds or 37.04% of the mean detection time) and the number of replications (45) were the smallest.

The probability P was calculated by (*ibid.*):

$$t_{2(1-P)} = \frac{\delta}{(\frac{2}{r})^{\frac{1}{2}}\sigma} - t_{P_\alpha} \tag{4.3}$$

where t - Student's random variable

δ - mean of the detected difference

σ - standard error per unit

r - number of replications

and P_α - level of significance

From the analysis of variance of failure-detection times, the following values were obtained:

$\delta = 37.04\%$

$\sigma = 49.98\%$ with 156 d.f.

Letting, for this "worst case" computation, $P_\alpha = 0.05$ one has, for 156 d.f.,

$$t_{0.05,\phi=156} \simeq Z_{0.05} = 1.95996$$

hence

$$Z_{2(1-P)} = \frac{37.04}{(\frac{2}{45})^{\frac{1}{2}}(49.98)} - 1.95996 = 1.5537 \tag{4.4a}$$

or

$$2(1-P) \simeq 0.125 \qquad \therefore \quad P \simeq 93.7\% \tag{4.4b}$$

That is, the probability of a true difference being detected as a significant difference is quite high, and the number of replicates in the experiment was sufficient for the accuracy sought.

4.5.2 Simulator System

The simulator was intended to resemble a large transport jet aircraft in the final approach flight envelope. The actual flight parameters of a DC-8 were initially used and later modified, following a series of flight tests by an experienced Boeing-707 instructor captain. The flight tests included adjustment, with the aid of a stop-watch, of the simulated aircraft's throttle and control responses and of the effects of the flaps, landing gear and speed brakes.

A subjective evaluation was solicited of the pilots who flew the simulated aircraft (Appendix C and Figures 3.17-3.20). According to this evaluation, the simulated aircraft was rated as corresponding to 4.0 points on the Cooper-Harper rating scale (Cooper and Harper, 1969, p. 12). This rating represents an aircraft in which adequate performance is attainable with tolerable pilot workload but which has some annoying deficiencies. It should be kept in mind that the pilots evaluated the total aircraft system, including the intentionally simulated failures.

Due to technical and economic limitations, we used a fixed-base,

or static, simulator in this research. The case for the importance of motion cues in flight simulations has been made by many investigators (*cf.* Gibino, 1968; Jacobs *et al.*, 1973). Our main purpose in this research, however, was to document the pilot's failure detection performance. The simulated failures were very subtle and it is our belief that motion cues would not have aided the pilot in the detection task, especially in the presence of the noise introduced by turbulence and wind gusts, which are quite common during a bad-weather approach.

4.5.3 Subjects

All of the fifteen subjects who participated in the formal experiment were professional pilots from two major domestic airlines who were highly motivated, enthusiastic and intelligent. All but four flew jet transport aircraft regularly; the four who did not (one pilot who flew turbo-prop transport aircraft, two second officers and one retired captain) did not reveal any difference in performance (RMS tracking errors, workload scores, touchdown performance and failure detection times) when compared to the other pilots. We are convinced that our subjects were a representative sample of the population of airline pilots.

CHAPTER V

SUMMARY AND CONCLUSIONS

5.1 Summary

In the last decade, a great deal of thought has been given to Category III landings and their implications. One area of intensive investigation centers around the role of the crew during the approach. Current thought is polarized around two extremes:

1. The crew is in the control loop and flies the aircraft in accordance with instrument-generated steering signals.

2. Steering signals are coupled directly into the autopilot, with the crew monitoring the system.

It is axiomatic that a pilot should be capable of detecting and identifying failures in the landing guidance system accurately, reliably and with minimal time delay. The purpose of this research was the study of the pilot's short-term decisions regarding performance assessment and failure monitoring. We wished to investigate the relationship between the pilot's ability to detect failures, his degree of participation in the control task and his overall workload

level. Also, we wished our findings to be applicable to the general population of pilots who fly low-visibility approaches in commercial jet transport aircraft.

To this end, this research consisted of an experimental investigation which was carried out in a static ground simulator. Fifteen airline pilots flew zero-visibility landing approaches with different degrees of automation and at different workload levels which were induced by simulated wind disturbances. The pilots' ability to detect failures and to provide a reliable manual back-up capability was monitored and recorded.

The data were analyzed to identify statistically significant relationships among the experimental treatments and the factors which produced the optimal performance were sought.

Two hypotheses were tested in this research:

1. Both the participation mode of the operator in the control task and his overall workload level affect his information processing capability. The effects, then, of the operator's participation mode and workload level on his failure detection performance are additive. Manual tracking will result in longer detection times than will

monitoring a coupled, automatic approach, and higher workloads will effect longer detection times than will low workload levels.

2. As the flight instruments display angular, rather than linear, deviations from the localizer course and from the glide-path, they increase in sensitivity as distance to touchdown decreases. In addition, the penalty for error increases with increased proximity to the ground. Additional processing demands are therefore placed on the pilot and hence his workload increases in inverse relationship to altitude or to distance-to-go.

To measure the pilot's workload, a "warning-light"-type subsidiary task was selected for this research. It consisted of two small red lights mounted above each other outside the subject's peripheral vision field, and a rocker thumb switch mounted on the left horn of the control yoke. The lights provided the stimuli. During the run the upper or lower light, with equal probability, was lit at a random time for a maximum of two seconds. A correct response by the subject to this stimulus consisted of turning the light off by a proper motion of the rocker thumb switch. The subject's responses were processed and converted into a workload index.

For the purpose of this research, a simulator capability

including a digital graphics computer and a fixed-base cockpit simulator has been developed. An integrated-cue flight director system has been designed for the simulator. Also, a two-axis autopilot has been incorporated into the simulation which is capable of flying ILS-coupled approaches, in either axis or in both axes, to touchdown. We also had the capability to add wind disturbances to the simulation to induce different workload levels. The simulation did not include any displays of a mode progress annunciator, movable bugs or a fault annunciator panel, nor were there any warning flags.

The experimental variables to be investigated in this study were the pilot's participation mode in the piloting task, the workload induced by the control dynamics and by external disturbances, and the pilot's failure detection performance. The experiment involved four levels of participation:

1. Passive monitoring.
2. Split axis, yaw manual.
3. Split axis, pitch manual.
4. Full manual control.

Three failure conditions were used:

1. No failure.
2. Failure in the yaw axis. In this condition the autopilot, if coupled, or the flight director would steer the aircraft away from

the localizer course.

3. Failure in the pitch axis, similar in nature to a failure in the yaw axis.

In addition there were three levels of wind disturbances.

The effects of the level of participation and of the wind diturbance on the pilot's workload were investigated in a full-rank 4 x 3 factorial experiment. The effects of the level of participation and of the wind disturbance on the pilot's failure detection performance were investigated in a separate 4 x 3 x 3, partially-confounded factorial experiment. The "no failure" condition was incorporated in the design so that the subjects would not anticipate a failure on each and every approach.

The following results were obtained:

1. The workload scores were sensitive to both participation mode and the presence of wind disturbances.

2. There was a very marked increase in workload scores at altitudes below 500 feet AGL, which was inversely related to distance-to-go. This increase was observed even in fully automatic approaches, which seems to indicate the effects, possibly, of the pilot's mental state arising from his awareness of the proximity of the ground, and, therefore, that a significant reduction in the pilot's workload at

low altitudes cannot be achieved by improved display design alone.

3. Detection times in a manually-controlled axis were significantly longer than detection times in an automatically-controlled axis.

4. Detection times for lateral failures were significantly longer than detection times for longitudinal failures at comparable workload levels. This result can possibly be attributed to some combination of the following factors:

a. A lateral failure, as simulated in our experiment, resulted in a one-dot deviation in approximately 100 seconds, while a longitudinal failure required only about 30 seconds to cause a one-dot deviation. The reasons for this are the differences in the dynamics of the simulated aircraft in the lateral and longitudinal axes and the larger linear distance represented by a one-dot lateral deviation (1.25°), compared to the distance represented by a one-dot longitudinal deviation (0.35°).

b. As the lowest altitude at which a failure was presented was 800 feet AGL, which corresponds to a distance of over 2 miles from the runway threshold, the pilots may have assigned, in that phase of the approach, a higher priority to vertical positioning of the simulated aircraft than to runway centerline alignment; consequently, they may have been more sensitive to excursions of the glide-slope deviation indicator.

c. Both position and rate information are directly available to the pilot in the vertical plane by means of the GSI and the vertical speed indicator, respectively. Lateral rate information, on the other hand, is available only indirectly by means of the heading displayed on the HSI; furthermore, this information is contaminated by extraneous inputs, such as lateral drift due to the wind. The ready availability of vertical rate information, which relieves the pilot of the need to generate a large phase lead, may be responsible, in part, for the better failure detection performance in the longitudinal axis.

5. Detection times increased in direct relationship to workload:

$$T_{detection} = 20.9 + 16.5\underline{M} + 15.4\underline{A} + 0.10WL$$

where $\underline{M} = \begin{cases} 1 & \text{if the failed axis is controlled manually} \\ 0 & \text{otherwise} \end{cases}$

$\underline{A} = \begin{cases} 1 & \text{if the failure occurs in the lateral axis} \\ 0 & \text{if the failure occurs in the longitudinal axis} \end{cases}$

WL = normalized workload index

and $T_{detection}$ is measured in seconds.

The model correlated with the data at the $P << 0.001$ level of significance.

6. Finally, the touchdown performance was poor under all

conditions, with the exception of the fully-automatic, no-failure case. Of the attempted landings, 67% were acceptable under the split-axis, yaw-manual mode of control; 34% were acceptable in the aplit-axis, pitch-manual mode and only 19.8% of the attempted landings were successful on fully-manual approaches. We could not ascertain from the available data whether the poor landing performance was due to insufficient information presented by the displays, overloading of the pilot in the final stages of the landing, deficiencies in the simulat[illegible] some other causes.

5.2 Conclusions

Our goal in this research was to identify the participation mode and workload level which optimize the pilot's failure-detection performance. For the failures considered here the results suggest that a coupled, fully-automatic landing with the lowest possible workload is called for in Category III operations, with the crew monitoring the progress of the landing via a cockpit display. Furthermore, as manual touchdown performance with the simulated conventional flight instruments was unacceptable by commercial operational standards, a failure in the automatic landing system may have to be followed by the initiation of a mandatory missed approach and a diversion to a better visibility alternate field, unless the required progress is

made in display design and technology to radically improve manual touchdown performance.

The detection times for pitch failures in a fully-automatic mode ranged in our experiments from 7 seconds to 56 seconds, with a mean of approximately 24 seconds. Yaw failures detection times under the same conditions - that is, a fully-automatic approach - ranged from 17 seconds to 52 seconds, with a mean of approximately 35 seconds. Assuming a rate of descent of 10 feet per second on the final approach, our data suggest that below Category I decision height a failure of the automatic landing system (as simulated in our study) may not be detected at all or, at least, it may not be detected in time to allow safe initiation of a missed approach. Performance monitors and fault annunciator panels may alleviate the problem somewhat and shorten detection times. They are inadequate at altitudes below 100 feet, however (Vreuls *et al.*, 1968*a*); also, they are not infallible, and additional warning lights and buzzers in the cockpit provide only more opportunities for malfunctions and for crew confusion.

One possible answer to the dilemma may lie in the Independent Landing Monitor concept. The monitor is completely independent of the guidance system and of current landing aids, thus reducing the probability of simultaneous failures. It presents to the crew a

perspective life-like synthesized analog display of the runway environment, enabling the pilot to monitor the performance of the automatic landing system or to fly the aircraft manually, following an autopilot failure, by reference to artificial visual cues. One proposed IIM system (Parks and Tubb, 1970) was based on microwave transmitters or radio reflectors installed along the runway edges. The display, when augmented with aiding symbology (*cf.* Van Houtte, 1970) may lead to safe Category III operations.

5.3 Recommendations for Further Research

A very marked increase in workload scores at altitudes below 500 feet has been observed, even on fully-automatic approaches. As the pilot's failure detection performance was shown to be inversely related to his workload, this phenomenon should be carefully investigated and its causes identified; an effort should be made to reduce the flying pilot's workload during the final phases of the approach, either through display design or by crew task allocation.

The pilot's failure-detection performance should be investigated at a constant workload level, to validate our findings. An invariant workload level across participation modes can be induced, possibly, by a cross-adaptive concomitant loading task.

In our experiments the failure detection performance in the longitudinal axis was significantly better than in the lateral axis. One possible explanation of this result (see Section 5.1) is the availability of explicit rate information in the longitudinal axis. This hypothesis should be tested and, if verified, the findings should be applied to the design of the lateral deviation instruments.

As stated in Sections 3.3 and 4.3 all missed alarms occurred in manually-controlled axes; no failures were missed when the failed axis was under automatic control. An attempt to explain this result by variations in the signal-to-noise ratio of the displayed tracking error failed, as the RMS tracking errors on approaches which resulted in missed alarms were not statistically different from the tracking errors on other approaches under comparable experimental conditions. Other possible explanations of the difference in missed alarm performance between manually- and automatically-controlled axes may be:

1. As detection times in manually-controlled axes were longer than detection times in automatically-controlled axes, there was a higher probability when the failed axis was controlled manually that the approach would terminate (at touchdown) prior to detection. This explanation leaves something to be desired as it does not address the question of the basic cause of the difference in detection performance

between manually- and automatically-controlled axes.

2. When faced with simultaneous demands for monitoring and control the pilot may divide his attention between the two tasks. Under such "single channel" theory the fraction of attention allotted to one of these tasks is not available to the other (even though the pilot derives the information for both tasks from the same set of displays), thus resulting in a better failure detection performance when an axis is monitored by the pilot (and controlled automatically) as compared to simultaneous monitoring and control.

Further study is clearly necessary to effect a better understanding of the causes of the reported missed-alarm performance and their implications in the context of low-visibility landings.

Finally, the behavior of the pilot during the last phases of the approach is not well understood. Factors affecting the pilot's touchdown performance should be studied and his information requirements and processing mechanisms identified, as a prerequisite to pilot-aircraft interface design; the design must be optimized if future Category III operations are to maintain the excellent safety record of commercial aviation.

APPENDIX A

SIMULATOR DYNAMICS

A.1 Equations of Motion

In order to describe fully the motion of a rigid airplane, three frames of reference were used. They were the body-fixed frame of reference and the cartesian axes ξ, η and ζ associated with it; the so-called wind frame of reference and the spherical coordinates ξ_v, γ and ψ associated with it; and the inertial earth-fixed frame of reference and the cartesian coordinates X, Y and Z associated with it.

A.1.1 Body-Fixed Frame

In the body-fixed frame of reference ξ is the longitudinal axis of the airplane, positive forward; η is the pitch axis, positive to the right; and ζ is the yaw axis, positive down, thus completing a right-handed orthogonal triad.

In this coordinate system, assuming small angular rates, one has:

$$\dot{p} = \ell/I_{\xi} \tag{A.1}$$

$$\dot{q} = m/I_{\eta} \tag{A.2}$$

$$\dot{r} = n/I_{\zeta} \tag{A.3}$$

where p, q and r are the angular velocities around the ξ, η and ζ axes, respectively,

ℓ, m and n are the moments

and I_{ξ}, I_{η} and I_{ζ} are the principal moments of inertia.

A.1.2 Local-Wind Spherical Coordinates

In the local-wind frame of reference ξ_v is along the velocity vector $\bar{v}$, γ is the angle, in a vertical plane, between ξ_v and the local horizontal, positive upward; and ψ is the heading azimuth angle of the velocity vector, measured clockwise from the north. The relationship between the body-fixed and wind frames is shown in Figure A.1. Transforming vectors from the body-fixed coordinate system to the spherical wind coordinates, one has (Miele, 1962):

$$\dot{\alpha} = q\cos\beta - p\sin\beta - \dot{\gamma}\cos\phi - \dot{\psi}\cos\gamma\sin\phi \tag{A.4}$$

$$\dot{\beta} = \dot{\psi}(\cos\gamma\cos\phi\cos\alpha - \sin\gamma\sin\alpha) - \dot{\gamma}\sin\phi\cos\alpha - r \tag{A.5}$$

$$\dot{\phi} = p\cos\beta\cos\alpha + q\sin\beta\cos\alpha - \dot{\gamma}\sin\alpha - \dot{\psi}\sin\gamma \tag{A.6}$$

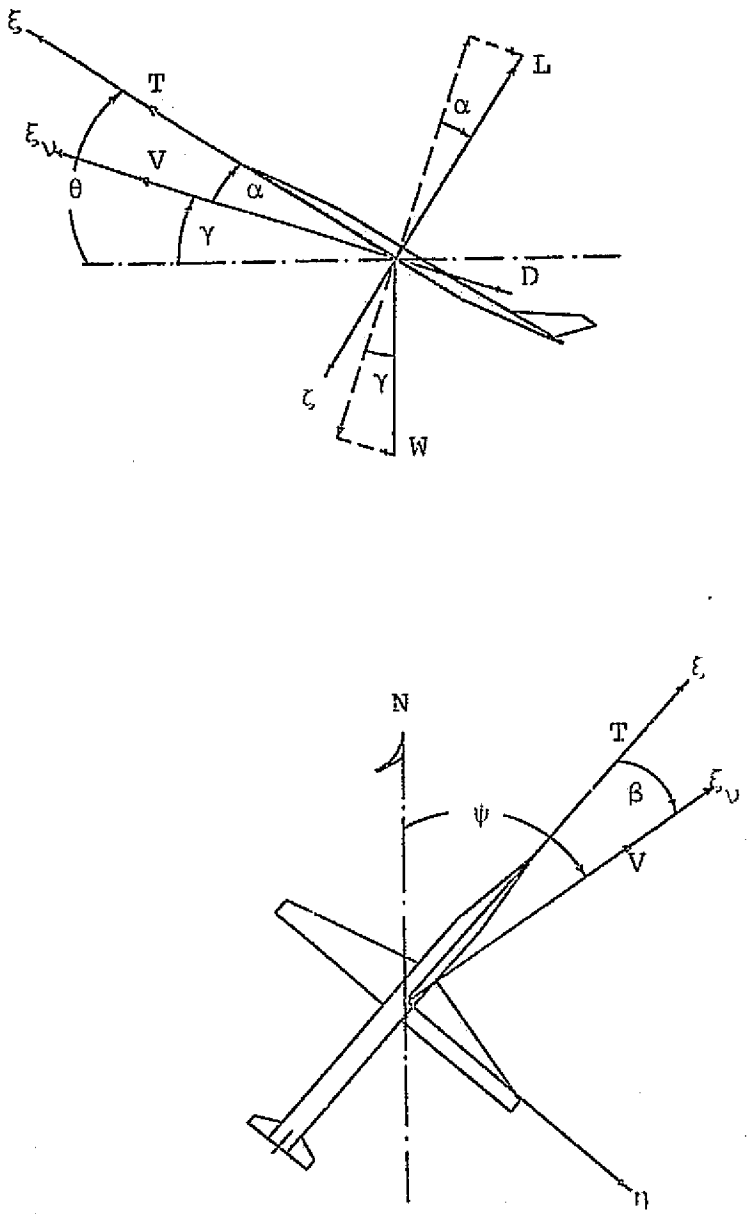

Fig. A.1 Body-Fixed and Local Wind Reference Frames

While the equations of motion in the wind coordinates are

$$\dot{V} = \frac{g}{W} (T \cos\beta \cos\alpha - D - L \sin\alpha - W \sin\gamma) \tag{A.7}$$

$$\dot{\psi} = \frac{g}{W V \cos\gamma} (-T \sin\beta \cos\phi \cos\alpha + L \sin\phi) \tag{A.8}$$

$$\dot{\gamma} = \frac{g}{W V} \{(T \sin\alpha \cos\beta + L \cos\alpha)\cos\phi - W \cos\gamma\} \tag{A.9}$$

and

$$\theta = (\alpha + \gamma)\cos\phi + \beta\sin\phi \tag{A.10}$$

where α - angle of attack

β - side-slip angle

ϕ - bank angle

θ - pitch angle

g - gravitational acceleration

W - aircraft weight

T - thrust

L - lift

D - drag

Equations A.1 through A.9 were developed under the following assumptions:

1. The aircraft has a left-right symmetry.

2. All engines produce equal thrust, and the resultant thrust axis coincides with the aircraft's longitudinal axis.

3. All rates of rotation are small and hence, all products of inertia are negligible.

4. Fuselage side forces and secondary forces produced by air hitting the jet intakes at an angle to the thrust axis are negligible.

5. Effects of curvature of the flight path due to motion about the earth are negligible.

A.1.3 Aerodynamic Forces and Moments

The aerodynamic lift and drag forces appearing in Equations A.1 through A.9 were defined as follows:

$$L = \frac{1}{2}\rho S C_\ell V^2 \qquad (A.11)$$

$$D = \frac{1}{2}\rho S C_d V^2 \qquad (A.12)$$

where ρ - density of air

S - wing area

C_ℓ, C_d - coefficients of lift and drag, respectively

As this model was meant for use in final approach studies ρ was assumed to remain constant at 0.0023 $lb.sec^2/ft^4$. The lift-curve of the wing was assumed to be piece-wise linear with the

angle of attack (see Figure A.2) and consequently, a lumped coefficient of lift C_L^*

$$C_L^* \triangleq \frac{1}{2}\rho S \partial C_\ell / \partial \alpha \tag{A.13}$$

and a lumped coefficient of drag C_D^*

$$C_D^* \triangleq \frac{1}{2}\rho S \partial C_d / \partial \alpha \tag{A.14}$$

were introduced. The final relationships for the lift and drag forces were then

$$\begin{aligned} L &= C_L^* \alpha V^2 && 0 < \alpha \leq 23^\circ \\ &= \frac{(C_L^*)_{\alpha=23^\circ}}{5}(28^\circ - \alpha)V^2 && 23^\circ < \alpha \leq 27^\circ \\ &= 0 && 27^\circ < \alpha \end{aligned} \tag{A.15}$$

$$D = C_D^* \alpha V^2 \tag{A.16}$$

The lumped coefficient of lift was a function of flaps position

$$C_L^* = C_{L_0}^* + C_{L_F}^* F \tag{A.17}$$

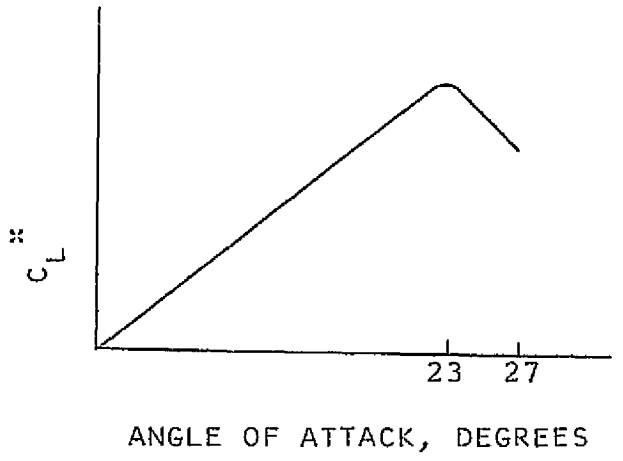

Fig. A.2 Simulated Lift Curve

The lumped coefficient of drag was a function of flaps position, landing gear position and speed brake position

$$C_D^* = C_{D_0}^* + C_{D_f}^* F + C_{D_g}^* G + C_{D_s}^* S \tag{A.18}$$

In addition, ground effect was included in the model, obeying the relationship

$$C_L = C_L^*\left(1 + \frac{k_g - \dot{h}/k_{\dot{h}}}{h + k_h}\right) \tag{A.19}$$

where h is the altitude and k_g, k_h and $k_{\dot{h}}$ are constant coefficients. The aerodynamic moments ℓ, m and n were computed by passing the appropriate control deflections through a simple gain

$$\ell = (k_{\ell\ell}\phi_c + k_{\ell n}\psi_c)V^2 \tag{A.20}$$

$$m = k_{m\theta_c}V^2 + \frac{1}{P_k}(L\cos\alpha\cos\phi - \omega\cos\gamma) \tag{A.21}$$

(taking into account pitching moments caused by lift and by the fact that the center of gravity is located forward of the aerodynamic center)

$$n = \{k_{nn}(\psi_c + \beta - k_{\frac{r}{rV}}) - k_{n\ell}\phi_c\}V^2 \tag{A.22}$$

(including a yaw damper in the model).

In Equations A.20 - A.22, ϕ_c, θ_c, and ψ_c are the roll, pitch and yaw commands, respectively, and $k_{\ell\ell}$, $k_{\ell n}$, k_m, P_k, k_r and $k_{n\ell}$ are constants.

As a first approximation, the parameters of a DC-8 were used in the equations of motion (Teper, 1969). The various parameters were later refined following a series of flight tests by an American Airlines senior instructor captain with considerable Boeing 707-123 experience. The actual values can be found in Section A.5.

A.1.4 Earth-Fixed Frame

The origin of the earth-fixed coordinates for the model was set at the glide-slope touchdown point of runway 4R at Logan Airport in Boston. In this frame of reference X lies along the runway center-line, positive toward the far end of the runway; Y is normal to it in the horizontal plane, positive to the right; and Z is normal to both X and Y, positive up, thus completing a left-handed orthogonal triad. The earth-fixed coordinates are shown in Figure A.3 together with various landmarks and navigation aids.

The geometry of the runway environment is defined, in this coordinate system, by:

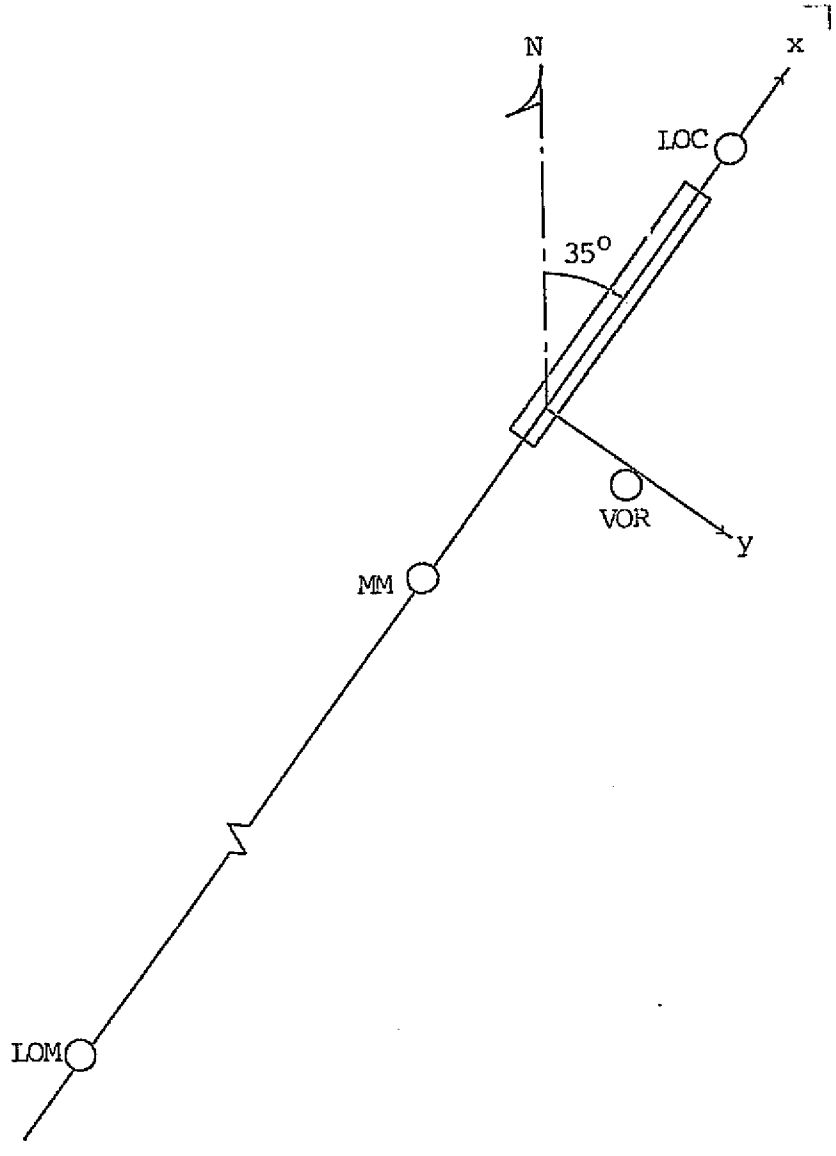

Fig. A.3 Runway Environment

Localizer antenna is at X = 7500 feet, Y = 0

Runway threshold is at X = -1153 feet

Middle marker is at X = -4800 feet, Y = 0

Outer marker is at X = -5.49 n.m., Y = 0

Boston VOR is at X = -250 feet, Y = 4200 feet

Glideslope beam originates at X = 0, and the glide-slope angle is 3.03°.

All approaches began at X = -12 n.m., Y = -1 n.m. and Z = 2500 feet, at aircraft heading and course of 65°. This course resulted in localizer interception angle of 30° at approximately 11 n.m. from the runway threshold, well beyond the outer marker.

By simple transformation of the spherical wind axes one obtains the kinematic equations of motion of the airplane's center of gravity in the earth-fixed axes:

$$\dot{Z} = V \sin\gamma \tag{A.23}$$

$$\dot{X} = V \cos\gamma \cos(\psi - 35°) \tag{A.24}$$

$$\dot{Y} = V \cos\gamma \sin(\psi - 35°) \tag{A.25}$$

For the purpose of various measurements during the approach (see Section 2.6) an X^*-coordinate, distance from the runway threshold,

was introduced and defined by

$$X^{*} = X + 1153 \text{ feet} \tag{A.26}$$

A.2 Wind Disturbances

Both horizontal and vertical disturbances were modelled as random wind gusts. A random numbers generator was incorporated in the computer program as follows:

Define

$$x'_{n+1} \triangleq (7701\, x'_n + 3927) \bmod (10000) \qquad x'_o = 7129 \tag{A.27}$$

to obtain a pseudo-random number in the range $0 \leq x'_n < 10000$ with the probability distribution shown in Figure A.4.

Define

$$x_n \triangleq \left(\frac{x'_n}{10000} - \frac{1}{2}\right)(2P) \qquad P << 10000 \tag{A.28}$$

to obtain a random number in the range $-P \leq x_n < P$ with the square probability distribution shown in Figure A.5.

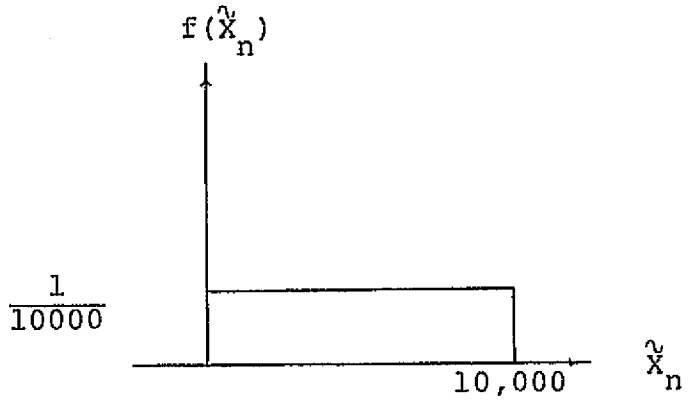

Fig. A.4 Probability Distribution of $\tilde{X}_n$

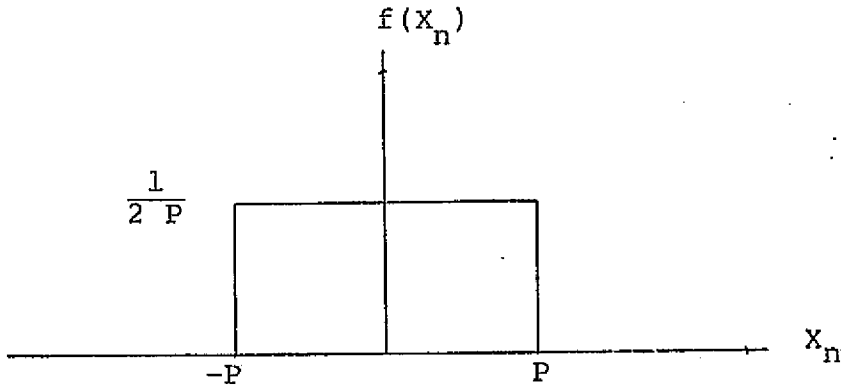

Fig. A.5 Probability Distribution of X_n

Since, for a square distribution,

$$\sigma_x^2 = (2P)^2/12$$

$$\therefore P = \sqrt{12}\,\sigma_x/2 \qquad \text{(A.29)}$$

The gust sequence y_n was obtained from the random sequence x_n by passing it through a first-order filter G(s):

$$G(s) = 1/(s + \omega_i) \qquad \text{(A.30)}$$

The output of the filter was sampled by the program at intervals of T seconds (the program's update rate), to obtain the gust sequence

$$y_{n+1} = e^{-\omega_i T} y_n + T x_{n+1} \qquad y_o = 0 \qquad \text{(A.31)}$$

Hence, the gust sequence has the following statistics:

$$\bar{y}_n = T\,\bar{x}_n \quad \text{but} \quad \bar{x}_n = 0 \quad \therefore \bar{y}_n = 0 \qquad \text{(A.32)}$$

$$\sigma_y^2 = e^{-2\omega_i T} \sigma_y^2 + T^2 \sigma_x^2 \qquad \text{(A.33)}$$

or

$$\frac{\sigma_x}{\sigma_y} = \frac{(1 - e^{-2\omega_i T})^{\frac{1}{2}}}{T} \qquad \text{(A.34)}$$

It was desired that the wind gusts y_n should not exceed some preset maximum value V_{max} 99.75% of the time (which, for normal distributions, corresponds to $3\sigma_y$). Therefore, $\sigma_y = V_{max}/3$ and

$$\sigma_x = \frac{V_{max}}{3} (1 - e^{-2\omega_i T})^{\frac{1}{2}}/T \tag{A.35}$$

$$\therefore \quad P = \sqrt{12}\, \sigma_x/2 = \frac{\sqrt{12}}{2} \frac{V_{max}}{3} \frac{(1 - e^{-2\omega_i T})^{\frac{1}{2}}}{T}$$

$$= \frac{V_{max}}{T} \left(\frac{1 - e^{-2\omega_i T}}{3}\right)^{\frac{1}{2}} \tag{A.36}$$

The use of the normal distribution property is justified as the output of a linear filter has approximately normal statistics.

To summarize:

1. A random sequence was generated

$$x'_{n+1} = (7701\, x'_n + 3927) \bmod (10000) \qquad x'_o = 7129$$

2. A modified sequence was defined

$$x_n = \left(\frac{x'_n}{10000} - \frac{1}{2}\right) \frac{2V_{max}}{T} \left(\frac{1 - e^{-2\omega_i T}}{3}\right)^{\frac{1}{2}}$$

where V_{max} - the desired maximal gust velocity

ω_i - the gusts' cutoff frequency, set at $\pi/6$ rad/sec

and T - the program's update rate, ≈0.2 seconds.

3. The sequence x_n was passed through a filter G(s)

$$G(s) = \frac{1}{(s + \omega_i)}$$

to obtain the random wind gusts.

4. As a final step, a steady (constant) wind was superimposed on the gusts.

In a series of tests the actual mean and standard deviation of the generated gusts were found to be within less than 1.2% of the predicted values, even when as few as 150 sample points were used, and t- and F-tests could not reject the hypotheses that the actual statistics of the gusts were equivalent to the predicted ones. A typical time-history of the gusts over 200 seconds is shown in Figure A.6.

A.2.1 Dynamics

The aircraft was assumed to posses two separate motions:

1. Motion relative to the air (wind axes)

2. Motion of the air relative to the ground, defined by the wind speed V_w and its heading, ψ_w.

The vector addition of these two motions defined the motion of the

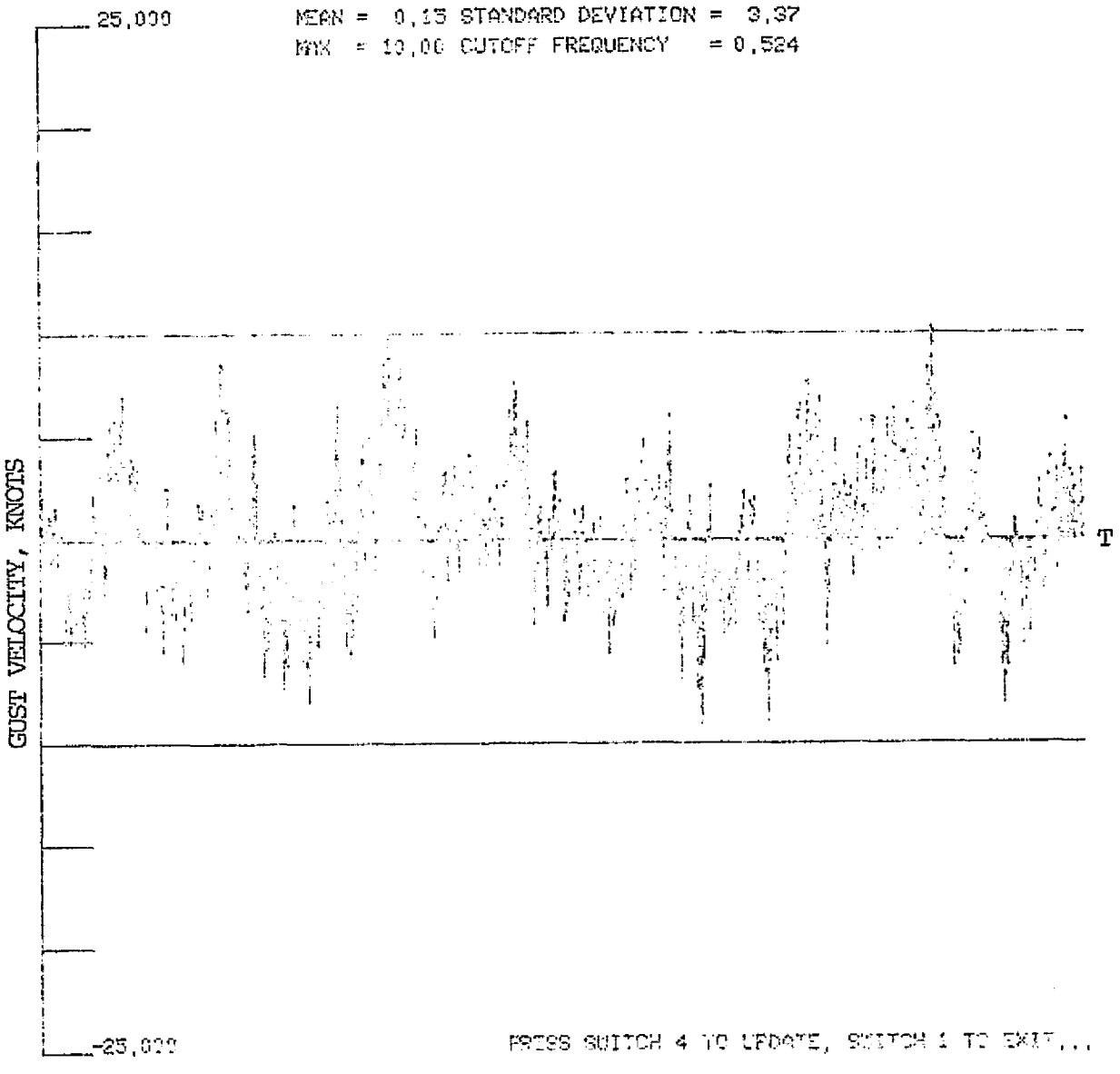

Figure A.6 Time History of Gust Disturbance

aircraft relative to the ground.

Also, if there was a component of the wind, V_{nw}, normal to the heading of the aircraft ψ, the aircraft was assumed to acquire a component of velocity V_n in that direction (normal to its heading) relative to the ground according to the relationship

$$\frac{V_n(s)}{V_{nw}(s)} = \frac{1}{\tau s + 1} \tag{A.37}$$

or

$$\dot{V}_n = \frac{1}{\tau}(V_{nw} - V_n) = \frac{1}{\tau}\{V_w \sin(\psi_w - \psi) - V_n\} \tag{A.38}$$

The ground speed, V_g, was then computed from the airspeed V_a and the wind velocity V_w:

$$V_g = V_a + V_w \cos(\psi_w - \psi) \tag{A.39}$$

and the total side-slip angle β_T is

$$\beta_T = \beta + \arctan(V_{nw} - V_n)/V_a \tag{A.40}$$

The components of the aircraft's ground speed along the principal earth axes were computed from

$$V_x = [V_a + V_w \cos(\psi_w - \psi)]\cos(\psi - 35°) - V_n \sin(\psi - 35°)$$
$$V_y = [V_a + V_w \cos(\psi_w - \psi)]\sin(\psi - 35°) - V_n \sin(\psi - 35°) \quad \text{(A.41)}$$

The geometry is illustrated in Figure A.7. For the purpose of the simulation, the following values were used:

τ = 1 second

ψ_w = 80° (45° to the runway heading, which was 35°)

and three values for V_w:

1. $V_w = 0$, $V_{max} = 0$ (no wind).
2. V_w = 5 knots steady wind plus gusts ranging between ±10 knots.
3. V_w = 10 kt. steady wind plus gusts ranging between ±20 knots.

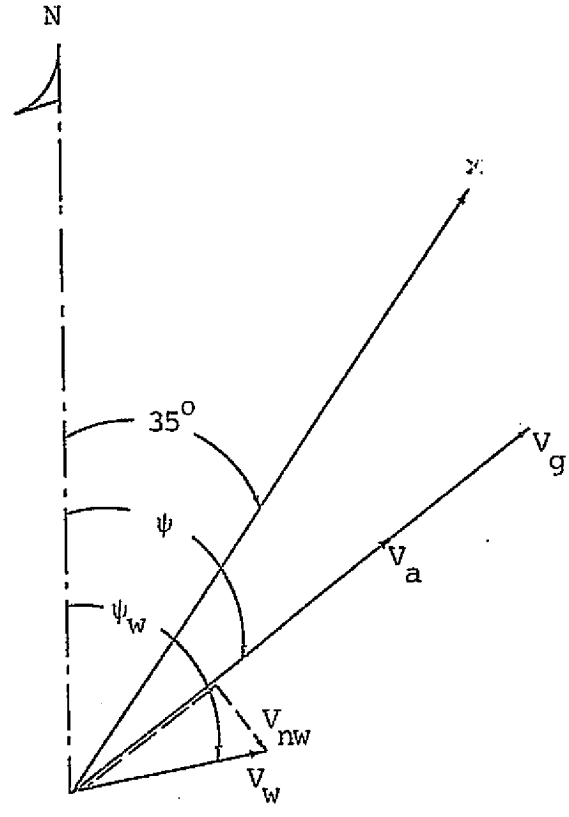

Fig. A.7 Geometry of Wind Environment

A.3 Flight Directors and Autopilot

An integrated-cue flight director display was used in the simulation. At the initiation of each approach the flight director was slaved to the artificial horizon and commanded the straight-and-level condition. The lateral (LOC) mode engaged automatically at two-dot deviation (2.5°) from the localizer course; the longitudinal mode (APPR) engaged at one-dot deviation (0.35°) from the glide slope. At an altitude of approximately 60 feet above the runway elevation the flare mode became operational and the letters FLR appeared on the flight director display.

A.3.1 Longitudinal Mode

First-order transfer was utilized in the longitudinal director (Weir and Klein, 1970):

$$FD_p = -3.6(0.0005\ h_e + \frac{0.5\ \dot{\theta}}{s + 0.034}) \tag{A.42}$$

where FD_p is the flight-director's pitch attitude command and h_e, the altitude deviation in feet from the glide path, was computed by

$$h_e \triangleq Z - X \tan(-3.03°) \tag{A.43}$$

and

$$\dot{h}_e = \dot{z} - \dot{x} \tan(-3.03°) \tag{A.44}$$

The time-rate of pitch, $\dot{\theta}$, in radians per second, was found from Equation A.10:

$$\dot{\theta} = (\dot{\alpha} + \dot{\gamma})\cos\phi + \dot{\beta} \sin\phi + [\beta \cos\phi - (\alpha + \gamma)\sin\phi]\dot{\phi} \tag{A.45}$$

The control sequence FD_p was mechanized digitally by a trapezoidal integration:

$$(\dot{FD}_p)_{n+1} = -3.6[0.0005(\dot{h}_e + 0.034\ h_e) + 0.5\ \dot{\theta}] - 0.034(FD_p)_n$$

and (A.46)

$$(FD_p)_{n+1} = (FD_p)_n + (\dot{FD}_p)_{n+1}\ \Delta t$$

A.3.2 Flare Path

During the flare maneuver it is desired to cause the aircraft to approach the ground asymptotically while following an exponential flight path. Referring to Figure A.8 one has

$$h = h_o\ e^{-t/\tau} + h_T \tag{A.47}$$

$$\therefore\ \dot{h} = -(h_o/\tau)e^{-t/\tau} \tag{A.48}$$

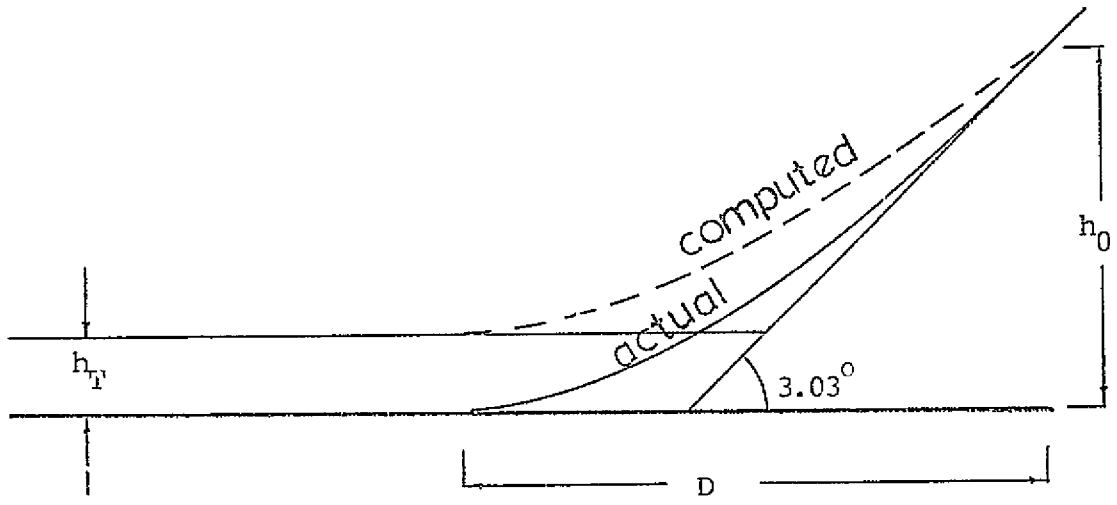

Fig. A.8 Flare Path

but, from Eq. A.47

$$h_o\, e^{-t/\tau} = h - h_T \tag{A.49}$$

$$\therefore\ \dot{h} = \frac{1}{\tau}\,(h - h_T)\cdot(-1) \tag{A.50}$$

and

$$h = h_T - \tau\dot{h} \tag{A.51}$$

Assuming that $h \approx h_T$ in N time-constants τ and that $\dot{X}$ is approximately invariant, then

$$D = N\cdot\tau\cdot\dot{X} \qquad \therefore\ \tau = D/N\dot{X} \tag{A.52}$$

and

$$h = h_T - D\cdot\dot{h}/(N\cdot\dot{X}) \tag{A.53}$$

at the initiation of the flare maneuver t=0 and

$$h_o = h_T - D\cdot\dot{h}_o/(N\cdot\dot{X}) \tag{A.54}$$

D is the distance downrange that the aircraft will travel between the initiation of flare and touchdown.

We introduced the bias h_T because of the delay in the response of the aircraft to control inputs: It is assumed that at touchdown the aircraft will be below the computed path by this amount.

Equation A.53 was used to compute the nominal path; deviations from this path were fed to the longitudinal flight director as altitude-error signals during the flare.

The parameters h_T, D and N were adjusted empirically. As $\dot{X} = V\cos\gamma$, $\dot{h}_o = V\sin\gamma$ one has, from Equation A.54

$$D = N\frac{h_o - h_T}{\tan(\gamma)} \tag{A.55}$$

On a nominal glide path $\gamma = 3.03°$; for the best touchdown performance, in terms of sink rate at touchdown and longitudinal dispersion, values of D = 2550 feet at N = 3 and h_T = 15 feet were used. These yielded a nominal flare altitude of 60 feet; the actual altitude at which flare command was to be initiated, based on the airplane's ground speed and sink rate, was computed in real time from Equation A.54.

A.3.3 Lateral Mode

Second-order transfer was utilized in the lateral flight director (*ibid.*):

$$FD_r = -0.2\cdot\left[\frac{a(b\dot{\psi} + c\dot{\phi} + d\dot{\varepsilon})}{(s + \tau_1)(s + \tau_2)} + f\phi + g\varepsilon\right] \tag{A.56}$$

where $a = 0.62$

$b = 8.6$

$c = 0.9$

$d = 180$

$f = 2.7$

$g = 15.6$

$\tau_1 = 1.06$

$\tau_2 = 0.16$

and where ε, the angular deviation in radians from the localizer course, was computed by

$$\varepsilon \triangleq Y/(-X) \qquad \text{(positive to the right)} \tag{A.57}$$

Now,

$$\frac{a}{(s+\tau_1)(s+\tau_2)} = \frac{R}{s+\tau_2} - \frac{R}{s+\tau_1}$$

$$R = \frac{a}{\tau_1 - \tau_2} = 0.6889 \tag{A.58}$$

and

$$FD_r = -0.2\left[\frac{R}{s+\tau_2}(b\dot{\psi} + c\ddot{\phi} + d\dot{\varepsilon}) - \frac{R}{s+\tau_1}(b\dot{\psi} + c\dot{\phi} + d\dot{\varepsilon}) + f\phi + g\varepsilon\right] \tag{A.59}$$

The control sequence FD_r was mechanized digitally by a trapezoidal numerical integration in a way similar to that of the longitudinal director (Equation A.46).

A.3.4 Autopilot

The autopilot was mechanized by feeding a function of the flight-director's commands as control inputs:

$$\theta_c = k_1 \, (FD_p) + k_2 \, (\dot{FD}_p) \tag{A.60}$$

$$\psi_c = k_3 \, (FD_r) + k_4 \, (\dot{FD}_r) \tag{A.61}$$

$$\phi_c = - \beta \tag{A.62}$$

At altitude of 200 feet the pitch autopilot stopped tracking the longitudinal flight director and maintained, instead, a glide path of 3.03° in an open-loop fashion until the flare maneuver was to be initiated; during the flare maneuver the lateral autopilot disengaged from the flight director and maintained wings-level attitude.

The autothrottles were mechanized by computing the appropriate thrust required to null the velocity time-rate-of-change (Eq. A.7) at a nominal reference airspeed (see Table A.1).

Table A.1 Approach Reference Speeds

Flaps, degrees	Reference Airspeed, Knots
0	170
30	150
50	130

A.4 Failures

Failures in the guidance system were simulated by feeding a constant bias deviation into the appropriate flight director system (but not into the raw-data indicators, that is, the CDI or the GSI). The bias was computed to correspond to one-dot deviation at the point of failure occurrence; from that point on, until the failure was correctly identified, the aircraft was guided to intercept and track a path parallel to the nominal path but translated by the amount of the bias, as shown in Figures A.9 and A.10. This enabled us to introduce failures at different altitudes without having the data contaminated by unwanted effects, such as differences in the aircraft's rate-of-turn or sink rate and in the rate of motion of the deviation indicators, following a failure.

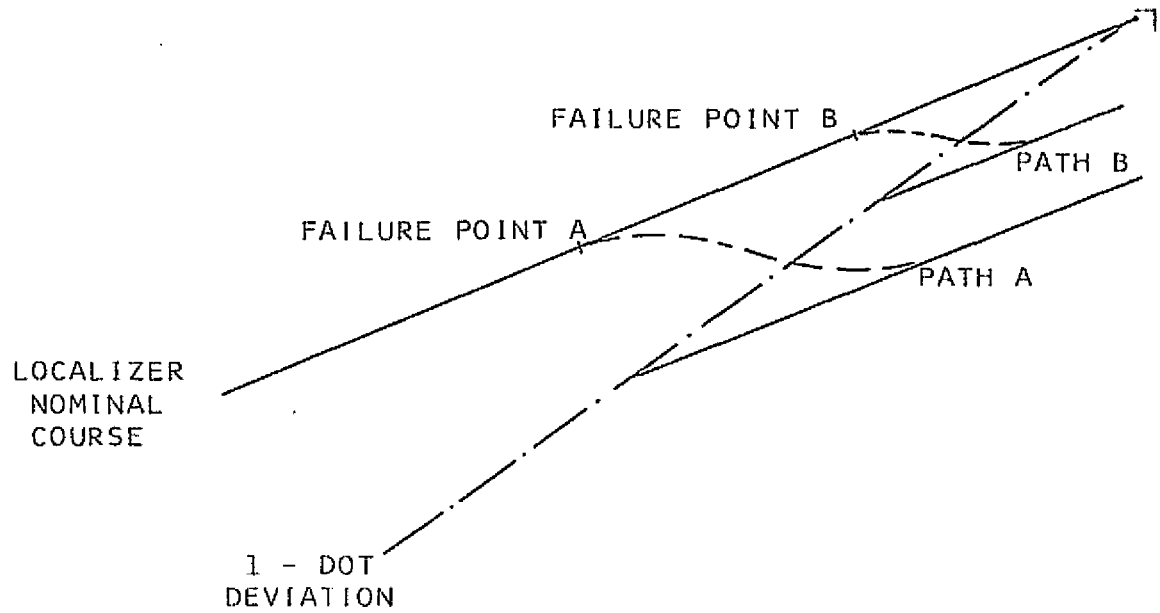

Fig. A.9 Schematics of Lateral Failure

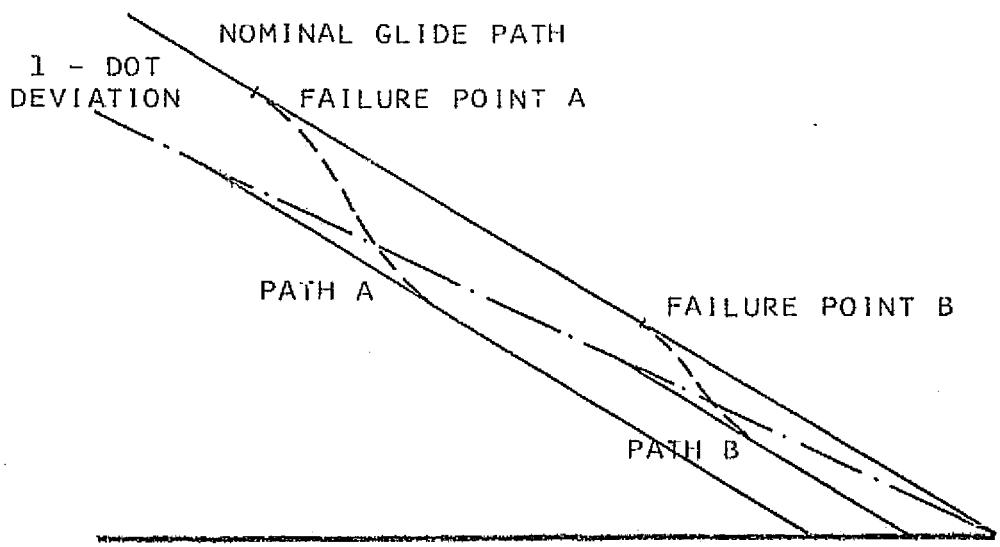

Fig. A.10 Schematics of Longitudinal Failure

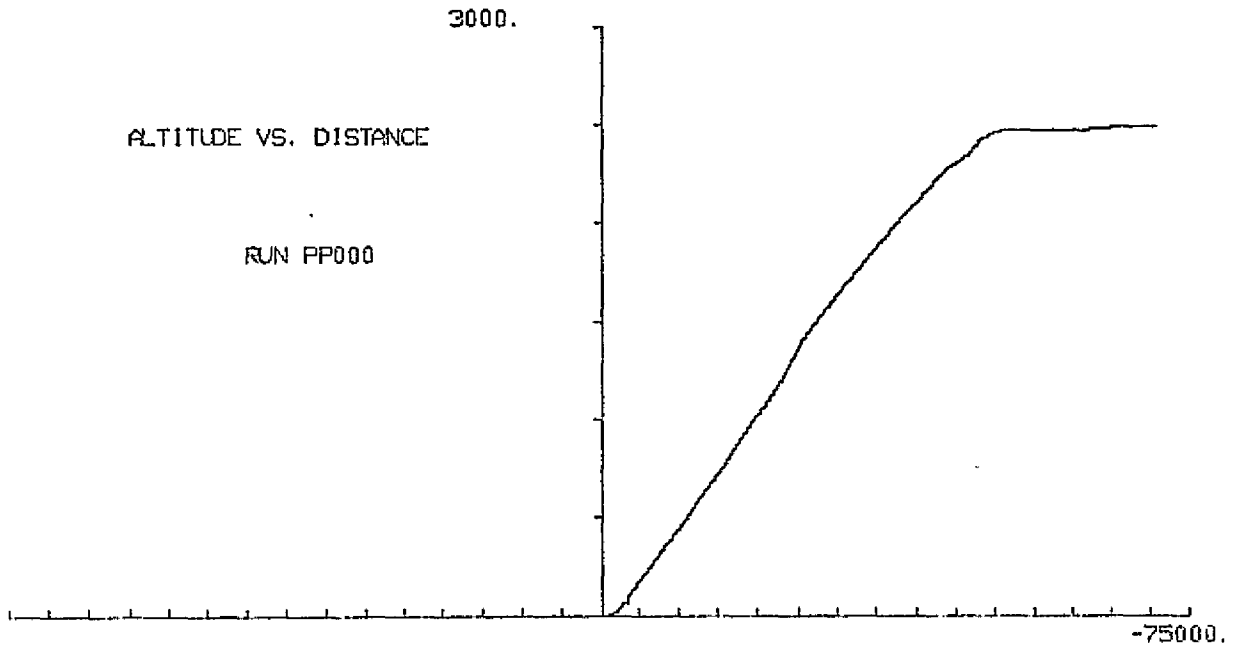

Figure A.11 Longitudinal Failure

(Autopilot control)

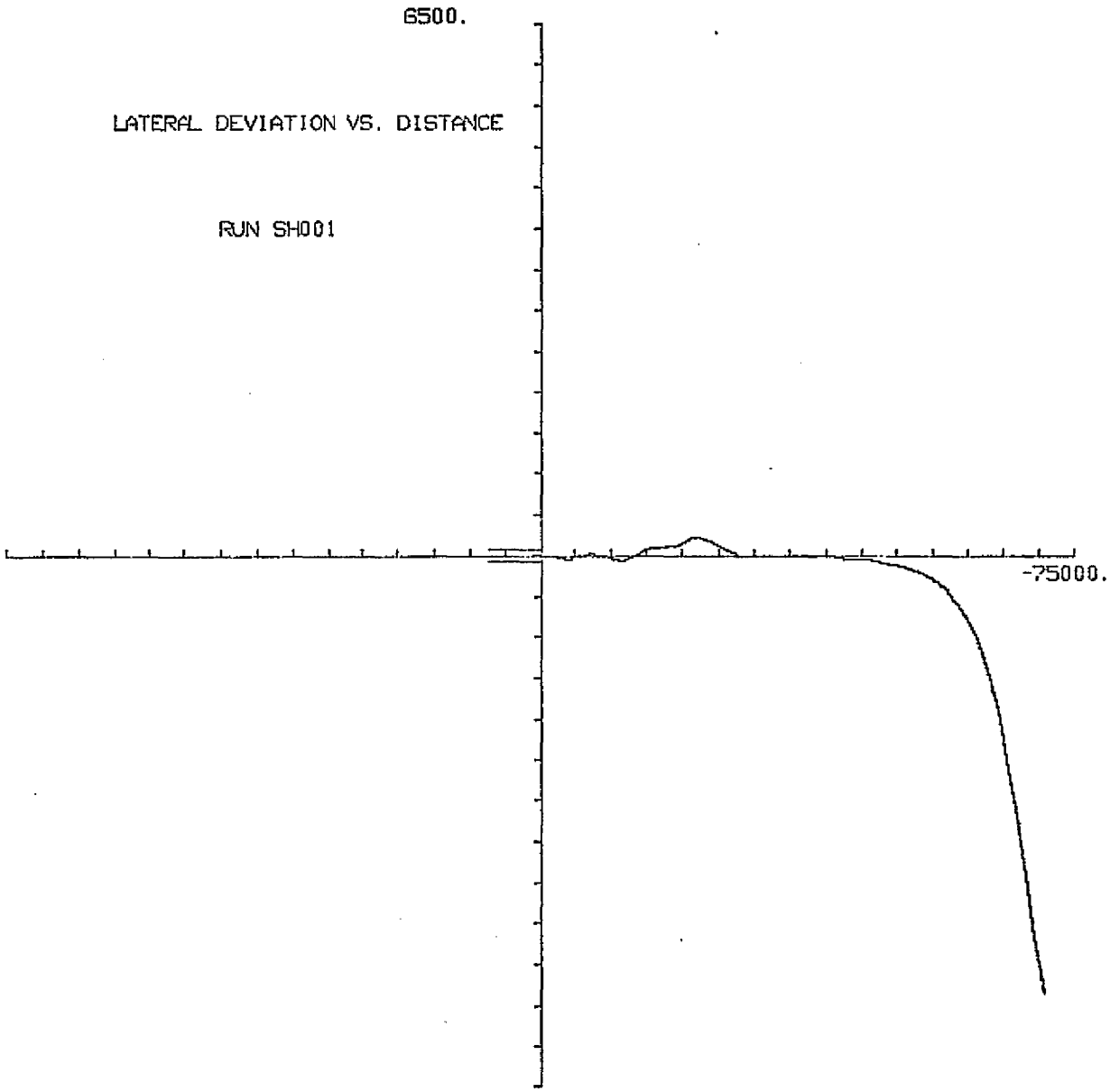

Figure A.12 Lateral Failure
(Autopilot control. Subject recovered manually)

When a failure occurred in a manually-controlled axis the pilot was guided by the flight director to intercept and track the new path. When the failure occurred in an autopilot-coupled axis the autopilot, driven by the flight director, tracked the new path. In each case the subject was expected to detect the failure by reference to the raw-data indicators, which did not fail. To this end the flight director display was biased out of view whenever the autopilot was coupled.

Failures were presented at altitudes between 1800 and 800 feet. The choice of altitudes was randomized, as were the order of presentation and the direction of the failure, i.e., left-right for a lateral failure and up-down for a longitudinal one.

A.5 Computer Programs

Three computer programs were used: A "No Failure" program which included the workload measurement subroutine, a "Pitch Failure" program and a "Yaw Failure" program; both of the latter accepted as inputs the altitude at which a failure was to occur and its direction. At the begining of each run the appropriate program was loaded from a console in a room adjacent to the simulator.

Documentation and listings of the programs are presented in the remainder of this Appendix.

```
      PROGRAM PNF
C
C***        PROGRAM: NO FAILURES
C
      GLOBAL ITIME,NF
      IMPLICIT FRACTION (F)
      LOGICAL CONE
      REAL FLAPS
L             OTSERRORS=SHORT
      COMMON/CSTASK/MSTSK,TOTTX,ETIME,LTON,NSWOLD,TIMEON,TIMEOFF
      COMMON/CNTRL/T,FLAPS,CTETA,CPHI,CXI,GEAR,AFLARE,SPBRK
      COMMON/CNTRL/BTETA,BPHI,BXI
      COMMON/PRMTR/V,XI,VG,VW,COSXW,SINXW,COS35,SIN35,BETAG,VNORM,CRAB
      COMMON/PRMTR/GAMMA,ALPHA,BETA,PHI,VX,VY,VZ,THETA,A,XM,Y,R
     1    /DPRMTR/DV,DXI,DGAMA,DALFA,DBETA,DPHI,DT,DVZ
     2    /ANG/SINA,SING,SINP,SINB,SINX,COSA,COSG,COSP,COSX
      COMMON/FRAC/FV,FBNK,FPICH,FA,FA100,FVZ,FHDG,FADF,FVOR,FCPICH
      COMMON/FRAC/FCBNK,FER,FHER,DME(5),MODE(6),FTETA0
      COMMON/FD/ADF,VOR,CPICH,CBNK,EPS,HER,RHO,GUST,THETA0
      COMMON/AUTO/DCBNK1,DCBNK2,DCPICH,CAPTR,GW,W,VZ0,,FLARE
      COMMON STORT(100),TOTT(150),STOPX(150),STORA(150),STORY(150)
      COMMON LOCT,LOCD,NI$$,XNIS$(100),XHIT(100)
      DATA RAD/57.296/,W/165000./,GW/0.0001155/
      DATA TMRKR1/0.4815/,TMPKR2/0.068/,TMRKR/0.0076/
      DATA TNGSA/-0.052933/
      DATA COSXW/0.173648/,SINXW/0.984808/
      DATA COS35/0.819152/,SIN35/0.573576/
      WRITE(10,2005)
      READ(10,2006,NAME
2005  FORMAT(' ENTER 5-LETTER CODE'/)
2006  FORMAT(A5)
      DECODE(5,2008,NAME,H)INAME
      IF(INAME.EQ.40404040408)NAME=NAME.R.18
      DECODE(5,2007,NAME,H)IDIST
2007  FORMAT(3X,I1)
2008  FORMAT(2X,A3)
      VW0=IDIST*5.
      PRAND=IDIST*11.6936
      IF(NAME.EQ.777777404OB)PRAND=0.
      ENTRY NF
C
C***        TURN OFF ALL LIGHTS AND SAMPLE SIDE-TASK SWITCH
C
    1 CONTINUE
A             ADEPT
              MDAR TURNOFF
              ARIC'A'F
              MDAR MSTASK
              S6AR'A'F
              JPLS MSTSKON
```

```
FORTRAN
      MSTSK=0
      GO TO 8
A           ADEPT
MSTASK:     0!H00200
MSTSKON:    NOOP
FORTRAN
      MSTSK=1
8     CONTINUE
C
C***        INITIALIZE ALL VALUES
C
      GAMMA=0.
      DGAMA=0.
      XI=65.
      PHI=0.
      FBNK=0.0F
      ALPHA=6.
      THETA0=4.
      BETAG=0.
      BETA=0.
      CRAB=0.
      A=2500.
      DRNG=2550.
      AFLARE=0.
      IFLARE=0
      IOM=INM=IIM=0
      JJFF=0
      ETIME=TOTTX=0.
      LOCT=LOCD=0
      LTON=MISS=NSWOLD=0
      TIMEON=5.
      TIMEOFF=2.
      XM=-12.
      Y=-6030.2
      VOR=43.047
      ADF=43.732
      VG=170.
      VX=VG*0.866026
      VY=VG*0.5
      VZ=0.
```

```
VZ0=-1.
IRNUM=7129
GUST=0.
VW=VW0+GUST
VNORM=0.
V=VG-VW*(COSXW*0.422618+SINXW*0.906308)
R=0.
THETA=ALPHA-2.
DIST=SQRT((XM+0.0411)**2+(Y/6080.2-0.6908)**2)
GSLOCK=0.
MODFD=""
LABEL(MODE)
ZSET(0.0F)
MOVE(0.23F,0.66F)
WRITE(16,556)MODFD
ENDLIST
LABEL(DME)
ZSET(0.F)
MOVE(-0.305F,-0.01434F)
WRITE(16,555)DIST
ENDLIST
XFEET=XM*6080.2
EPS=Y/(-(XM-1.23)*6080.2)
HEP=A-XFEET*(-0.052933)
CPICH1=CPICH=0.
DCPIC4=0.
CBNK1=CBNK=CBNK2=0.
DCBNK1=DCBNK2=0.
BTETA=BPHI=BXI=0.
CALL SAMPLE
BTETA=CTETA
BPHI=CPHI
BXI=CXI
CALL RTOF
CALL TRIG
```

```
C
C***        START THE DISPLAY
C
A           JPSR $GRAFX
A                $DIALS
A                5
C
C***        INITIALIZE DATA-UPDATE CLOCK
C
    2 ITIME=1
C
C***         ENTER WAIT LOOP IF SWITCH 8 (START) IS NOT ON
C
      IF(.NOT.SWITCH(8))GO TO 2
C
C***        EXECUTE UNLESS SWITCH 12 (FREEZE) IS ON
C
    6 IF(.NOT.SWITCH(12))GO TO 3
C
C***        AFTER SWITCH 12 HAS BEEN PRESSED, EXIT IF SWITCH 16 IS ON...
C
    7 IF(SWITCH(16))GO TO 4
C
C***        OR INITIALIZE VALUES IF SWITCH 4 (IC) IS ON...
C
      IF(SWITCH(4))GO TO 5
C
C***        OR START EXECUTION AGAIN IF SWITCH 8 IS ON...
C
      IF(SWITCH(8))GO TO 6
C
C***        OR INITIALIZE DATA-UPDATE CLOCK AND ENTER A WAITING LOOP
C
      ITIME=1
      GO TO 7
    5 CONTINUE
C
C***        STOP THE DISPLAY AND GO BACK TO INITIAL VALUES
C
A   JPSR $NHALT
A   NOOP
      GO TO 1
```

```
C
C***        START EXECUTION OF A NEW DATA-UPDATE CYCLE:
C***        COMPUTE DT (=TIME IN SECS OF PREVIOUS CYCLE)
C***        AND INITIALIZE DATA-UPDATE CLOCK
C
    3 TIME=ITIME
      ITIME=0
      DT=TIME/120.
      CALL DYNNF
      CALL TRIG
C
C***        COMPUTE RANDOM DISTURBANCE (GUSTS)
C
L     INTEGER*5=LONG
      IRNUM=MOD((7701*IRNUM+3927),10000)
      RNUM=IRNUM
L     INTEGER*5=SHORT
      DVW1=(RNUM/10000.-0.5)*PRAND
      GUST=GUST+(DVW1-0.10472*GUST)*DT
      VW=VW0+GUST
      XFEET=XW/6080.2
      IF(XFEET.EQ.0.)XFEET=1.
      YMILE=Y/6080.2
C
C***        COMPUTE THETA-DOT (=PITCH-ANGLE TIME-RATE OF CHANGE)
C
      TDOT=(DALFA+DGAMA)*COSP+DBETA*SINP+(BETA/RAD+COSP-(ALPHA+GAMMA)
     1 *SINP/RAD)*DPRI
C
C***        FLARE COMMAND COMPUTATION
C
      IF(IFLARE)33,35
35    DENOM=3.*                .3367
      AFLARE=AMAX1(                3.-DRNG*VZ/DENOM),120.)
      IF(A.GT.AF                 )GO TO 31
      IFLARE=1
```

```
      TAU=DRNG/DENOM
      VZ0=AMIN1((VZ+150.),-150.)
      CPICH1=0.
      MODFD="FLR."
      LABEL(MODE)
      ZSET(0.F)
      MOVE(0.23F,0.66F)
      WRITE(16,556)MODFD
      ENDLIST
556   FORMAT("@S",B4)
33    HER1=A+TAU*VZ-15.
      HEDOT=VZ/60.+TAU*DVZ
      GO TO 32
31    HER=A-XFEET*TNGSA
      HER1=HER
      HEDOT=VZ/60.+VX*1.68894*(-TNGSA)
C
C***        FLIGHT-DIRECTOR PITCH COMMAND
C
32    DCPICH=-0.6*(0.0005*(HEDOT+0.034*HER1)+0.5*TDOT)-0.034*CPICH1
      CPICH1A=CPICH1+DCPICH*DT
      DCPICH=(-0.6*(0.0005*(HEDOT+0.034*HER1)+0.5*TDOT)-0.034*
     1 CPICH1A+DCPICH)/2.
      CPICH1=CPICH1+DCPICH*DT
      CPICH=CPICH1+PAD*3.+(1.+IFLARE*(2.*ABS((VZ+150.)/VZ0)-1.))
      IF(IFLAPE)8001,8002
8001  IF(VZ.GT.-150.)CPICH=AMIN1(0.,(-ABS(CPICH)))
8002  CONTINUE
      IF(A.LE.AFLAPE)GO TO 22
C
C***        CENTER FLIGHT-DIRECTOR COMMAND-BARS IF OUTSIDE OF
C***        GLIDE-SLOPE RECEIVER RANGE
C
      CAPTR=1.
      IF(ABS(HER/XFEET).LE.0.006)GSLOCK=1.
      IF(GSLOCK)22,402
402   CONTINUE
      CPICH=-GAMMA
      DCPICH=-DGAMA
      CPICH1=0.
      CAPTR=0.
22    CONTINUE
      CPICH=AMOD(CPICH,360.)
```

```
C
C***          FLIGHT-DIRECTOR LATERAL COMMAND
C
      IF(XM.EQ.1.23)XM=1.2301
      EPS=YMILE/(1.23-XM)
      EPSDT=VX/3600.*YMILE/((XM-1.23)*(XM-1.23))-VY/3600./(XM-1.23)
      DCBNK1=-(0.1*(5.9244*DXI+3.32*DPHI+139.6*EPSDT
     1 +0.432*PHI/RAD+2.49*EPS)+0.16*CBNK1)
      DCBNK2=0.06889*(8.6*DXI+0.9*DPHI+180.*EPSDT)-1.06*CBNK2
      CBNK=CBNK+(DCBNK1+DCBNK2)*DT*RAD
      CBNK1=CBNK1+DCBNK1*DT
      CBNK2=CBNK2+DCBNK2*DT
      IF(ABS(EPS).LE.0.045)GO TO 21
      CBNK=CBNK1=CBNK2=DCBNK1=DCBNK2=0.
21    CONTINUE
      CBNK=AMOD(CBNK,360.)
      IF(XM.EQ.-5.4896)XM=-5.4895
C
C***          VOR, ADF AND DME INFORMATION
C
      ADF=35.-ATAN(YMILE/(-XM-5.4896))*PAD
      IF(XM.GT.-5.4896)ADF=ADF+180.
      IF(XM.EQ.-0.0411)XM=-0.0410
      VOR=35.-ATAN((YMILE-0.6908)/(-0.0411-XM))*PAD
      IF(XM.GT.-0.0411)VOR=VOR+180.
      ADF=AMOD(ADF,360.)
      VOR=AMOD(VOR,360.)
      CALL RTOF
      CALL STASK
      DIST=SQRT((XM+0.0411)**2+(YMILE-0.6908)**2)
      LABEL(DME)
      ZSET(0.07)
      MOVE(-0.105F,-0.01434F)
      WRITE(16,555)DIST
555   FORMAT("$",F4.1)
      ENDLIST
```

```
      CONE=.FALSE.
      IOM=IMM=IIM=0
      IF(EPS.LE.0.05.AND.EPS.GT.-0.05)CONE=.TRUE.
C
C***        TURN OUTER MARKER LIGHT ON
C
      IF(ABS(XM+5.4896).LE.TMRKR1.AND.CONE)IOM=1
C
C***        TURN MIDDLE MARKER LIGHT ON
C
      IF(ABS(XM+0.7896).LE.TMRKR2.AND.CONE)IMM=1
C
C***        TURN INNER MARKER LIGHT ON
C
      IF(ABS(XM+0.1896).LE.TMRKR.AND.   CONE )IIM=1
      CALL BEACONS(IOM,IMM,IIM,JJFF)
C
C***        EXIT IF ALTITUDE=0
C
      IF(A)4,4,6
    4 CONTINUE
C
C***        STOP THE DISPLAY, TURN ALL LIGHTS OFF
C
A        JPSR $NHALT
      CALL STASK
A        ADEPT
         MOAR TURNOFF
         ARIC'A'F
         JUMP .+2
TURNOFF: 77076!H57777
         NOOP
FORTRAN
      XFF=XM+6080.2+1153.
     %KDT=1./DT
```

```
C
C***        SHOW PARAMETERS AT TOUCHDOWN ON THE CRT SCREEN
C
      WRITE(25,2000)
      WRITE(25,2001)XFF,Y,V
      WRITE(25,2002)VZ
      WRITE(25,2004)AFLARE
      XI=XI-BETAG
      TRACK=XI+CRAB
      WRITE(25,2003)THETA,PHI,XI,TRACK,CRAB,DT,FDT,LOCD,LOCT,MISS
2000  FORMAT(/////27X,"PARAMETERS AT TOUCHDOWN OR AT STOPACTION"//)
2001  FORMAT(27X,"DISTANCE FROM THRESHOLD ",F15.0," FT."/
     1       27X,"DISTANCE FROM CENTERLINE",F15.0," FT."/
     2       27X,"INDICATED AIRSPEED      ",F15.0," KNOTS")
2002  FORMAT(27X,"VERTICAL SPEED          ",F15.0," FPM")
2004  FORMAT(27X,"FLARE COMMANDED AT ALT. ",F15.1," FT.")
2003  FORMAT( /27X,"PITCH ANGLE      ",F5.0," DEGS."/
     1          27X,"BANK ANGLE       ",F5.0," DEGS."/
     2          27X,"HEADING          ",F5.0," DEGS."/
     7          27X,"GROUND TRACK     ",F5.0," DEGS."/
     3          27X,"CRAB ANGLE       ",F5.0," DEGS."//
     4          27X,"    DT           =",F7.4/
     5          27X,"DATA UPDATE RATE =     ",I2/
     6          27X,"LOCD=",I3," HITS=",I3," MISS=",I3)
C
C***        OUTPUT FLIGHT DATA TO DISK
C
      IF(INAME.EQ.4040404040B)GO TO 601
      CALL OUTPUT
601   CONTINUE
      EXIT
```

```
      SUBROUTINE OUTPUT
C
C***        SUBROUTINE TO OUTPUT DATA TO DISK
C
      DIMENSION IBUFF(208)
      TDETECT=0.
      TIDENT=0.
      OPEN(21,0,2,0IBUFF,NAME)
      WRITE(21)XFF,Y,V,VZ,THETA,PHI,XI,CRAB,TDETECT,TIDENT,NAME
      WRITE(21)LOCD,(TOTT(I),STORX(I),STORA(I),STORY(I),I=1,LOCD)
      DO 1 K=1,50
      CONTINUE
1     CONTINUE
      CLOSE(21)
      OPEN(22,0,2,0IBUFF,'*HITSTASK*')
      WRITE(22)LOCT
      IF(LOCT.EQ.0)GO TO 130
      WRITE(22)(STORT(I),XHIT(I),I=1,LOCT)
130   CONTINUE
      DO 2 K=1,50
      CONTINUE
2     CONTINUE
      CLOSE(22)
      OPEN(23,0,2,0IBUFF,'*MISSTASK*')
      WRITE(23)MISS
      IF(MISS.EQ.0)GO TO 40
      WRITE(23)(XMISS(I),I=1,MISS)
40    CONTINUE
      DO 3 K=1,50
      CONTINUE
3     CONTINUE
      CLOSE(23)
      RETURN
      END
```

```
      SUBROUTINE SAMPLE
C
C***        SUBPOUTINE TO SAMPLE COCKPIT CONTROLS
C
      IMPLICIT FRACTION(F)
      REAL FLAPS
      COMMON/PRMTR/V,XI,VG,VW,COSXW,SINXW,COS35,SI 35,BETAG,VNORM,CRAB
      COMMON/CNTRL/T,FLAPS,CTETA,CPHI,CXI,GEAR,AFLARE,SPBRK
      COMMON/CNTRL GTETA,GPHI,GXI
A             ADEPT
              FPRI
              MD07'F 0
              0;0;0
              MD07'F 10
              0;0
              S5MD FSPBRK
              MD07'F 20
              0;0
              S5MD FT1
              MD07'F 40
              0;0
              S5MD FT2
              MD07'F 100
              0;0
              S5MD FT3
              MD07'F 200
              0;0
              S5MD FT4
              MD07'F 0
              0;0;0
              MD07'H C1
              0;0;0
              MD07'L; 1!H1
              0;0
              S5MD FFLAPS
              MD07'L; 1!H2
              0;0
              S5MD FYOKE
              MD07'L; 1!H4
              0;0
              S5MD FWHEEL
              MD07'L; 1!H10
              0;0
              S5MD FPEDL
              MD07'H C1
              0;0;0
              UPRI
```

```
            MDAR MASK
            S6AR'A'F
            ARAR'H'F
            JPLS DOWN
            MDAR ZERO
            ARMD FGEAR
            JUMP BACK
DOWN:       MDAR ONE
            ARMD FGEAR
            JUMP BACK
MASK:       00100!H0
ZERO:       0!H0
ONE:        0!H37777
FGEAR:      0
FSPBRK:     0
FT1:        0
FT2:        0
FT3:        0
FT4:        0
C1:         0!H00001
FFLAPS:     0
FYOKE:      0
FWHEEL:     0
FPEDL:      0
BACK:       NOOP
FORTRAN
      SPBRK=FTOR(FSPBRK)
      FLAPS=AMAX2(0.0F,FFLAPS)*2.5663
      CTETA=-FTOF(FYOKE)*18.75-BTETA
      CPHI=-FTOF(FWHEEL)*42.5-BPHI
      CXI=FTOF(FPEDL)*20.5-BXI
      THRUST=FTOR(FT1+FT2)+FTOF(FT3+FT4)
      IF(THRUST-1.048)201,201,200
200   T=60000.+(THRUST-1.048)*173)8.
      GO TO 203
201   T=60000.-(1.048-THRUST)*84821.
      IF(THRUST-.376)202,202,203
202   T=3000.-(.376-THRUST)*8108.
203   IF(V-200.)204,204,205
204   T=T*300./(V+100.)
      GO TO 206
205   T=T*(50000./(V*V+10000.))
206   GEAR=FTOF(FGEAR)
      RETURN
      END
```

```
      SUBROUTINE BEACONS(IOM,IMM,IIM,JJFF)
C
C***        SUBROUTINE TO OPERATE MARKER-BEACONS' LIGHTS
C
      IF(IOM.OR.IMM.OR.IIM)9,10
9     CONTINUE
      JJFF=JJFF+1
      GO TO (8,8,6,10),JJFF
8     CONTINUE
      IF(IOM)1,4
 4    IF(IMM)2,5
5     IF(IIM)3,6
C
C***        NONE OF THE LIGHTS SHOULD BE ON:
C***        TURN THEM ALL OFF
C
10    JJFF=0
6     CONTINUE
A     ADEPT
      MDAR BCN
      ARIC'A'F
      JUMP .+2
BCN:77277!H57777
      NOOP
FORTRAN
      GO TO 7
1     CONTINUE
A     MDAR OUTER
A     ARIC'O
      GO TO 7
2     CONTINUE
A     MDAR MIDLE
A     ARIC'O
      GO TO 7
3     CONTINUE
A     MDAR INNER
A     ARIC'O
      GO TO 7
A     ADEPT
OUTER:20000
MIDLE:00400!H
INNER:00100!H
FORTRAN
7     CONTINUE
      RETURN
      END
```

```
      SUBROUTINE STASK
C
C***        SUBROUTINE TO OPERATE THE WORK-LOAD SIDE-TASK.
C
      IMPLICIT FRACTION (F)
      COMMON/CSTASK/MSTSK,TOTTX,ETIME,LTON,NSWOLD,TIMEON,TIMEOFF
      COMMON/PRMTR/V,XI,VG,VW,COSXW,SINXW,COS35,SIN35,BETAG,VNORM,CRAB
      COMMON/PRMTR/GAMMA,ALPHA,BETA,PHI,VX,VY,VZ,THETA,A,XM,Y,R
      COMMON/DPRMTR/DV,DXI,DGAMA,DALFA,DBETA,DPHI,DT,DVZ
      COMMON STORT(100),TOTT(150),STORX(150),STORA(150),STORY(150)
      COMMON LOCT,LOCD,MISS,XMISS(100),XHIT(100)
C
C***        UPDATE RUNNING CLOCK AND LIGHT CLOCK
C
      TOTTX=TOTTX+DT
      IF(MSTSK>16,100
16    CONTINUE
      ETIME=ETIME+DT
C
C***        IS LIGHT ON?
C
      IF(LTON)1,2
1     CONTINUE
A         ADEPT
      MOAR MASKUP          [SAMPLE RESPONSE SWITCH
      S6AR'A'F             [IS IT UP?
      JPLS SWUP            [YES
      MOAR MASKDN
      S6AR'A'F
      JPLS SWDN            [IT IS DOWN
FORTRAN
C
C***        SWITCH IS NOT ON
C
      INSW=0
      GO TO 3
A        ADEPT
MASKUP:10000
MASKDN:04000
SWUP:  NOOP
```

```
FORTRAN
      INSW=2
      GO TO 3
A        ADEPT
SWDN:  NOOP
FORTRAN
      INSW=1
3     GO TO(7,5,4,14,5),INSW+LTON+1
C
C***        CORRECT RESPONSE
C
4     LOCT=LOCT+1
      STORT(LOCT)=ETIME
      XHIT(LOCT)=XM+6080.2+1153.
      GO TO 9
5     IF(INSW-NSWOLD)6,7
C
C***        INCORRECT RESPONSE
C
6     MISS=MISS+1
      XMISS(MISS)=XM+6080.2+1153.
      NSWOLD=INSW
7     IF(ETIME-TIMEOFF)100,8,8
C
C***        TIME TO TURN LIGHT OFF (WITHOUT CORRECT RESPONSE)
C
8     CONTINUE
      IF(NSWOLD)9,18
18    MISS=MISS+1
      XMISS(MISS)=XM+6080.2+1153.
9     CONTINUE
A        ADEPT
      MOVAR MASKOFF
      ARIC'A'F
      JUMP .+2
MASKOFF:77576!H77777
      NOOP
FORTRAN
C
C***        DETERMINE TIME TO TURN LIGHT ON AGAIN
C***        AND RESET LIGHT-CLOCK AND FLAG
C
      ETIME=0.
      TIMEON=AMOD(ABS(XM+6080.2),4.5)+0.5
      LTON=0
```

```
      GO TO 100
2     IF(ETIME-TIMEON)100,10,10
L   INTEGER*S=LONG
C
C***        TIME TO TURN LIGHT ON AGAIN: DETERMINE WHICH LIGHT
C
10    NXFEET=ABS(XM*6080.2)
      LTON=MOD(NXFEET,2)+1
L   INTEGER*S=$HORT
      GO TO (11,12),LTON
11    CONTINUE
A        ADEPT
      MDAR MASK2
      ARIC'O'F
      JUMP .+3
MASK2:00200!H
MASK3:00001!H
      NOOP
FORTRAN
      GO TO 13
12    CONTINUE
A     MDAR MASK3
A     ARIC'O'F
13    ETIME=0.
      INSW=NSWOLD=0
      GO TO 100
14    WRITE(10,15)
15    FORMAT(5X,' ERROR IN SWITCHING LOGIC')
100   CONTINUE
C
C***        STORE TOTAL ELAPSED TIME, X,A,AND Y AT 5 SEC
C***        INTERVALS; UNLESS ALTITUDE IS LESS THAN 150,
C***        IN WHICH CASE STORE THEM AT 1 SEC INTERVALS
C
      TINT=5.
      IF(A.LE.150.)TINT=1.
      IF(AMOD(TOTTX,TINT).GT.DT)GO TO 101
      LOCD=LOCD+1
      TOTT(LOCD)=TOTTX
      STORX(LOCD)=XM*6080.2+1153.
      STORA(LOCD)=A
      STORY(LOCD)=Y
101   CONTINUE
      RETURN
      END
```

```
      SUBROUTINE DYNMF
C
C***        DYNAMICS-COMPUTING SUBROUTINE
C
      GLOBAL DVZ,DT,MP,APP,P,Q,DR
      REAL L,FLAPS
      COMMON/CNTRL/T,FLAPS,CTETA,CPHI,CXI,GEAR,AFLARE,SPBRK
      COMMON/CNTRL/BTETA,BPHI,BXI
      COMMON/PPMTR/V,XI,VG,VW,COSXW,SINXW,COS35,SIN35,BETAG,VNORM,CRAB
      COMMON/PFMTR/GAMMA,ALPHA,BETA,PHI,VX,VY,VZ,THETA,A,XM,Y,R
      COMMON/DPRMTR/DV,DXI,DGAMA,DALFA,DBETA,DPHI,DT,DVZ
      COMMON/ANG/SINA,SING,SINP,SINB,SINX,COSA,COSG,COSP,COSX
      COMMON/AUTO/DCBNK1,DCBNK2,DCPICH,CNPTR,GW,W,V20,IFLARE
      COMMON/FD/ADF,VOR,CPICH,CBNK,EPS,HER,RAD,GUST,THETAJ
      CALL SAMPLE
C
C***        COMPUTE GROUND EFFECT AND ALT. EFFECT
C
      GREFF=1.+(0.6-VZ/583.)/(A+6.)
      A18=A/1800.
      AEFF=2.*A18-A18*A18
      VW=VW*AEFF
      CL=(0.6502+0.4902*FLAPS)*GPEFF
      CD=0.05+0.0789*FLAPS+0.0347*GEAR+0.157*SPBRK
      V2=V*V
      V=ABS(V-1.)+1.
C
C***        VERTICAL GUSTS CORRELATED TO LATERAL GUSTS
C
      GUSTZ=GUST/200./GREFF*AEFF
      ALFA1=ALPHA-GUSTZ
      D=CD*V2*AL.41
      ITETA=0
      IF(ALFA1.LE.23.)GO TO 9
      IF(ALFA1.LE.27.)GO TO 10
      L=0.
      GO TO 11
    9 L=CL*ALFA1*V2
      GO TO 11
   10 L=CL*4.60*(28.-ALFA1)*V2
   11 CONTINUE
C
C***        SAMPLE AUTOPILOT MODE-SELECT SWITCHES
C
A           ADEPT
       S&AR'F
       MDAR'A MSKAPP
       ARAR'H'F
       JPLS APP
       JUMP MP
```

```
MSKAPP:04000!H0
MSKAPR:02000!H0
APP:   NOOP
FORTRAN
C
C***  COMPUTE PITCH COMMAND
C
      ITETA=1
      IF(A.LT.200.,AND.A.GT.AFLARE)GO TO 12
      TCOM1=(3.-2.5*CAPTR)*CPICH+3.*DCPICH*RAD
      GO TO 15
12    TCOM1=-3.*(GAMMA+3.03)-3.*DGAMA*RAD
15    CONTINUE
      CTETA=AMIN1(10.,AMAX1(TCOM1,-10.))
A           ADEPT
MP:    NOOP
       S6AR'F
       MDAR'A MSKAPR
       ARAR'H'F
       JPLS APR
       JUMP MANR
APR:   NOOP
FORTRAN
C
C***        COMPUTE YAW AND ROLL COMMANDS
C
      CPHI=-BETA
      IF(A.LT.AFLARE)CPHI=-(PHI+DPHI*RAD*3.)
      CXI=CBNK+(DCBNK1+DCBNK2)*RAD*3.
      IF(A.LE.(-VZ/120.))CXI=(35.-XI+BETAG)*5.
A  MANR: NOOP
      P=(0.0107*CPHI+0.0057S+CXI)*V2/16386.656
      Q=(0.005+CTETA*V2+(L+COSA+COSP-W*COSG)/1000.)/15641.808
      DR=(0.03*(CXI+BETA-12490.53/V+R)-0.00183*CPHI)*V2/40966.64*DT
      R=R+DR
      IF(ITETA)13,14
13    CONTINUE
C
C***        COMPUTE THRUST IF IN AUTO PITCH MODE
C
      TC=170.
      IF(FLAPS.GT.0.5)TC=150.
      IF(FLAPS.GT.0.8)TC=130.
      IF(A.LE.5.)TC=120.
      T=((TC-V)/(20.*DT*GW)+D+L*SINA+W*SING)/COSA
      T=AMIN1(T,75000.)
```


C. 3

```
14    CONTINUE
      DVNORM=VW*(SINXW*COSX-COSXW*SINX)-VNORM
      VNORM=VNORM+DVNORM*DT
      DV=GW*(T*COSA-D-L*SINA-W*SING)*DT
      DXI=GW/V*COSG*(L*SINP-T*SINB*COSP*COSA+DVNORM)*DT
      DGAMA=GW/V*((L*COSA+T*SINA)*COSP-W*COSG)*DT
      DALFA=(Q-P*SINB)*DT-DGAMA*COSP-DXI*SINP*COSG
      DBETA=DXI*(COSA*COSG*COSP-SINA*SING)-DGAMA*COSA*SINP-R*DT
      DPHI=(P*COSA+D*SINB*COSA+R*SINA)*DT+DXI*SING
      XI=XI+DXI*RAD
      BETAG=BETAG+DBETA*RAD
      BETA=BETAG-DVNORM/V*RAD
      CRAB=BETAG+ATAN2(VNORM,VG)*RAD
      PHI=PHI+DPHI*RAD
      A=A+VZ/60.*DT
      XM=XM+VX/3600.*DT
      Y=Y+VY*1.68894*DT
      VG=VG+DV
      V=VG-VW*(COSXW*COSX+SINXW*SINX)
      VX=VG*COSG*(COS35*COSX+SIN35*SINX)
     1 -VNORM*(COS35*SINX-SIN35*COSX)
      VY=VG*COSG*(COS35*SINX-SIN35*COSX)
     1 +VNORM*(COS35*COSX+SIN35*SINX)
      VZ=VG*SING+101.3387
      DVZ=(DV*SING+VG*COSG*DGAMA)*1.68894/DT
      ALPHA=ALPHA+DALFA*RAD
      GAMMA=GAMMA+DGAMA*RAD+GUSTZ
      THETA=(ALPHA-2.*GAMMA)*COSP+BETA*SINP
      THETA0=(165000./CL/V2-2.*GAMMA)*COSP
      XI=AMOD(XI,360.)
      PHI=AMOD(PHI,360.)
      GAMMA=AMOD(GAMMA,360.)
      THETA=AMOD(THETA,360.)
      A=AMAX1(A,0.)
      RETURN
      END
```

```
      SUBROUTINE RTOF
C
C***        SUBROUTINE TO CONVERT DATA REAL-TO-FRACTION
C
      GLOBAL TRIG,FPICH1,FPCH1
      IMPLICIT FRACTION (F)
      COMMON/PRMTR/V,XI,VG,VW,COSXW,SINXW,COS35,SIN35,BETA3,VNORM,CRAB
      COMMON/PRMTR/GAMMA,ALPHA,BETA,PHI,VX,VY,VZ,THETA,A,XW,Y,R
      COMMON/ANG/SINA,SING,SINP,SINB,SINX,COSA,COSG,COSP,COSX
      COMMON/FRAC/FV,FBNK,FPICH,FA,FA100,FVZ,FHDG,FADF,FVOR,FCPICH
      COMMON/FRAC/FCBNK,FER,FHER,DME(5),MODE(6),FTETA0
      COMMON/FD/ADF,VOR,CPICH,CBNK,EPS,HER,RAD,GUST,THETA0
      FV=(200.-AMOD(V,400.))/200.
      FBNK1=PHI/360.
      FBNK=FBNK1+FBNK1
      FPICH1=-THETA/360.
      FPICH=FPICH1+FPICH1
      FTETA0=THETA0/180.
      IF(A.LT.0.)A=0.
      FA=(500.-AMOD(A,100.))/500.
      FA100=(5000.-AMOD(A,10000.))/5000.
      FVZ=-FMIN1(1.,AMAX1(VZ/4000.,-1.))
      FHDG1=AMOD((XI-BETAG),360.)/360.
      FHDG=FHDG1+FHDG1
      FADF1=-ADF/360.
      FADF=FADF1+FADF1
      FVOR1=-VOR/360.
      FVOR=FVOR1+FVOR1
C
C***        SAMPLE FLIGHT-DIRECTOR MODE SELECTOR
C
A           ADEPT
            S6AR'F'H
            MDAR'A MSKBTH
            JPLS FDON
            MDAR UNO
            ARMD FCPICH
            JUMP L2
FDON:       S6AR'F'H
            MDAR'A MSKFDP
            JPLS PON
            MDAR ZRO
            ARMD FCPICH
```

```
ROLL:       S6AR'F'H
            MDAR'A MSKFDR
            JPLS RON
            MDAR ZRO
            ARMD FCBNK
            JUMP L2
MSKBTH:     01400
MSKFDP:     01000
MSKFDR:     00400
ZRO:        0!H0
UNO:        0!H37777
RON:        NOOP
FORTRAN
      FPCH1=CPICH/360.
      FPCH1=FMIN2(0.1F,FMAX2(FPCH1,-0.1F))
      FCPICH=4.*FPCH1
A           JUMP ROLL
A   RON:    NOOP
      FBNK1=-CBNK/360.
      FBNK1=FMIN2(0.1F,FMAX2(FBNK1,-0.1F))
      FCBNK=FBNK1*4.
A   L2:     NOOP
      ERR=EPS*RAD
      TEMPP=AMAX1(ERR,-2.5)
      ERR=AMIN1(2.5,TEMPP)
      FER=-ERR*0.24
      IF(XM.EQ.0.)XM=0.0001
      AHER=HER*RAD/(XM*6080.2)
      TEMPP=AMAX1(AHER,-0.7)
      TEMP=AMIN1(0.7,TEMPP)
      FHER=TEMP*0.22857
      RETURN
```

```
      SUBROUTINE TRIG
C
C***        SUBROUTINE TO COMPUTE TRIG FUNCTIONS
C***        ONCE FOR EACH DATA-UPDATE CYCLE
C
      FRACTION COSN
      ALP=ALPHA/RAD
      ALP2=ALP*ALP
      SINA=ALP-ALP*ALP2/6.
      SINB=BETA/RAD
      COSA=1.-ALP/2.+ALP2*ALP2/24.
      FGAMA=GAMMA/360.
      FGAMA=FGAMA+FGAMA
      FPHI=PHI/360.
      FPHI=FPHI+FPHI
      FXI=XI/360.
      FXI=FXI+FXI
      SING=FSIN(FGAMA)
      COSG=FTOR(1$COSN)
      SINP=FSIN(FPHI)
      COSP=FTOR(1$COSN)
      SINX=FSIN(FXI)
      COSX=FTOR(1$COSN)
      RETURN
      END
```

```
      IMAGE DIALS
C
C***        SUBROUTINE TO DISPLAY THE INSTRUMENT PANEL
C
      INTEGER *FTIMX
      IMPLICIT FRACTION(F)
      COMMON/FRAC/FV,FBNK,FPICH,FA,FA100,FVZ,FHDG,FADF,FVOR,FCPICH
      COMMON/FRAC/FCBNK,FER,FHER,DME(5),MODE(6),FTETA0
      LINKAGE PTR(8),CBARS(12),LYNE(4),PNTR1(10),PNTR(20)
      LINKAGE GSI(8),LOCI(5),ADFN(10),VORN(10),HDNG(5)
C
C***        ADD FTIMX TO ITIME, TO UPDATE THE
C***        DATA-UPDATE CLOCK
C
      *ITIME=$ITIME+*FTIMX
      POSCHAR(0.2417F,-0.01434F,-0.3F,"0S35")
      POSCHAR(DME)
      POSCHAR(MODE)
      DY(FHER)
      TABLE2D(GSI)
      LDY(0.F)
      TABLE2D(HDNG)
      LDX(FER*0.2667F)
      TABLE2D(LOCI)
      LDX(-0.75F)
      LDY(0.49F)
      LSCL(0.275F)
      LRZ(FV)
      TABLE2D(PNTR)
      LDX(0.71F)
      LDY(0.52F)
      LSCL(0.28F)
      LRZ(FA)
      TABLE2D(PNTR)
      LRZ(FA100)
      TABLE2D(PNTR1)
      LDX(0.71826F)
      LDY(-0.20575F)
      LSCL(0.285F)
      LRZ(FVZ-0.5F)
      TABLE2D(PNTR)
```

```
                LDX(0.F)
                LDY(-0.323F)
                LSCL(0.33F)
                LRZ(FHDG)
                TABLE2D($COARD)
A               2DT BUG
                ROTZ(-0.19444F)
                DX(FER)
                TABLE2D(LYNE)
                LRZ(FHDG)
                LDX(-0.745F)
                LDY(-0.212F)
                LSCL(0.275F)
                ROTZ(FADF)
                TABLE2D(ADFN)
                ROTZ(FVOR-FADF)
                TABLE2D(VORN)
                LRZ(FHDG)
                TABLE2D($COARD)
                LDX(0.F)
                LDY(0.66F)
                LSCL(0.32F)
                LRZ(FBNK)
                TABLE2D(PTR)
                LSCL(1.0F)
                ROTX(FPICH)
                LAI(166,1.0F)
                LAI(178,0.5F)
                TABLE3D($HRZON)
                LSCL(0.32F)
                ROTX(FCPICH+FTETA0)
                ROTZ(FCBNK)
                TABLE2D(CBARS)
                TABLE2D(CBARS)
                RETURN
```

```
DATA2D(LYNE)
ZSET(0.0F)
LINE(0.F,0.43F,0.F,-0.5286F)
ENDLIST
ENDDATA

DATA2D(PNTR1)
ZSET(0.0F)
MOVE(-0.02F,0.04F)
DRAW(-0.02F,-0.3F)
DRAW(0.0F,-0.36F)
DRAW(0.02F,-0.3F)
DRAW(0.02F,0.04F)
DRAW(-0.02F,0.04F)
ENDLIST
ENDDATA

DATA2D(PNTR)
ZSET(0.0F)
MOVE(0.0F,-0.5F)
DRAW(-0.02F,-0.56F)
DRAW(-0.02F,-0.74F)
DRAW(0.0F,-0.9F)
DRAW(0.02F,-0.74F)
DRAW(0.02F,-0.56F)
DRAW(0.0F,-0.5F)
DRAW(0.0F,-0.26F)
DRAW(0.04F,-0.2F)
DRAW(0.04F,0.0F)
DRAW(0.06F,0.1F)
DRAW(-0.06F,0.1F)
DRAW(-0.04F,0.0F)
DRAW(-0.04F,-0.2F)
DRAW(0.0F,-0.26F)
MOVE(0.0F,0.0F)
DRAW(0.0F,0.0F)
ENDLIST
ENDDATA
```

```
DATA2D(GSI)
ZSET(0.0F)
MOVE(-0.3F,0.55F)
DRAW(-0.36F,0.59F)
DRAW(-0.3F,0.63F)
MOVE(-0.3F,-0.30F)
DRAW(-0.36F,-0.34F)
DRAW(-0.3F,-0.38F)
ENDLIST
ENDDATA

DATA2D(LOCI)
ZSET(0.0F)
MOVE(-0.04F,0.16F)
DRAW(0.0F,0.12F)
DRAW(0.04F,0 16F)
ENDLIST
ENDDATA

DATA2D(ADFN)
ZSET(0.0F)
MOVE(-0.1F,0.5F)
DRAW(-0.1F,-0.7F)
DRAW(0.0F,-0.8F)
DRAW(0.1F,-0.7F)
DRAW(0.1F,0.5F)
DRAW(-0.14F,0.5F)
DRAW(0.0F,0.8F)
DRAW(0.14F,0.5F)
DRAW(0.1F,0.5F)
MOVE(0.0F,0.9F)
DRAW(0.0F,0.8F)
MOVE(0.0F,0.0F)
DRAW(0.0F,0.0F)
MOVE(0.0F,-0.8F)
DRAW(0.0F,-0.9F)
ENDLIST
ENDDATA
```

```
      DATA2D(VORN)
      ZSET(0.0F)
      MOVE(0.0F,0.8F)
      DRAW(-0.04F,0.6F)
      DRAW(-0.04F,-0.8F)
      DRAW(0.04F,-0.8F)
      DRAW(0.04F,0.6F)
      DRAW(0.0F,0.8F)
      MOVE(0.0F,0.9F)
      DRAW(0.0F,-0.9F)
      ENDLIST
      ENDDATA
A     ADEPT
BUG: 0
    1631224426;163'221261;1314423345;1631224427
    2000026743;1146211662;1146215461;0631414431
    0767613244;1146215461;6631462316;6314655465
    6000013054;6000013055;6000013055;7000005462
    7000005463;7000005463;1000072314;1000072315
    1000072315;2000064022;2000064023;1777764023
FORTRAN

      DATA2D(PTR)
      ZSET(0.F)
      MOVE(0.F,0.8333F)
      DRAW(-0.15F,0.6667F)
      DRAW(0.15F,0.6667F)
      DRAW(0.0F,0.8333F)
      ENDLIST
      ENDDATA

      DATA2D(CBARS)
      ZSET(-1.0F)
      MOVE(0.0F,0.0F)
      DRAW(-0.75F,-0.37F)
      DRAW(-0.75F,-0.25F)
      DRAW(0.0F,0.0F)
      DRAW(0.75F,-0.37F)
      DRAW(0.75F,-0.25F)
      DRAW(0.0F,0.0F)
      ENDLIST
      ENDDATA
```

```
DATA2D(HDNG)
ZSET(0.0F)
MOVE(-0.015F,0.03625F)
DRAW(0.F,0.0025F)
DRAW(0.015F,0.03625F)
ENDLIST
ENDDATA
RETURN
END
```

```
      PROGRAM PFP
C
C***        PROGRAM: FAIL PITCH
C
      GLOBAL ITIME,FP
      IMPLICIT FRACTION (F)
      LOGICAL CONE
      REAL FLAPS
L             OTSERRORS=SHORT
      COMMON/CSTASK/MSTSK,TOTTX,ETIME,LTON,NSWOLD,TIMEON,TIMEOFF
      COMMON/CNTRL/T,FLAPS,CTETA,CPHI,CXI,GEAR,AFLARE,SPBRK
      COMMON/CNTPL/DTETA,DPHI,DXI
      COMMON/PRMTR/V,XI,VG,VW,COSXW,SINXW,COS35,SIN35,BETAG,VNORM,CRAB
      COMMON/PRMTR/GAMMA,ALPHA,BETA,PHI,VX,VY,VZ,THETA,A,XM,Y,R
      COMMON/DPRMTR/DV,DXI,DGAMA,DALFA,DBETA,DPHI,DT,DVZ
      COMMON/ANG/SINA,SINS,SINP,SINB,SINX,COSA,COSS,COSP,COSX
      COMMON/FRAC/FV,FBNK,FPICH,FA,FA100,FVZ,FHDS,FHDF,FVOR,FCPICH
      COMMON/FFAC/FCBNK,FER,FNER,DME(5),MODE(6),FTETH0
      COMMON/FD/ADF,VOR,CPICH,CBNK,CPS,HER,FAD,GUST,THETA0
      COMMON/AUTO/DCBNK1,DCBNK2,DCPICH,CAPTR,GW,W,VZ0,IFLARE
      COMMON LOCD,TOTT(150),STORX(150),STORA(150),STORY(150)
      DATA RAD/57.296/,W/165000./,GW/0.0001155/
      DATA TMPKP1/0.4915/,TMPKR2/0.069/,TMRKR/0.0976/
      DATA TNGSA/-0.052933/
      DATA COSXW/0.173648/,SINXW/0.984808/
      DATA COS35/0.819152/,SIN35/0.573576/
      WRITE(10,2005)
      READ(10,2006,NAME,AFAIL
2005  FORMAT(' ENTER 5-LETTER CODE AND ALT.:'/)
2006  FORMAT(A5/F6.0)
      DECODE(5,2008,NAME,H)INAME
      IF(INAME.EQ.4040404040B)NAME=NAME.R.18
      DECODE(5,2007,NAME,H)IDIST
2007  FORMAT(3X,I1)
2008  FORMAT(2X,A3)
      VW0=IDIST*5.
      PRAND=IDIST*11.6936
      IF(NAME.EQ.777777404QB)PRAND=0.
      ENTRY FP
```

```
C***        INITIALIZE ALL VALUES
    1 CONTINUE
A             ADEPT
              MDAR MSTSKON
              ARMD PRDET
              MDAR MSTASK
              ARMD SELECTOR
              MDAR TURNOFF
              ARIC'A'F
              MDAR MSTASK
              S6AR'A'F
              JPLS MSTSKON
FORTRAN
      MSTSK=0
      GO TO 8
A             ADEPT
MSTASK:       01H00200
MSTSKON:      NOOP
FORTRAN
8     CONTINUE
      MSTSK=0
      GAMMA=0.
      DGAMA=0.
      XI=65.
      PHI=0.
      FBNK=0.0F
      ALPHA=6.
      THETA0=4.
      BETAG=0.
      BETA=0.
      CRAB=0.
      A=2500.
      DRNG=2550.
      AFLARE=0.
      IFLARE=0
      ION=IMM=IIM=0
      JJFF=0
      ETIME=TOTTX=TDETECT=TIDENT=TFAIL=0.
      IFAIL=IDETECT=IDENT=0
      LOCT=LOCD=0
      LTON=MISS=NSWOLD=0
      TIMEON=5.
      TIMEOFF=2.
```

```
XM=-12.
Y=-6080.2
VOR=43.047
ADF=45.732
VG=170.
VX=VG*0.866026
VY=VG*0.5
VZ=0.
VZ0=-1.
IRNUM=7129
GUST=0.
VW=VW0+GUST
VNORM=0.
V=VG-VW*(COSXW*0.422618+SINXW*0.906308)
R=0.
THETA=ALPHA-2.
DIST=SQRT((XM+0.0411)**2+(Y/6080.2-0.6908)**2)
GSLOCK=0.
MODFD=""
LA?EL(MODE)
ZSET(0.0F)
MOVE(0.23F,0.66F)
WRITE(16,556)MODFD
ENDLIST
LABEL(DME)
ZSET(0.F)
MOVE(-0.305F,-0.01434F)
WRITE(16,555)DIST
ENDLIST
XFEET=XM*6080.2
EFS=Y/(-(XM-1.29)*6080.2)
HER=A-XFEET*TNGSA
CPICH1=CPICH=0.
DCPICH=0.
CBNK1=CBNK=CBNK2=0.
DCBNK1=DCBNK2=0.
BTETA=BPHI=BXI=0.
CALL SAMPLE
BTETA=CTETA
BPHI=CPHI
BXI=CXI
CALL RTOF
CALL TRIG
```

```
C***        START THE DISPLAY
A           JPSR $GRAFX
A                $DIALS
A                5
C***        INITIALIZE DATA-UPDATE CLOCK
    2 ITIME=1
C***         ENTER WAIT LOOP IF SWITCH 8 (START) IS NOT ON
      IF(.NOT.SWITCH(8))GO TO 2
C***        EXECUTE UNLESS SWITCH 12 (FREEZE) IS ON
    6 IF(.NOT.SWITCH(12))GO TO 3
C***        AFTER SWITCH 12 HAS BEEN PRESSED, EXIT IF SWITCH 16 IS ON...
    7 IF(SWITCH(16))GO TO 4
C***        OR INITIALIZE VALUES IF SWITCH 4 (IC) IS ON...
      IF(SWITCH(4))GO TO 5
C***        OR START EXECUTION AGAIN IF SWITCH 8 IS ON...
      IF(SWITCH(8))GO TO 6
C***        OR INITIALIZE DATA-UPDATE CLOCK AND ENTER A WAITING LOOP
      ITIME=1
      GO TO 7
    5 CONTINUE
C***        STOP THE DISPLAY AND GO BACK TO INITIAL VALUES
A   JPSR $NHALT
A   NOOP
      GO TO 1
C***        START EXECUTION OF A NEW DATA-UPDATE CYCLE:
C***        COMPUTE DT (=TIME IN SECS OF PREVIOUS CYCLE)
C***        AND INITIALIZE DATA-UPDATE CLOCK
    3 TIME=ITIME
      ITIME=0
      DT=TIME/120.
      CALL DYNNF
      CALL TRIG
C***        COMPUTE RANDOM DISTURBANCE (GUSTS)
L     INTEGER*5=LONG
      IRNUM=MOD((7701*IRNUM+3927),10000)
      RNUM=IRNUM
L     INTEGER*5=SHORT
      DVWI=(RNUM/10000.-0.5)*PRAND
      GUST=GUST+(DVWI-0.10472*GUST)*DT
      VW=VW0+GUST
```

```
      IF(IFAIL*IDETECT)10,11
C***        STORE TIME OF FAILURE IDENTIFICATION
10    CONTINUE
A           ADEPT
            S6AR'F
            ARAR'H'F
            MDAR'A CORRECT   [IS PITCH A.P. OR PITCH F.D. "ON"?
            JPLS NOCHANGE    [YES. NO IDENTIFICATION OCCURED.
            ARMD TSELECTOR   [NO. STORE 0 IN TSELECTOR
            MDXO SELECTOR    [IS THERE ALREADY A 0 IN SELECTOR?
            JPLS CHANGE      [NO. IDENTIFICATION HAS JUST OCCURED.
            JUMP NOCHANGE    [YES. IDENTIFICATION ALREADY RECORDED.
CORRECT:    0!H05000
TSELECTOR:  0
SELECTOR:   1
CHANGE:     MDAR TSELECTOR
            ARMD SELECTOR
FORTRAN
      TIDENT=TOTTX
      IDENT=1
      CPITCH1=0.
A  NOCHANGE: NOOP
11    CONTINUE
      XFEET=XN*6080.2
      IF(XFEET.EQ.0.)XFEET=1.
      YMILE=Y/6080.2
C***        COMPUTE THETA-DOT (=PITCH-ANGLE TIME-RATE OF CHANGE)
      TDOT=(DALFA+DGAMA)*COSP+DBETA*SINP+(BETA/RAD*COSP-(ALPHA+GAMMA)
     1 *SINP/RAD)*DPHI
C***        FLARE COMMAND COMPUTATION
      IF(IFLARE)33,35
35    DENOM=3.*VX*101.3367
      AFLARE=AMIN1((15.-DRNG*VZ/DENOM),120.)
      IF(A.GT.AFLARE)GO TO 31
      IFLARE=1
```

```
      TAU=DRNG/DENOM
      V20=AMIN1((V2+150.),-150.)
      CPICH1=0.
      MODFD="FLR."
      LABEL(MODE)
      ZSET(0.F)
      MOVE(0.23F,0.66F)
      WRITE(16,556)MODFD
556   FORMAT("0S",B4)
      ENDLIST
33    HER1=A+TAU*V2-15.
      HEDOT=V2/60.+TAU*DVZ
      GO TO 32
31    HER=A-XFEET*TNGSA
      HER1=HER
      HEDOT=V2/60.-VX*1.68894*TNGSA
32    IF(IFAIL)405,401
401   IF(A-ABS(AFAIL))403,403,400
403   IFAIL=1
      TFAIL=TOTTX
405   IF(IDENT)400,404
404   HER1=HER+0.1156935*AFAIL
C***       FLIGHT-DIRECTOR PITCH COMMAND
400   DCPICH=-0.6*(0.0005*(HEDOT+0.034*HER1)+0.5*TDOT)-0.034*CPICH1
      CPICH1A=CPICH1+DCPICH*DT
      DCPICH=(-0.6*(0.0005*(HEDOT+0.034*HER1)+0.5*TDOT)-0.034*
     1 CPICH1A+DCPICH)/2.
      CPICH1=CPICH1+DCPICH*DT
      CPICH=CPICH1+RAD*3.*(1.+IFLARE*(2.*ABS((V2+150.)/V20)-1.))
      IF(IFLARE)8001,8002
8001  IF(V2.GT.-150.)CPICH=AMIN1(0.,(-ABS(CPICH)))
8002  CONTINUE
      IF(A.LE.AFLARE)GO TO 22
C***        CENTER FLIGHT-DIRECTOR COMMAND-BARS IF OUTSIDE OF
C***        GLIDE-SLOPE RECEIVER RANGE
      CAPTR=1.
      IF(ABS(HER/XFEET).LE.0.006)GSLOCK=1.
      IF(GSLOCK)22,402
402   CONTINUE
      CPICH=-GAMMA
      DCPICH=-DGAMA
      CPICH1=0.
      CAPTR=0.
22    CONTINUE
      CPICH=AMOD(CPICH,360.)
```

```
C***      FLIGHT-DIRECTOR LATERAL COMMAND
      IF(XM.EQ.1.23)XM=1.2301
      EPS=YMILE/(1.23-XM)
      EPSDT=VX/3600.*YMILE/((XM-1.23)*(XM-1.23))-VY/3600./(XM-1.23)
      DCBNK1=-(0.1*(5.9244*DXI+3.32*DPHI+139.6*EPSDT
     1 +0.432*PHI/RAD+2.49*EPS)+0.16*CBNK1)
      DCBNK2=0.06889*(8.6*DXI+0.9*DPHI+180.*EPSDT)-1.06*CBNK2
      CBNK=CBNK+(DCBNK1+DCBNK2)*DT*RAD
      CBNK1=CBNK1+DCBNK1*DT
      CBNK2=CBNK2+DCBNK2*DT
      IF(ABS(EPS).LE.0.045)GO TO 21
      CBNK=CBNK1=CBNK2=DCBNK1=DCBNK2=0.
21    CONTINUE
      CBNK=AMOD(CBNK,360.)
      IF(XM.EQ.-5.4896)XM=-5.4895
      ADF=35.-ATAN(YMILE/(-XM-5.4896))*RAD
      IF(XM.GT.-5.4896)ADF=ADF+180.
      IF(XM.EQ.-0.0411)XM=-0.0410
      VOR=35.-ATAN((YMILE-0.6908)/(-0.0411-XM))*RAD
      IF(XM.GT.-0.0411)VOR=VOR+180.
      ADF=AMOD(ADF,360.)
      VOR=AMOD(VOR,360.)
      CALL RTOF
      CALL PCORD
      DIST=SQRT((XM+0.0411)**2+(YMILE-0.6908)**2)
      LABEL(DME)
      ZSET(0.0F)
      MOVE(-0.305F,-0.01434F)
      WRITE(16,555)DIST
555   FORMAT("0S",F4.1)
      ENDLIST
```

```
      CONE=.FALSE.
      ION=INN=IIN=0
      IF(EPS.LE.0.05.AND.EPS.GT.-0.05)CONE=.TRUE.
C***        TURN OUTER MARKER LIGHT ON
      IF(ABS(XM+5.4896).LE.TMRKR1.AND.CONE)ION=1
C***        TURN MIDDLE MARKER LIGHT ON
      IF(ABS(XM+0.7896).LE.TMRKR2.AND.CONE)INN=1
C***        TURN INNER MARKER LIGHT ON
      IF(ABS(XM+0.1896).LE.TMRKR.AND.   CONE )IIN=1
      CALL BEACONS(ION,INN,IIN,JJFF)
      IF(IFAIL)12,13
12    CONTINUE
C***        STORE TIME OF FAILURE DETECTION
A           ADEPT
            MDAR DETECT
            S6AR'A'F       [SAMPLE DETECTION SWITCH
            JPLS DETON     [IT IS "ON"
            JUMP DETOFF    [IT IS "OFF"
DETECT:0!H01000
PRDET: 0
DETON:      MDXO PRDET     [WAS IT "ON" BEFORE?
            JPLS .+2       [NO
            JUMP DETOFF    [YES
            ARMD PRDET
FORTRAN
      TDETECT=TOTTX
      IDETECT=1
A  DETOFF: NOOP
13    CONTINUE
C***        EXIT IF ALTITUDE=0
      IF(A)4,4,6
    4 CONTINUE
A        JPSR $NHALT
      CALL RECRD
A        ADEPT
         MDAR TURNOFF
         ARIC'A'F
         JUMP .+2
TURNOFF: 77076!H57777
         NOOP
FORTRAN
      XFF=XM*6080.2+1153.
```

```
      WRITE(25,2000)
      WRITE(25,2001)XFF,Y,V
      WRITE(25,2002)VZ
      WRITE(25,2004)AFLARE
      XI=XI-BETAG
      TRACK=XI+CRAB
      TDETECT=TDETECT-TFAIL
      TIDENT=TIDENT-TFAIL
      WRITE(25,2003)THETA,PHI,XI,TRACK,CRAB,DT,LOCD,TDETECT,
     1 TIDENT
2000  FORMAT(/////27X,"PARAMETERS AT TOUCHDOWN OR AT STOPACTION:"/)
2001  FORMAT(27X,"DISTANCE FROM THRESHOLD ",F15.0," FT."/
     1       27X,"DISTANCE FROM CENTERLINE",F15.0," FT."/
     2       27X,"INDICATED AIRSPEED      ",F15.0," KNOTS")
2002  FORMAT(27X,"VERTICAL SPEED          ",F15.0," FPM")
2004  FORMAT(27X,"FLARE COMMANDED AT ALT. ",F15.1," FT.")
2003  FORMAT( /27X,"PITCH ANGLE      ",F5.0," DEGS."/
     1          27X,"BANK ANGLE       ",F5.0," DEGS."/
     2          27X,"HEADING          ",F5.0," DEGS."/
     7          27X,"GROUND TRACK     ",F5.0," DEGS."/
     3          27X,"CRAB ANGLE       ",F5.0," DEGS."//
     4          27X,"    DT           =",F7.4/
     5          27X,"LOCD=",I3/
     6          27X,"TIME TO DETECTION    = ",F6.1," SECS."/
     7          27X,"TIME TO IDENTIFY     = ",F6.1," SECS.")
      IF(INAME.EQ.4040404040B)GO TO 601
      CALL OUTPUT
601   CONTINUE
      EXIT
```

```
      SUBROUTINE OUTPUT
      DIMENSION IBUFF(208)
      OPEN(21,0,2,,IBUFF,NAME)
      WRITE(21)XFF,Y,V,VZ,THETA,PHI,XI,CRAB,TDETECT,TIDENT       ,NAME
      WRITE(21)LOCD,(TOTT(I),STORX(I),STORA(I),STORY(I),I=1,LOCD)
      DO 1 K=1,50
      CONTINUE
1     CONTINUE
      CLOSE(21)
      OPEN(22,0,2,,IBUFF,'*HITSTASK*')
      LOCT=0
      WRITE(22)LOCT
      DO 2 K=1,50
      CONTINUE
2     CONTINUE
      CLOSE(22)
      OPEN(23,0,2,,IBUFF,'*MISSTASK*')
      MISS=0
      WRITE(23)MISS
      DO 3 K=1,50
      CONTINUE
3     CONTINUE
      CLOSE(23)
      RETURN
      END
```

```
      SUBROUTINE RECRD
C
C***        SUBROUTINE TO RECORD RUN DATA
C
      IMPLICIT FRACTION (F)
      COMMON/CSTASK/NSTSK,TOTTX,ETIME,LTON,NSWOLD,TIMEON,TIMEOFF
      COMMON/PRMTR/V,XI,VG,VW,COSXW,SINXW,COS35,SIN35,BETAG,VNORM,CRAB
      COMMON/PRMTR/GAMMA,ALPHA,BETA,PHI,VX,VY,VZ,THETA,A,XN,Y,R
      COMMON/DPRMTR/DV,DXI,DGAMA,DALFA,DBETA,DPHI,DT,DVZ
      COMMON LOCD,TOTT(150),STORX(150),STORA(150),STORY(150)
C
C***        UPDATE RUNNING CLOCK
C
      TOTTX=TOTTX+DT
C
C***        STORE TOTAL ELAPSED TIME, X,A,AND Y AT 5 SEC
C***        INTERVALS; UNLESS ALTITUDE IS LESS THAN 150,
C***        IN WHICH CASE STORE THEM AT 1 SEC INTERVALS
C
      TINT=5.
      IF(A.LE.150.)TINT=1.
      IF(AMOD(TOTTX,TINT).GT.DT)GO TO 101
      LOCD=LOCD+1
      TOTT(LOCD)=TOTTX
      STORX(LOCD)=XN*6080.2+1153.
      STORA(LOCD)=A
      STORY(LOCD)=Y
101   CONTINUE
      RETURN
      END
```

APPENDIX B

INSTRUCTIONS TO THE SUBJECTS

INSTRUCTIONS TO PILOT

You are the pilot-in-command of a Boeing-707-123 on a flight to Boston.

You will be asked to fly a number of ILS approaches to touchdown on Runway 4R at Logan in zero-ceiling, zero-visibility conditions. Your task is to stay as close as you can to the nominal ILS path and to execute the best landing possible under the circumstances.

The approaches will be flown with the autopilot in different modes: Some may be fully automatic, some may have autopilot coupling in one axis, and some may be fully manual, with flight-director guidance.

The guidance-and-control equipment that you have on board is not too reliable and has been known to malfunction occasionally in the past. Therefore, you should keep up your instrument scan to detect discrepancies which might indicate a guidance-and-control system failure.

All the approaches will start from the same point: You are 12 miles south-west of the airport at 2500 feet AGL, flying heading 065 to intercept the localizer inbound.

INSTRUCTIONS TO PILOT - WORKLOAD MEASUREMENT

This is our "Pilot Workload Assessment" experiment. You have two tasks to perform:

The piloting task, which should be your major concern at all times, consists of flying an ILS approach to touchdown on Runway 4R.

Your secondary task is identifying, and responding to, the two lights above the center panel. One or the other of the lights will illuminate at random times and will stay on for two seconds. Your response consists of moving the thumb-switch which is mounted on the left horn of the yoke in the direction of the light - UP for the upper light, DOWN for the lower light.

To be scored as correct, your response must be made while the light is on.

Let me again emphasize that your primary concern should be to do the best that you can flying the approach. Respond to the lights if, and only if, you feel that you can do so without sacrificing your piloting performance.

APPENDIX C

PILOT QUESTIONNAIRES

QUESTIONNAIRE - PERSONAL DATA.

Name _____ Age _____ Sex _____

Airline _____ Position _____

Pilot's License _____

Type Ratings _____

Commercial Flight Experience:

Transport Aircraft - Jets: Hours _____

Types _____

Recip.: Hours _____

Types _____

Military Flight Experience:

Jets: Hours _____ Types _____

Rec.: Hours _____ Types _____

Private Flight Experience:

Hours _____ Types _____

Simulator Experience: _____

Experience With Flight Directors:

- ☐ Cross-Pointers (Sperry)
- ☐ Roll Bars (Collins, Bendix)
- ☐ Other - specify: _____
- ☐ None

Total ILS Approaches Flown _____

ILS Approaches Flown In Last Six Months _____

Last ILS Approach Flown _____

Total Hours Flown In Last Six Months _____

Dominant Hand: _____ Wearing Glasses When Flying? _____

QUESTIONNAIRE - WORKLOAD EVALUATION.

Please give only one answer per question.

I. In my opinion, with respect to response characteristics, the simulated aircraft was:

[ ] Excellent

[ ] Good

[ ] Fair

[ ] Somewhat uncomfortable: Quite sensitive or quite sluggish

[ ] Very uncomfortable: Extremely sensitive or extremely sluggish

[ ] Nearly uncontrollable

[ ] Uncontrollable

II. In my opinion, with respect to control characteristics, the simulated aircraft was:

[ ] Extremely easy to control with excellent precision

[ ] Easy to control with good precision

[ ] Controllable, with somewhat inadequate precision

[ ] Controllable, but with very little precision

[ ] Difficult to control

[ ] Nearly uncontrollable

[ ] Uncontrollable

III. In my opinion, with respect to the demands placed on me as the pilot, the simulated aircraft was:

[ ] Completely undemanding, very comfortable to fly

[ ] Largely undemanding, comfortable to fly

[ ] Mildly demanding of pilot attention, skill or effort

[ ] Very demanding of pilot attention, skill or effort

[ ] Nearly uncontrollable

[ ] Uncontrollable

IV. In my opinion, the following is true with respect to the deficiencies in the simulated aircraft:

[ ] No noticeable deficiencies

[ ] Very mild deficiencies with no significant effect on performance

[ ] Deficiencies with effects on performance which are easily compensated for by the pilot

[ ] Moderately objectionable deficiencies

[ ] Very objectionable deficiencies

[ ] Nearly uncontrollable

[ ] Uncontrollable

CODE:

m.:

s.d.:

V. In my opinion, turning off the lights interfered with my performance on the piloting task:

[ ] Not at all, no interference

[ ] To a negligible extent

[ ] Some interference, resulted in few piloting errors

[ ] Moderate interference, caused some piloting errors

[ ] Definite interference, resulted in considerable piloting errors

[ ] Nearly complete interference, piloting was severely impaired

[ ] Complete interference, could not perform piloting task

VI. In my opinion, the following is true with respect to my responses to the lights:

[ ] Always responded immediately

[ ] Always responded, but occasionally too late

[ ] Usually responded, and responses were never late

[ ] Usually responded, but responses were sometimes late

[ ] Often failed to respond, but responses were usually on time

[ ] Often failed to respond and responses were usually too late

[ ] Only rarely responded

---

m.:

s.d.: CODE:

REFERENCES

Afifi, A.A. and S.P. Azen, Statistical Analysis - A Computer Oriented Approach. New York: Academic Press, 1972.

Baty, D.L., *Human Transformation Rates During One-to-Four Axis Tracking with a Concurrent Audio Task*, Memo, NASA-Ames Research Center, Moffett Field, Calif.

Bencivenga, V.L., *Test and Evaluation of an Advanced Integrated Landing System for All-Weather Landing*, National Aviation Facilities Experimental Center, Atlantic City, N.J., August 1970. FAA-RD-70-28.

Blakelock, J.H., Automatic Control of Aircraft and Missiles. New York: John Wiley & Sons, 1965.

Broadbent, D.E., *A Mechanical Model for Human Attention and Immediate Memory*, Psych. Rev., 64:205-215, 1957.

Broadbent, D.E., Decision and Stress. New York: Academic Press, 1971.

Brown, I.D., *The Measurement of Perceptual Load and Reserve Capacity*, The Trans. Assoc. Industrial Medical Officers, 14:44-49, 1964.

Clement, W.F., H.R. Jex and D. Graham, *A Manual Control-Display Theory Applied to Instrument Landings of a Jet Transport*, IEEE Trans. on Man-Machine Sys., Vol. MMS-9, 4:93-110, December 1968.

Cochran, W.G. and G.M. Cox, Experimental Design. 2d. ed. New York: John Wiley & Sons, 1968.

Cooper, G.E. and R.P. Harper, Jr., *The Use of Pilot Rating in the Evaluation of Aircraft Handling Qualities*, NASA TN-D-5153, April 1969.

DeCelles, J.L. *et al.*, *The Fail-Safe Landing*, Report of the ALPA All-Weather Flying Committee presented at ALPA's 17th Air Safety Forum, San Francisco, Calif., July 1970.

Dillow, J.D., *The Paper Pilot - A Digital Computer Program to Predict Pilot Rating for the Hover Task*, Air Force Flight Dynamics Laboratory, Wright-Patterson AFB, Ohio, March 1971. AFFDL TR-70-40.

Dixon, W.J. (ed.), BMD - Biomedical Computer Programs. University of California Press, 1973.

Dommasch, D.O. *et al.*, Airplane Aerodynamics. 4th ed. New York: Pitman Publishing Co., 1967.

Dunbar, J. and C. Collins, *Demonstration of the French Thomson-CSF, All-Weather Approach and Landing Monitor HUD*, Memo, Charles Stark Draper Laboratory, Cambridge, Mass., Oct. 2, 1972.

Ekstrom, P.J., *Analysis of Pilot Workload in Flight Control Systems with Different Degrees of Automation*, paper presented at the IRE International Congress on Human Factors Engineering in Electronics, Long Beach, Calif., May 1962.

Gai, E.G., *Psychophysical Models for Signal Detection with Time-Varying Uncertainty*, Ph.D. Thesis, Dept. of Aero. and Astro., M.I.T., January 1975.

Gai, E.G. and R.E. Curry, *Failure Detection by Pilots During Automatic Landings: Model and Experiments*, paper presented at 11th Annual Conference on Manual Control, NASA-Ames Research Center, May 1975.

Gainer, C.A. *et al.*, *All-Weather Landing Simulation for Category III Airborne Configuration: Summary of Studies on Flight Directors and Split Axis Control*, Bunker-Ramo Corp., Canoga Park, Calif., July 1967. SRDS RD-67-56/1.

Gibino, D.J., *Effects of Presence or Absence of Cockpit Motion in Instrument Flight Trainers and Flight Simulators*, Wright-Patterson AFB, Ohio, June 1968. AF ASD TR-68-24.

ICAO All-Weather Operations Panel, Second Meeting, Montreal, Canada, May 1965. ICAO Document No. 8512.

ICAO Procedures for Air Navigation Services: Aircraft Operations. 2d. ed., 1970.

Jacobs, R.S. *et al.*, *Simulator Motion as a Factor in Flight-Director Display Evaluation*, Human Factors 15(6):569-582, 1973.

Jenney, L.L. *et al.*, *Head-Up Displays - A Study of their Applicability in Civil Aviation*, Matrix Research Division, URS Systems Co., Fall Church, Va. January 1971. NASA CR-117135.

Jester, D., *Implementation of the DC-10 Performance and Failure Assessment Monitor (PAFAM)*, McDonnel-Douglas Co., May 1973. MDC J4121D.

Jones, S.S.D., *Guidance and Control Philosophy for All-Weather Landing*, J. Inst. Nav., Vol. 3, 3:277-301, July 1970.

Kayton, M. and W.R. Fried (ed.), Avionics Navigation Systems, pp. 520-548. New York: John Wiley & Sons, 1969.

Kelley, C.R., *Design Applications of Adaptive (Self-Adjusting) Simulators*, paper presented at the Working Conference on Manual Control, Cambridge, Mass., Feb. 28-March 2, 1966.

Knowles, W.B., *Operator Loading Tasks*, Human Factors 5:155-161, 1963.

Levison, W.H., *A Model for Task Interference*, paper presented at the 6th Annual Conference on Manual Control, Wright-Patterson AFB, Ohio, April 1970.

Levison, W.H., *A Control-Theory Model for Human Decision Making*, paper presented at the 7th Annual Conference on Manual Control, Los Angeles, Calif. June 1971.

Li, C.C., Introduction to Experimental Statistics. New York: McGraw-Hill, 1964.

Li, J.C.R., *Design and Statistical Analysis of Some Confounded Factorial Experiments*, Iowa State College of Agriculture and Mechanic Arts' Agricultural Experiment Station, Ames, Iowa, Research Bulletin 333, pp. 482-486, June 1944.

McRuer, D.T. and H.R. Jex, *A Review of Quasi-Linear Pilot Models*, IEEE Trans. on Human Factors in Electronics, Vol. HFE-8, 3:231-249, Sept. 1967.

McRuer, D.T. and D.H. Weir, *Theory of Manual Vehicular Control*, IEEE Trans. on Man-Machine Sys., Vol. MMS-10, 4:257-291, Dec. 1969.

McRuer, D.T. *et al.*, *A System Analysis Theory for Displays in Manual Control*, Systems Technology, Inc., Hawthorne, Calif., Oct. 1967. AD 675 983.

Miele, A., Flight Mechanics - Theory of Flight Paths. Addison-Wesley Publishing Co., Inc., 1962.

Monroe, R.D., D. Vreuls and C.A. Semple, *Summary of All-Weather Landing Simulation Studies*, Bunker-Ramo Corp., Canoga Park, Calif., Feb. 1968. SRDS RD-68-13.

Parks, D.L. and D.G. Tubb, *Simulator Development and Flight Validation of a Perspective Display as an Independent Landing Monitor*, paper presented at the AIAA 2nd Aircraft Design and Operation Meeting, Los Angeles, Calif., July 1970.

Perkins, C.D. and R.E. Hage, Airplane Performance, Stability and Control. New York: John Wiley & Sons, 1958.

Phatak, A.V. and G.A. Bekey, *Decision Processes in the Adaptive Behavior of Human Controllers*, IEEE Trans. on Sys. Science and Cybernetics, Vol. SSC-5, 4:339-351, October 1969.

Pursel, R.H., *An Evaluation of an All-Weather Landing Panel Display*, National Aviation Facilities Experimental Center, Atlantic City, N.J., Aug. 1968. NAFEC NA-68-9.

Schneider, C.E., *FAA Answers All-Weather Critics*, Aviation Week and Space Technology, Aug. 10, 1970. pp. 58-59.

Semple, C.A. *et al.*, *Effects of a 100-ft. Option Altitude Rule and an Annunciator Panel on Failure Detection, Go-Around Decisions and Landing Performance*, Bunker-Ramo Corp., Canoga Park, Calif., Feb. 1968. SRDS RD-68-11.

Schrenk, L.P., *Aiding the Decision Maker - A Decision Process Model*, IEEE Trans. on Man-Machine Sys., Vol. MMS-10, 4:204-218, December 1969.

Schuman, H.G. and R. Staufenbiel, *Flight Control Systems with Respect to V/STOL Automatic Landing*, AGARD Conference Proceedings on Aircraft Landing Systems, Cambridge, Mass., May 1969. AGARD CP-59-70.

Schweizer, G. and G. Schmidt, *A V/STOL Guidance and Control System with Bad Weather Landing Capability*, Dornier-Post (English ed.), 3:11-16, 1970.

Singleton, W.T., *Display Design - Principles and Procedures*, IEEE Trans. on Man-Machine Sys., Vol. MMS-10, 4:181-193, Dec. 1969.

Smallwood, R.D., *Internal Models and the Human Instrument Monitor*, IEEE Trans. on Human Factors in Electronics, Vol. HFE-8, 3:181-187, Sep. 1967.

Sm[illegible]n, J.M. *et al.*, *Principles of Performance Monitoring with Application to Automatic Landing*, J. of Aircraft, Vol. 9, p. 339, May 1972.

St. John, O.B. and R.C. Morgan, *The Implication of All-Weather Landings in the U.K.*, Aerospace Proceedings, pp. 1111-1127, 1966.

Spyker, D.A. *et al.*, *Development of Techniques for Measuring Pilot Workload*, Honeywell, Inc., Roseville, Minn., Nov. 1971. NASA CR-1888.

Teper, G.L., *Aircraft Stability and Control Data*, System Technology, Inc., Hawthorne, Calif., April 1969. STI TR-176-1.

Todosiev, E.P. *et al.*, *Human Performance in Single- and Two-Axis Tracking Systems*, paper presented at the 2nd Annual NASA - University Conference on Manual Control, Cambridge, Mass., Feb. 28 - March 2, 1966.

Van Houtte, N.A.J., *Display Instrumentation for V/STOL Aircraft in Landing*, Sc.D. Thesis, Dept. of Aero. and Astro., M.I.T., June 1970.

Vreuls, D. *et al.*, *Pilot Failure Detection Performance with Three Levels of Fault Warning Information*, Bunker-Ramo Corp., Canoga Park, Calif., Feb. 1968*a*. SRDS RD-68-9.

Vreuls, D. *et al.*, *All-Weather Landing Flight Director and Fault Warning Display Simulator Studies*, Bunker-Ramo Corp., Canoga Park, California. Paper presented at the 5th Annual Symposium on Human Factors in Aviation, Los Angeles, Calif., June 1968*b*.

Weir, D.H. and R.H. Klein, *The Measurement and Analysis of Pilot Scanning and Control Behavior During Simulated Instrument Approaches*, System Technology, Inc., Hawthorne, California, June 1970. NASA CR-1535.

von Wieser, M.F. *et al.*, *Humanizing the All-Weather Approach*, Douglas Aircraft Division. A70 33819.

Wewerinke, P.H., *Human Operator Workload for Various Control Situations*, National Aerospace Laboratory, N.L.R., Amsterdam, the Netherlands.

Young, L.R. *et al.*, *The Adaptive Dynamic Response Characteristics of the Human Operator in Simple Manual Control*, 1964. NASA TN D-2255.

Young, L.R., *On Adaptive Manual Control*, IEEE Trans. on Man-Machine Sys., Vol. MMS-10, 4:292-331, December 1969.